NUMERICAL ANALYSIS OF REFRIGERANT FLOW IN ADIABATIC STRAIGHT CAPILLARY TUBE

A thesis submitted in partial fulfillment of the requirements for the award of

degree of

MASTER OF ENGINEERING

IN

THERMAL ENGINEERING

Submitted By**:**
INDERPREET SINGH
Roll No: 801083009

Under the guidance of:

Dr. MADHUP KUMAR MITTAL
Assistant Professor, Deptt. of Mechanical Engg.
Thapar University, Patiala

DEPARTMENT OF MECHANICAL ENGINEERING

THAPAR UNIVERSITY

PATIALA – 147004

JULY, 2012

DECLARATION

I hereby declare that work in this thesis entitled, **"Numerical analysis of refrigerant flow in adiabatic straight capillary tube"**, in partial fulfillment of the requirements for the award of degree of Master of Engineering in mechanical engineering with specialization in **THERMAL ENGINEERING** submitted in Mechanical Engineering Department of Thapar University, Patiala, is an authentic record of my own work carried out under the supervision of Dr. Madhup Kumar Mittal.

The matter presented in this thesis has not been submitted for the award of any other degree of this or any other university.

Date: 16-7-2012

Place: Patiala

Inderpreet Singh
(INDERPREET SINGH)

This is to certify that the above statement made by candidate is correct and true to the best of my knowledge.

Supervisor

Madhup
Dr. MADHUP KUMAR MITTAL
Assistant Professor, MED
Thapar University,Patiala

(Counter Signed by)

Dr. AJAY BATISH
Professor and Head, MED
Thapar University, Patiala

Dr. S.K. MOHAPATRA
Dean of Academic Affairs
Thapar University, Patiala

ACKNOWLEDGEMENT

I express my sincere gratitude to **Dr. Madhup Kumar Mittal , Assistant Professor, Mechanical Engineering Department ,Thapar University, Patiala,** for their valuable guidance, proper advice and constant encouragement of my work in this thesis.

I do not find enough words with which I can express my feeling of thanks to the entire faculty and staff of **Mechanical Engineering Department Thapar university, Patiala,** for their help, inspiration and moral support.

Inderpreet Singh

INDERPREET SINGH

ABSTRACT

In the present work a mathematical model based on homogenous two phase flow is developed to predict the flow characteristics of refrigerants in adiabatic straight capillary tube. The mathematical model has been developed by using equations of conservation of mass, momentum, and energy. The refrigerant usually enters the capillary tube in liquid state and remains in liquid state for certain length. At a certain point during the flow, the flashing of refrigerant takes place and beyond this point, the flow becomes two-phase flow till the exit of capillary tube. During the single phase flow, the refrigerant properties remains almost constant, therefore conservation equations are solved analytically in single phase region. However, during the two phase flow, the refrigerant properties keep on changing as the flow progresses, therefore the conservation equations are solved by using finite difference method in order to take into account the variation of refrigerant properties in the two-phase region. Friction factor also plays an important role during the flow of refrigerant through capillary tube. Churchill (1994) correlation is used to calculate the friction factor. Duklers *et al.* (1964) viscosity correlation has been used to evaluate the two phase viscosity of the refrigerant. A computer program coded in MATLAB has been developed to solve the mathematical model. The developed model for straight capillary tube geometries have been validated with the experimental data of Melo *et al.*(1999), Fiorelli *et al.* (2002) and Jabaraj *et al.* (2006). Finally after results of validation, simulation has been done with different refrigerants to analyse their flow characteristics for different geometries at different operating conditions. The results of simulation reveal the following points.

1. The flow characteristics of R-12 and R-134a are close to each other at same condenser pressure and same degree of subcooling.
2. The flow characteristics of R-22 and R-407C are close to each other at same condenser pressure and same degree of subcooling.
3. The pressure drop for refrigerants R-410A, R-407C, M-20 and R-22 are close to each other at same condenser pressure and same degree of subcooling.
4. By varying the model input parameters it has been found that for all refrigerants, the mass flow rate increases with increase in degree of subcooling, increases as diameter increases, increases as condenser temperature increases, decreases as roughness increases and decreases as length increases.

CONTENTS

Description	**Page No.**
Declaration	i
Acknowledgement	ii
Abstract	iii
Contents	iv-vi
List of figures	vii-xii
List of Tables	xiii
Nomenclature	xiv-xv
Chapter - I	
INTRODUCTION	**1-5**
1.1 General	1
1.2 Adiabatic Straight capillary tube	1-2
1.3 Diabatic Straight capillary tube	2-3
1.4 Use of refrigerants	3-4
1.5 Motivation for the present study	4
1.6 Organization of Thesis	4-5
Chapter – II	
LITERATURE REVIEW	**6-13**
2.1 Experimental investigations	6-10
2.1.1 Effect of evaporator pressure	7-8
2.1.2 Effect of inlet degree of subcooling	8
2.1.3 Flow visualization	8-9
2.1.4 Empirical mass flow rate correlations	9-10

2.1.5 Parametric study 10

2.2 Numerical investigations 10-13

Chapter – III

MATHEMATICAL MODELLING 14-20

3.1 Development of mathematical model 14-16

3.1.1 Straight capillary tube 16-20

3.1.1.1 Single-phase region 16-17

3.1.1.2 Two-phase region 17-20

Chapter – IV

RESULTS AND DISCUSSION 21-65

4.1 Validation of Mathematical Model 21-65

4.1.1 Validation of mathematical model with Melo *et al.* (1999) experimental data for R-12. 21-22

4.1.2 Validation of mathematical model with Melo *et al.* (1999) experimental data for R-134a. 22-23

4.1.3 Validation of mathematical model with Melo *et al.* (1999) experimental data for R-600a. 23-25

4.1.4 Validation of mathematical model with Fiorelli *et al.* (2002) experimental data R-407C. 26-27

4.1.5 Validation of mathematical model with Fiorelli *et al. (*2002) experimental data for R-410A. 27-29

4.1.6 Validation of mathematical model with Jabaraj *et al.* (2006) experimental data for R-22. 29-33

4.1.7 Validation of mathematical model with Jabaraj *et al.* (2006) experimental data for M-20. 33-38

4.1.8 Simulation of refrigerants M-20 and R-22 using Dukler viscosity model (1964). 38-42

4.1.9 Simulation of refrigerants R-410A, R-407C, M-20, R-22,R-12 and R-134a using Dukler viscosity model (1964) for R-410A,R-407C,M-20,R-22 and Cicchitti viscosity model (1960) for R-12 and R-134a. 43-52

4.1.10 Simulation of refrigerants R-12, R-134a and R-600a using Cicchitti viscosity model (1960). 52-57

4.1.11 Simulation of refrigerants R-22, R-407C and R-410A using Dukler viscosity model (1964). 57-61

4.1.12 Simulation of refrigerants R-22, R-407C and R-410A using Dukler viscosity model (1964). 61-62

4.1.13 Simulation of refrigerants R-22, R-407C and R-410A using Dukler viscosity model (1964). 62-63

4.1.14 Simulation of refrigerants R-407C, M-20, R-12 and R-134a using Dukler viscosity model (1964) for R-407C and M-20 whereas Cicchitti model for R-12 and R-134a (1960). 63-64

4.1.15 Simulation of refrigerants R-22, R-134a, R-407C and M-20 using Cicchitti viscosity model (1960) for R-134a whereas R-22, R-407C and M-20 using Dukler viscosity model (1964). 64-65

Chapter – V

CONCLUSIONS AND SCOPE OF FUTURE WORK **66-67**

REFERENCES **68-70**

LIST OF FIGURES

Fig. No.	Title	Page No.
Fig. 1.1	Adiabatic straight capillary tube	2
Fig. 1.2	Diabatic straight capillary tube	3
Fig. 2.1	Naked-eye view of the vaporization point	9
Fig. 3.1	Computational domain of straight adiabatic capillary tube	14
Fig. 3.2	Free body diagram of fluid element of straight tube	15
Fig. 3.3	Computational domain for two phase region	19
Fig.4.1 (a)	Comparison of Melo *et al.* (1999) experimental data with present numerical results at condenser pressure of 9 bar for the flow of R-12	21
Fig.4.1 (b)	Comparison of Melo *et al.* (1999) experimental data with present numerical results at condenser pressure of 11 bar for the flow of R-12	22
Fig.4.2 (a)	Comparison of Melo *et al.* (1999) experimental data with present numerical results at condenser pressure of 9 bar for the flow of R-134a	22
Fig.4.2 (b)	Comparison of Melo *et al.* (1999) experimental data with present numerical results at condenser pressure of 11 bar for the flow of R-134a	23
Fig.4.3 (a)	Comparison of Melo *et al.* (1999) experimental data with present numerical results at condenser pressure of 9 bar for the flow of R-600a	23
Fig.4.3 (b)	Comparison of Melo *et al.* (1999) experimental data with present numerical results at condenser pressure of 11 bar for the flow of R-600a	24
Fig.4.4 (a)	Comparison between measured mass flow rate and predicted mass flow rate in percentage for R-12, R-134a and R-600a using Cicchitti viscosity model (1960)	24
Fig.4.4 (b)	Comparison between measured mass flow rate and predicted mass flow rate deviation for R-600a using Dukler viscosity model (1964)	25

Fig.4.5	Comparison of measured mass flow rate with those predicted by model for refrigerants R-12, R-134a and R-600a	25
Fig.4.6	Comparison of Fiorelli *et al.* (2002) experimental data with present numerical results at condenser temperature of 37 °C and diameter of 1.101 mm for the flow of R-407C	26
Fig.4.7	Comparison of Fiorelli *et al.* (2002) experimental data with present numerical results at condenser temperature of 37 °C and diameter of 1.394 mm for the flow of R-407C	26
Fig.4.8	Comparison of Fiorelli *et al.* (2002) experimental data with present numerical results at condenser temperature of 37 °C and diameter of 1.641 mm for the flow of R-407C	27
Fig.4.9	Comparison of Fiorelli *et al.* (2002) experimental data with present numerical results at condenser temperature of 34 °C for the flow of R-410A	27
Fig.4.10	Comparison of Fiorelli *et al.* (2002) experimental data with present numerical results at condenser temperature of 37 °C for the flow of R-410A	28
Fig.4.11	Comparison of Fiorelli *et al.* (2002) experimental data with present numerical results at condenser temperature of 40 °C for the flow of R-410A	28
Fig.4.12	Comparison of measured mass flow rate with those predicted by model for refrigerants R-407C and R-410A	29
Fig.4.13 (a)	Comparison of Jabaraj *et al.* (2006) experimental data with present numerical results at condenser temperature of 37 °C and length of 0.75 m for the flow of R-22	29
Fig.4.13 (b)	Comparison of Jabaraj *et al.* (2006) experimental data with present numerical results at condenser temperature of 37 °C and length of 1.5 m for the flow of R-22	30
Fig.4.14 (a)	Comparison of Jabaraj *et al.* (2006) experimental data with present numerical results at condenser temperature of 42 °C and length of 0.75 m for the flow of R-22	30
Fig.4.14 (b)	Comparison of Jabaraj *et al.* (2006) experimental data with present numerical results at condenser temperature of 42 °C and length of 1.5 m for the flow of R-22	31
Fig.4.15 (a)	Comparison of Jabaraj *et al.* (2006) experimental data with present numerical results at condenser temperature of 37 °C and length of 0.75 m for the flow of R-22	31

Fig.4.15 (b)	Comparison of Jabaraj *et al.* (2006) experimental data with present numerical results at condenser temperature of 37 °C and length of 1.25 m for the flow of R-22	32
Fig.4.16 (a)	Comparison of Jabaraj *et al.* (2006) experimental data with present numerical results at condenser temperature of 42 °C and length of 0.75 m for the flow of R-22	32
Fig.4.16 (b)	Comparison of Jabaraj *et al.* (2006) experimental data with present numerical results at condenser temperature of 42 °C and length of 1.25 m for the flow of R-22	33
Fig.4.17 (a)	Comparison of Jabaraj *et al.* (2006) experimental data with present numerical results at condenser temperature of 37 °C and length of 0.75 m for the flow of M-20	33
Fig.4.17 (b)	Comparison of Jabaraj *et al.* (2006) experimental data with present numerical results at condenser temperature of 37 °C and length of 1.5 m for the flow of M-20	34
Fig.4.18 (a)	Comparison of Jabaraj *et al.* (2006) experimental data with present numerical results at condenser temperature of 42 °C and length of 0.75 m for the flow of M-20	34
Fig.4.18 (b)	Comparison of Jabaraj *et al.* (2006) experimental data with present numerical results at condenser temperature of 42 °C and length of 1.5 m for the flow of M-20	35
Fig.4.19 (a)	Comparison of Jabaraj *et al.* (2006) experimental data with present numerical results at condenser temperature of 37 °C and length of 0.75 m for the flow of M-20	35
Fig.4.19 (b)	Comparison of Jabaraj *et al.* (2006) experimental data with present numerical results at condenser temperature of 37 °C and length of 1.5 m for the flow of M-20	36
Fig.4.20 (a)	Comparison of Jabaraj *et al.* (2006) experimental data with present numerical results at condenser temperature of 42 °C and length of 0.75 m for the flow of M-20	36
Fig.4.20 (b)	Comparison of Jabaraj *et al.* (2006) experimental data with present numerical results at condenser temperature of 42 °C and length of 1.25 m for the flow of M-20	37
Fig.4.21	Comparison of measured mass flow rate with those predicted by model for refrigerants M-20 and R-22	37
Fig.4.22 (a)	Mass flow rate variation with degree of subcooling for M-20 and R-22 with different capillary length at 1.1176 mm diameter with	38

	condenser temperature of 37 ℃	
Fig.4.22 (b)	Mass flow rate variation with degree of subcooling for M-20 and R-22 with different capillary length at 1.1176 mm diameter with condenser temperature of 42 ℃	38
Fig.4.23 (a)	Mass flow rate variation with degree of subcooling for M-20 and R-22 with different capillary length at 1.27 mm diameter with condenser temperature of 37 ℃	39
Fig.4.23 (b)	Mass flow rate variation with degree of subcooling for different capillary length at 1.27 mm diameter with condenser temperature of 42 ℃	39
Fig.4.24 (a)	Mass flow rate variation with degree of subcooling for M-20 and R-22 with different capillary length at 1.397 mm diameter with condenser temperature of 37 ℃	40
Fig.4.24 (b)	Mass flow rate variation with degree of subcooling for M-20 and R-22 with different capillary length at 1.397 mm diameter with condenser temperature of 42 ℃	40
Fig.4. 25	Mass flow rate variation with diameter for refrigerants M-20 and R-22 at same degree of subcooling	41
Fig.4.26	Pressure and temperature variation with capillary tube length for refrigerants M-20 and R-22, at same condenser pressure and inlet temperature to capillary tube	42
Fig.4.27	Mass flow rate variation with degree of subcooling for R410A, R-407C, M-20, R-22, R-12 and R-134a at condenser temperature of 37 ℃	43
Fig.4.28	Mass flow rate variation with degree of subcooling for R410A, R-407C, M-20, R-22, R-12 and R-134a at condenser temperature of 42 ℃	44
Fig.4.29	Mass flow rate variation with degree of subcooling for R410A, R-407C, M-20, R-22, R-12 and R-134a with condenser temperature of 37 ℃ and diameter of 1.27 mm	44
Fig.4.30	Mass flow rate variation with degree of subcooling for R410A, R-407C, M-20, R-22, R-12 and R-134a with condenser temperature of 37 ℃ and diameter of 1.1176 mm	45
Fig.4.31	Mass flow rate variation with degree of subcooling for R410A, R-407C, M-20, R-22, R-12 and R-134a with condenser temperature of 37 ℃ and diameter of 1.27 mm	46
Fig.4.32	Mass flow rate variation with degree of subcooling for R410A, R-407C, M-20, R-22, R-12 and R-134a with condenser	46

temperature. of 42 ℃ and diameter of 1.27 mm

Fig.4.33 Mass flow rate variation with capillary tube diameter for R410A, R-407C, M-20, R-22, R-12 and R-134a at condenser temperature of 37 ℃ with subcooling of 2 ℃ 47

Fig.4.34 Mass flow rate variation with capillary tube length for R410A, R-407C, M-20, R-22, R-12 and R-134a at 1.1176 mm diameter with same condenser temperature and subcooling 47

Fig.4.35 Mass flow rate variation with capillary tube length for R410A, R-407C, M-20, R-22, R-12 and R-134a at 1.27 mm diameter with same condenser temperature and subcooling 48

Fig.4.36 Pressure variation along capillary tube length for refrigerants R410A, R-407C, M-20, R-22, R-12 and R-134a at same condenser pressure and subcooling to capillary tube 49

Fig.4.37 Pressure and temperature variation along capillary tube length for refrigerants R410A, R-407C, M-20, R-22, R-12 and R-134a at same inlet temperature to capillary tube 49-50

Fig.4.38 Pressure, temperature and dryness fraction variation with capillary tube length for refrigerants R410A, R-407C, M-20, R-22, R-12 and R-134a at same inlet temperature to capillary tube 50-51

Fig.4.39 Mass flow rate variation with capillary tube length for R-12, R-134a and R-600a at 11 bar condenser pressure with 5 ℃ of subcooling at inlet to capillary tube 52

Fig.4.40 Mass flow rate variation with capillary tube length for R-12, R-134a and R-600a at 11 bar condenser pressure with 10 ℃ of subcooling at inlet to capillary tube 52

Fig.4.41 Pressure, temperature and dryness fraction variation along capillary tube length for R-12, R-134a and R-600a at same condenser pressure and inlet temperature to capillary tube 53-54

Fig.4.42 Pressure variation with capillary tube length for R-12, R-134a and R-600a at same inlet temperature to capillary tube 54

Fig.4.43 Mass flow rate variation along capillary tube length for R-12, R-134a and R-600a at same condenser pressure 55

Fig.4.44 Mass flow rate variation with respect to degree of subcooling for R-12, R-134a and R-600a at same condenser pressure and temperature 55

Fig.4.45 Pressure and temperature variation along capillary tube length for R-12, R-134a and R-600a at same condenser pressure and same degree of subcooling 56

Fig.4.46	Mass flow rate variation along capillary tube length for R-22, R-407C and R-410A at same condenser pressure and inlet temperature to capillary tube	57
Fig.4.47	Mass flow rate variation with capillary tube length for R-22, R-407C and R-410A same condenser pressure and inlet temperature to capillary tube	58
Fig.4.48	Pressure and temperature variation with capillary tube length for R-22, R-407C and R-410A at same condenser pressure and inlet temperature to capillary tube	58-59
Fig.4.49	Temperature variation with capillary tube length for R-22, R-407C and R-410A at same condenser pressure and subcooling	59
Fig.4.50	Pressure, temperature and dryness fraction variation along capillary tube length for R-22, R-407C and R-410A at same inlet temperature to capillary tube	60-61
Fig.4.51	Pressure variation with capillary tube length for R-22, R-407C and M-20 at capillary tube diameter of 1.27 mm	61
Fig.4.52	Pressure variation with capillary tube length for R-22, R-407C and M-20 at capillary tube diameter of 1.1176 mm	62
Fig.4.53	Pressure and temperature variation with capillary tube length for R-12, R-134a, R-407C and R-410A at same condenser pressure and inlet temperature to capillary tube	63
Fig.4.54	Pressure variation with capillary tube length for M-20, R-407C, R-134a and R-12 at same condenser temperature and subcooling at inlet to capillary tube	64
Fig.4.55	Mass flow rate variation along capillary tube length for R-22, R-134a, R-407C and M-20 at same condenser pressure and subcooling with different diameters	64-65

LIST OF TABLES

Table No.	Title	Page No.
Table 2.1	Experimental investigation	8
Table 2.2	Numerical investigation	12
Table 3.1	Friction factor correlation models	19
Table 3.2	Two-phase viscosity correlation models	20
Table 4.1	Database used for validation of mathematical model for straight capillary tube	21

NOMENCLATURE

A	-	cross-section of capillary tube,m^2
d	-	diameter,mm
e	-	relative surface roughness, µm
f	-	friction factor
G	-	mass flux, kg/h m^2
h	-	specific enthalpy, J/kg
k	-	entrance loss coefficient
L	-	length , m
m	-	mass flow rate, kg/h
P	-	pressure , kPa
Re	-	Reynolds number
s	-	specific entropy ,J/kg K
T	-	temperature, °C
V	-	velocity, m/s
x	-	quality
Greek letters		
µ	-	dynamic viscosity, kg/m s
ρ	-	density, kg/m^3
υ	-	specific volume, m^3/kg
τ_w	-	shear stress at wall, N/m^2
Δ	-	difference of
Subscripts		

cd	-	condenser
e	-	evaporator
f	-	liquid
fg	-	vaporization
g	-	gas
i	-	inlet
sp	-	subcooled single phase
sub	-	subcooling
tp	-	two phase

Chapter - I

INTRODUCTION

1.1 General

The capillary tube is simple, reliable, inexpensive, and widely used as a throttling device in the small-scale vapor compression refrigeration appliances. It is used as an automatic flow rate controller for the refrigerant when varying load conditions and varying condenser and evaporator temperatures are to be encountered.

The capillary tube is employed where the cooling load is fairly constant and the cooling capacity is not more than 3 TR. Capillary tube is a long narrow hollow drawn copper tube with an internal diameter ranging from 0.5 to 2.0 mm**.** The refrigeration systems work on vapor compression cycle comprising of evaporator, compressor, condenser, and expansion device. A capillary tube permits hermetically sealed compressor to start in an unloaded condition by allowing the pressures between the condenser and evaporator to equalize during the off cycle, thus, reducing the starting torque of the compressor. Hence, a low starting torque motor can be used with the vapour compression systems having capillary tube as an expansion device. In addition, the small and critical refrigerant charge required by the refrigeration system employing capillary tube results not only in reducing the cost of the refrigerant but also in eliminating the need for a receiver tank in the system. Obviously, all the enunciated facts contribute to substantial savings in the built-up cost of the system.

1.2 Adiabatic straight capillary tube

The schematic diagram of adiabatic capillary tube is shown in Fig.1.1a. In adiabatic capillary tubes, the refrigerant expands from high pressure side to low pressure side with no heat exchange with the surroundings as the tube is adiabatic. The refrigerant from the condenser enters the capillary tube, usually in a subcooled condition. So long as the refrigerant remains in subcooled state in the capillary tube, the pressure drops linearly due to friction, while the temperature remains constant due to adiabatic flow. As the pressure of refrigerant falls below the saturation pressure corresponding to temperature of subcooled refrigerant, vaporization of refrigerant takes place, which result in two-phase flow in the capillary tube. This causes an increase in fluid velocity because of the fall in density of the refrigerant due to vaporization of refrigerant.

The acceleration of fluid due to vaporization causes acceleration pressure drop, in addition to the friction pressure drop in the capillary tube. So, the pressure of refrigerant starts falling rapidly after onset of flashing and correspondingly the temperature of refrigerant also falls.

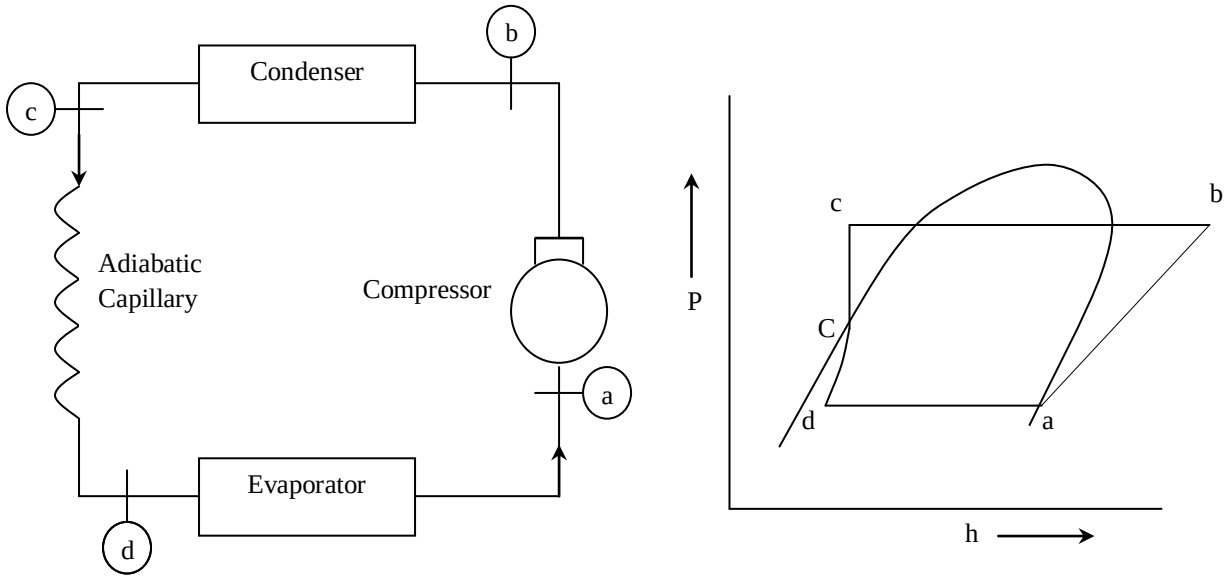

Fig. 1.1 Adiabatic capillary tube (a) block diagram (b) P-h diagram

Fig.1.1b shows the thermodynamic process of refrigerant in adiabatic capillary tube. So long as the refrigerant is in subcooled state, the enthalpy of refrigerant remains constant and as the flashing of refrigerant begins (at point 'C'in Fig.1.1b), the enthalpy starts decreasing due to increase in fluid velocity at the cost of decrease in enthalpy. However, stagnation enthalpy remains constant throughout the process due to adiabatic flow of refrigerant in capillary tube.

1.3 Diabatic straight capillary tube

Diabatic capillary tube act as heat-exchanger. In a diabatic flow arrangement, the capillary tube is bonded with the cold compressor suction line in a counter flow arrangement as shown in Fig. 1.2a. In this tube refrigerant expands from condenser pressure to evaporator pressure. As refrigerant expands through capillary tube from high to low pressure (c to d) it transfer its heat to refrigerant passing through the suction line of compressor (a to a$_1$) as shown in Fig.1.2b. So here liquid region length increases as compare to adiabatic capillary tube. As result of this refrigerating capacity increases, also cause improvement in efficiency of cycle.

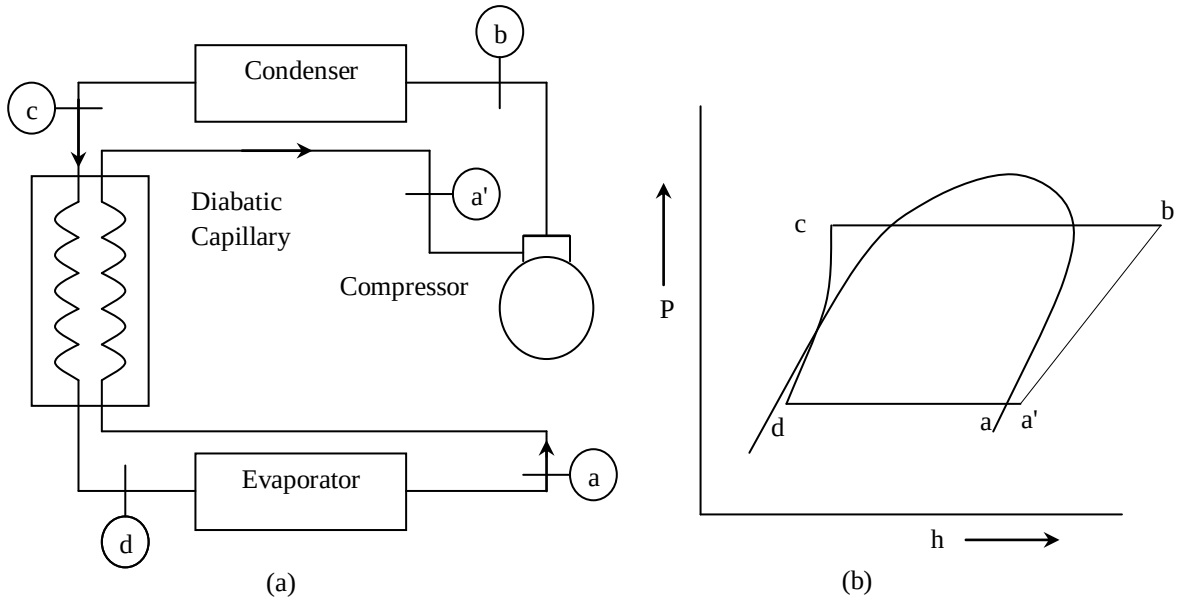

Fig.1.2: Diabatic capillary tube (a) block diagram (b) P-h diagram

As shown in Fig.1.2b, the enthalpy of refrigerant flowing in the diabatic capillary tube decreases at a higher rate than that in case of adiabatic capillary tube, which causes reduction in refrigerant quality entering the evaporator. Unlike adiabatic capillary tubes where the refrigerant temperature in the single phase region remains constant, heat transfer to the suction line causes the temperature of refrigerant to fall in the subcooled region, which causes a delay in the onset of vaporization. The delay of vaporization increases the liquid length, thus, the refrigerant mass flow rate through the diabatic capillary tube increases. The above two effects give a remarkable increase in refrigerating capacity of the system and results in the improvement of thermodynamic efficiency of the refrigeration system. In addition, the transfer of heat from capillary tube to the suction line diminishes the chances of liquid refrigerant entering the compressor.

1.4 Use of Refrigerants

Refrigerant is the substance which is necessary in an refrigeration system for producing cooling effect by going into phase change from liquid to vapour & vapour to liquid. Several evidences connecting halogenated compounds to stratospheric ozone layer depletion was collected in the last decades. One of such substances is the HCFC 22, largely used as refrigerant in equipment for commercial refrigeration, commercial and household air conditioners. These hydrochlorofluorocarbon & chlorofluorocarbon commonly called as HCFC & CFC, respectively are not used in refrigeration industries as they cause ozone layer depletion . This is due to the fact that free molecule of conventional refrigerant reaches the upper atmosphere, the strong solar

radiations break down the conventional refrigerant's molecule freeing chlorine atom from the structure. This chlorine reacts with ozone and converts it to oxygen. The conversion of ozone into oxygen will ultimately cause thinning of the layer to the extent that a hole is formed. This depleted zone of the ozone layer is termed as 'Ozone Hole'. The conventional refrigerants which are used in industries for refrigeration such as R-12, R-22 have varying degree of ozone depletion potential (ODP). The ozone depletion potential (ODP) of a refrigerant is the relative amount of degradation to the ozone layer it can cause.

Unfortunately up today research indicates that there is no pure substance that could be used as alternative for HCFC 22 small size units without the need of great modifications in existing equipment. The use of zeotropic or near-azeotropic refrigerant mixtures is the most suitable alternative so far. Among the possible alternatives manufacturers are using mainly the R-407C,a zeotropic mixture of HFC 32, HFC 125 and HFC134a (23%=25%=52% on mass basis) and the R-410A, a near-azeotropic mixture of HFC 32 and HFC 125. The use of such mixtures demands new experimental and numerical studies in order to evaluate how they affect the performance of refrigeration cycles as well as the design of cycle component. In this way the sizing of adiabatic capillary tubes using zeotropic mixtures is a subject of particular interest for small size air conditioning. Other refrigerants which are environment friendly also comes in market for utilization in refrigeration industries. This include M-20, R-502 and R-507a. M-20 is a mixture of R-407 , R-600a, R-290, R-502 is a mixture of R-22 and R-115 whereas R-507A is a mixture of R-125 and R-143a. Due to use of these hydrochlorofluorocarbon & chlorofluorocarbon refrigerants, global warming has increased in the world which are very dangerous sign for living beings as all the ecology gets disturb with this.

1.5 Objectives of the present study

1. Development of mathematical model for flow of refrigerant through adiabatic straight capillary tube.
2. To analyse flow characteristics of different refrigerants flowing through adiabatic capillary tube using the mathematical model.
3. To compare the flow characteristics of conventional and non-conventional refrigerants at different operating conditions, for different geometric parameters of the capillary tube.

1.6 Organization of thesis

The division of dissertation is mainly divided into five main parts. Experimental and numerical work are presented in this thesis. Validation and simulation results are explored on the basis of mathematical model of adiabatic straight capillary tube.

Chapter - I

This chapter is related to the capillary tube, its function in the refrigeration system and types of capillary tubes. It presents the adiabatic and diabatic straight capillary tubes to be used in vapor compression refrigeration systems. It also describes the various refrigerants used by authors in their study. R-12, R-22, R-134a, R-410A, R-407C and M-20 are the refrigerants which are used in their study.

Chapter - II

It is related to literature review. Extensive literature on experimental and numerical investigation is reviewed. The overview of experimental investigation including Flow visualization study, parametric study and empirical mass flow rate correlation are described in this chapter. Later in this chapter numerical investigation has been shown, that narrate mathematical model (two-phase model) that has been developed based on homogenous flow assumptions. The mathematical models are developed by using most reliable and frequently used correlations for friction factor and viscosity models available in the literature.

Chapter - III

This chapter deals with the mathematical model developed to predict the flow characteristics of refrigerant through geometries of straight capillary tube. The mass, momentum and energy conservation equations are described in this chapter to develop mathematical model. Friction factor and viscosity correlations are also studied.

Chapter - IV

It is related to various validation results obtained after comparing developed model for straight capillary tube geometries with the experimental data. In this chapter, the mass flow rates of refrigerants measured by Melo *et al.* (2002), Fiorelli *et al.* (1999) and Jabaraj *et al.* (2006) are compared with those predicted by the model. It also describe the simulation results obtained by comparing different refrigerants at different operating conditions and geometries.

Chapter - V

It is related to conclusion regarding validation and simulation results. Scope of future work is also narrated in this chapter.

Chapter – II

LITERATURE REVIEW

By means of experiments and numerical simulation, people gradually knew the flow characteristics of pure or mixed refrigerants through capillary tubes. Parameter analysis based on experimental data or numerical results is a general approach for people to understand and utilize the flow characteristics of a capillary tube.

2.1 Experimental investigations

The survey of literature has revealed that the most of the experimental investigations on capillary tube have been conducted for the flow of refrigerant through adiabatic straight capillary tubes using R-12 and R-22 as working fluid. As new eco-friendly refrigerants have come into the market, similar investigations are required for these refrigerants as well. In fact, after the implementation of Montreal Protocol (1992), new alternative refrigerants like R-134a, R-152a, R-600a, R-407C, R-410A and a number of blends are introduced in the market. The literature pertaining to the experimental investigation on the flow through adiabatic straight capillary tubes is listed in Table 2.1.

Table 2.1 Adiabatic straight capillary tube: Experimental investigations

author(s) (year)	***Refrigerants***	***Geometrical Parameters***	***Operating Parameters***	***study/remarks***
Bolstad and Jordan (1948)	R-12	d: 0.66 to 1.397 mm L: 1.83, 3.66, 5.49 m	P_{cd}: 827, 965, 1103 kPa P_e: 103.4 kPa	study of effect of evaporator pressure
Mikol (1963)	R-12 R-22	d: 1.41 mm L: 1.83 m	P_{cd}: 827, 965, 1100 kPa P_e: 103.4 kPa	flow visualization study
Koizumi and Yokoyama (1980)	R-22	d: 1.0, 1.5 mm L: 1.5, 1.9 m	P_{cd}: 1961 kPa P_e: 588 kPa	flow visualization study
Chang and Ro (1996)	R-32 R-125 R-134a	d: 1.2, 1.6 mm L: 1.5 m	P_{cd}: 1025 to 2800 kPa ΔT_{sub}: 1.8 to 12.2 °C	pressure drop studies of R-32, R-125 and R-134a

Melo *et al.* (1999)	R-12 R-134a R-600a	d: 0.77 to 1.05 mm L: 1.993 to 3.02 m	P_{cd}: 900, 1100 kPa ΔT_{sub}: 0 to 16 °C	empirical mass flow rate correlations
Motta *et al.* (2002)	R-404A R-404A/Oil	d: 0.8 mm L: 1.0 m	P_{cd}: 1825 kPa ΔT_{sub}: 6.2 to 21.5 °C	flow visualization study
Fiorelli *et al.* (2002)	R-407C R-410A	d:1.10, 1.39, 1.64 mm L:1.0, 1.25, 1.5 m	T_{cd}: 34 to 43 °C ΔT_{sub}: 1.0 to 6.0 °C	parametric study
Choi *et al.* (2003)	R-22 R-290 R-407C	d: 0.96, 1.2, 1.36 mm L: 0.7, 1.0, 1.3 m	T_{cd}: 38, 45, 52 °C ΔT_{sub}: 1.0 to 14.0 °C	generalized mass flow rate correlation
Chun-Lu Zhang (2004)	R-22 R-410A R-407C	d=1.2 to 1.3 mm L=1 to 1.5 m	T_{cd}: 35 ,40, 45 °C ΔT_{sub}: 4.0 to 8 °C	parametric study
Jabaraj *et al.* (2006)	R-22 M20(R-407C/ R-600a/R-290)	d: 1.1176, 1.397 mm L: 0.75 to 1.75 m	T_{cd}: 37 to 52 °C ΔT_{sub}: 2.0 to 14.0 °C	empirical mass flow rate correlations
Li Yang *et al.* (2008)	R-12, R-22 R-134a,R-152a R-410A,R-410C R-600a	d:0.2 to 5.0 mm L: 0.5 to 5 m	T_{cd}: 20 to 60 °C ΔT_{sub}: 0.0 to 20.0 °C	generalized mass flow rate correlation
V.Vacek.V.Vins (2009)	R-116 R-218 R-610	d:0.66 to 1.17 mm L=2.38 to 5.95 m	P_{cd}:0.82,0.98kPa ΔT_{sub}: 5.9°C ,13.3 °C	correlation for underpressure of vaporization

Various studies done by investigators are discussed below.

2.1.1 Effect of evaporator pressure

Bolstad and Jordan (1948) conducted experiments to determine the effect of evaporator pressure on mass flow rate of refrigerant for a constant inlet pressure and temperature. The experiments were conducted on the instrumented capillary tube. It was found that the variation in evaporator pressure had a marginal effect on the mass flow rate of refrigerant. In fact, in many of

the tests there was no effect on mass flow rate over the usual range of evaporator pressure. Later on this effect of evaporator pressure was also confirmed by Whitesel (1957).

2.1.2 Effect of inlet degree of subcooling

The studies conducted by Bolstad and Jordan (1948), Cooper *et al.* (1957), Lathrop (1948) showed that mass flow rate had propotional dependence on amount of subcooling. The studies showed that mass flow rate increases almost linearly with degree of subcooling. As the degree of subcooling increases, the liquid length in the capillary tube increases. Consequently, the mass flow rate increases because the liquid refrigerant offers less resistance to flow.

2.1.3 Flow visualization

Flow visualization is an extremely useful tool for research on two-phase flows and processes of heat transfer with phase change. Some researchers have used the visualization of refrigerant flow, through expansion devices of fixed area, with different objectives (e.g. two-phase flow characterization and metastable phenomenon verification). Cooper *et al.* (1957) were the first to used a glass capillary tube to compare the liquid length, measured visually, to that predicted by theoretical models. In all cases, the observed length was larger than the predicted, suggesting the presence of metastable flow. Additionally, pictures of the vaporization point described the two-phase flow as being a ‘‘fog flow.’’. Dudley (1962) and Mikol (1963) performed a visualization study using a glass capillary tube (internal diameter of 0.049 inches) to observe the two-phase flow. At first, pictures taken using a constant source of illumination (or‘‘naked-eye’’ pictures) as shown in Fig.2.1.It shows the two-phase flow having a ‘‘fog’’ appearance. (as reported before by Cooper *et al.*(1957). Trying to improve this procedure, pictures were taken using a stroboscope as a source of illumination. These pictures showed many small bubbles forming along the wall of the tube and moving toward the core of the flow; allowing the identification of the two-phase flow as being bubbly-type. Koizumi and Yokoyama (1980) used a glass capillary tube to verify the existence of a delay in the onset of vaporization due to metastable flow. Additionally, these authors described the two phase flow as being a ‘high-speed bubble flow’, confirming the observations of Mikol (1963). A few years back, another experimental study to visualize the in-tube flow of pure R-404A and R-404A/oil (5.6-6.9 % by mass) was carried out by Motta *et al.* (2002). While performing the experiments, they observed electric discharges at the exit of capillary tube. However, it could not be concluded with certainty if the similar phenomenon also appears in copper capillary tubes. V.Vacek.V.Vins (2009) has done visualization investigation on capillary tube.In this experimental investigation V.Vacek.V.Vins (2009) detects the existence of metastable region. He determined a correlation for ‘underpressure’ of vaporization.

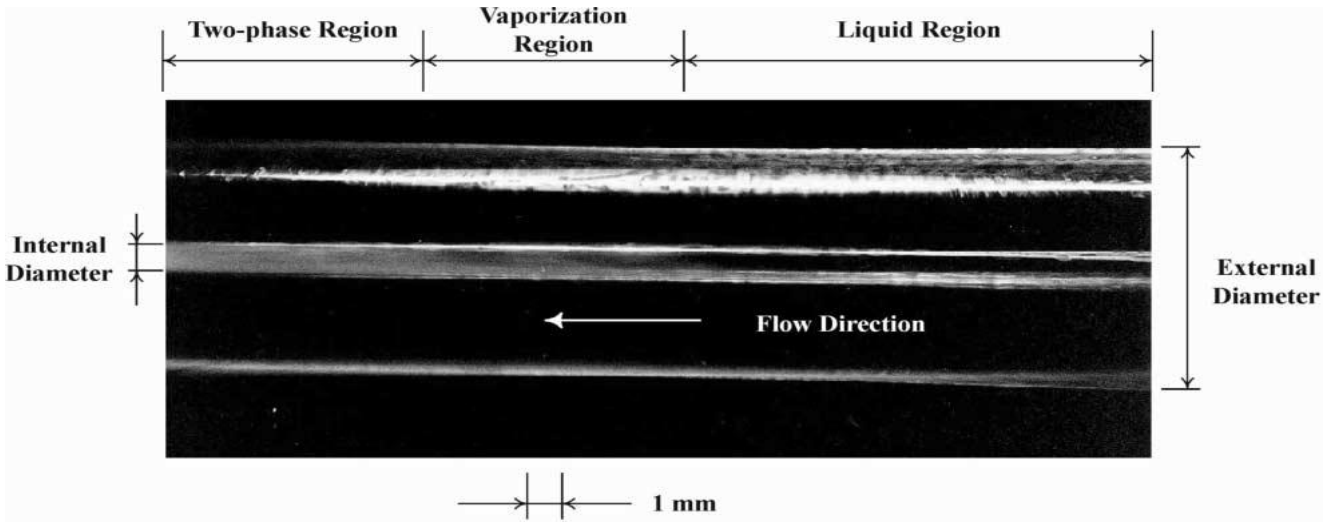

Fig. 2.1. Naked-eye view of the vaporization point.

2.1.4 Empirical mass flow rate correlations

A number of empirical correlations for the prediction of mass flow rate of various refrigerants in straight capillary tubes have been proposed. These empirical correlations have been developed by generating dimensionless parameters for operating conditions, capillary tube geometry and refrigerant properties using the Buckingham-π theorem. Wolf *et al.* (1995) developed a set of refrigerant specific correlations for refrigerants R-134a, R-22, R-410A and R-152a. They also proposed generalized correlation based on experimental data of R-134a, R-22 and R-410A. Melo *et al.* (1999) developed individual correlations for refrigerants R-12, R-134a and R-600a. They also proposed combined correlation for refrigerants R-12, R-134a and R-600a. Choi *et al.* (2003) developed a generalized correlation based on extensive experimental data of R-22, R-290 and R-407C. They validated their correlation by comparing the predictions from their correlation with the experimental data R-12, R-134a, R-152a, R-410A and R-600a available in the open literature. Choi *et al.* (2003) employed simplified dimensionless parameters in their correlation, by modifying the original dimensionless parameters obtained from Buckingham-π theorem. Further, Choi *et al.* (2004) proposed another modified generalized mass flow rate correlation using R-12, R-22, R-134a, R-152a, R-410A and R-600a experimental data of previous researchers. Choi *et al.* (2004) also generated rating charts with the help of their correlation to predict the mass flow rate of refrigerants R-12, R-22, R-134a, R-152a, R-410A and R-600a. Jabaraj *et al.* (2006) have proposed mass flow rate correlation for the flow of R-22 and M20 (R-407C/R-600a/R-290) through a straight adiabatic capillary tube. Li Yang et al (2008) developed generalized correlation

for refrigerant mass flow rate through capillary tube for R-12, R-22, R-134a, R-152a, R-410A, R-410C and R-600a with approximate analytic solutions based on their data. The collected data base about capillary tubes covers diameter from 5 mm to 2 mm, the condensing temperature from 20°C to 60 with subcooling ranges from 0°C to 20°C.

2.1.5 Parametric study

Various investigators perform parametric studies to insight into the flow characteristics of capillary tube. Fiorelli *et al.* (2002) proposed that capillary tube mass flow rates increase as condensing temperature and subcooling degree increases. For two-phase inlet conditions, mass flow rate increases as condenser temperature increases and the quality decreases. It is also verified that there is an increase in mass flow rate as diameter increases, due to the minor pressure drop imposed by bigger diameters. On the other mass flow rate increases as capillary tube length diminishes. Similarly to diameter, a bigger capillary tube length means a bigger pressure drop and a smaller mass flow rate. Chun-Lu Zhang (2004) also studied influences of geometrical parameters and inlet parameters on mass flow rate through a straight adiabatic capillary tube. It was found that mass flow rate was linear function of subcooling and varies reciprocally with inlet quality.

2.2 Numerical investigations

Numerical modelling is a method used to predict the flow characteristics of refrigerant in the capillary tube without conducting laborious experimental work. It is basically the simulation of experiment results developed by various researchers in their investigations. From the survey of literature it has been found that mathematical model (two-phase model) developed was based on homogenous flow assumptions. The mathematical models are developed by using most reliable and frequently used correlations for friction factor and viscosity models available in the literature. The developed model for straight capillary tube geometries are validated with the experimental data of previous studies as well as those of the present study.

Bolstad and Jordan (1949) presented a numerical solution for the flow of refrigerant through adiabatic capillary tubes. The numerical solution was based on homogenous flow and constant friction factor was considered throughout the flow. The conservation equations of mass, momentum and energy were solved using simplified methods. Later Marcy (1949) did a similar study except that he used liquid viscosity for the calculation of two-phase Reynolds number. Hopkins (1950) presented a graphical method to integrate flow equations used in Bolstad and Jordan's (1949) and Marcy's (1949) study. He also developed rating charts for the flow of R-12 and R-22, which covered the variables like tube diameter, tube length, condensing temperature, liquid subcooling and the refrigerant mass flow rate.

Literature survey of numerical investigation performed by various investigators is summarized in Table 2.2.

Table 2.2 - Adiabatic straight capillary tube: Numerical investigations

Author(s) (year)	Model Developed	Friction factor used	Two-phase Viscosity used
Wong and Ooi (1995)	Homogenous flow model	Colebrook (1939)	McAdams (1942), Cicchitti (1960), Dukler (1964), Beattie and Whalley (1981)
Wong and Ooi (1996a)	Homogenous flow model	Colebrook (1939)	Dukler (1964)
Chung (1998)	Homogenous flow model	Moody (1944)	Dukler (1964)
Bansal and Rupasinghe (1998)	Homogenous flow model	Churchill (1977)-single phase Lin *et al.* (1991)-two-phase	Lin *et al.* (1991)
Jung *et al.* (1999)	Homogenous flow model	Stoecker (1982)	McAdams (1942)
Sami and Maltais (2000)	Homogenous flow model	Beattie (1981)	McAdams (1942)
Wongwises *et al.* (2000b)	Homogenous flow model	Colebrook (1939)	McAdams (1942), Cicchitti (1960), Dukler (1964)
Wongwises *et al.* (2001)	Homogenous flow model	Colebrook (1939)	McAdams (1942), Cicchitti (1960), Dukler (1964), Lin *et al.* (1991)
Wongwises *et al.* (2002)	Homogenous flow model	Colebrook (1939)	Dukler (1964)
Trisaksri and Wongwises (2003)	Homogenous flow model	Colebrook (1939)	McAdams (1942), Dukler (1964)
Bansal and Wang (2004)	Homogenous flow model	Churchill (1977)	Dukler (1964)
Park *et al.* (2007)	Homogenous flow model	Colebrook (1939)	McAdams (1942)
Chingulpitak and Wongwises (2011)	Homogenous two phase flow model	Churchill (1977)	McAdams (1942)

In literature survey most of the mathematical models available have considered the two-phase flow as homogenous flow. In homogenous two-phase flow, it is assumed that the two phases move with the same velocity.

The design and analysis of capillary tubes has received the most attention, both analytically and experimentally, mostly for pure refrigerants. Mostly homogenous two-phase flow assumption has been used extensively. Wong and Ooi (1995) developed a mathematical model, considering the homogenous flow model, to investigate the effect of various two-phase viscosity correlations on the length of capillary tube. They did not take into account the phenomenon of metastablility in their model. It was concluded that Dukler (1964) mixture viscosity correlation provided the best

prediction of capillary tube length for a given mass flow rate of refrigerant. Wong and Ooi (1996a) used the same model to determine the performance of R-12 and R-134a under similar operating conditions. It was evolved from their study that, although there was a minor difference in the properties of the two refrigerants, yet the difference in capillary length for a given mass flow rate was quite significant. The length of capillary tube for a given flow rate was reduced by more than 15 percent as the refrigerant R-12 was replaced by R-134a. Bansal and Rupasinghe (1998) developed a mathematical model considering the homogeneous flow model i.e. CAPIL. It is obtained by applying fundamental equations of conservation of mass, momentum and energy. The model use the REFPROP data base to calculate the refrigerant properties. However, the phenomenon of metastability was ignored in the model. Another model that used homogeneous two-phase flow theory was proposed by Sami and Tribes (1998). The model was used to predict the flow behavior of R-12, R-22, alternative pure and binary blends to CFCs as well, inside the adiabatic capillary tube. But the phenomenon of metastability was ignored by them. It was found that the model predicted well the refrigerant behaviour inside the capillary tubes and was found in good agreement with the experimental data of previous researchers. Chung (1998) numerically analyzed the flow of R-407C, a ternary non-azeotropic mixture of refrigerants, through an adiabatic capillary tube. The phenomenon of metastability and capillary entrance effects were ignored by Chung (1998). Dukler *et al.* (1964) two phase viscosity correlation was employed for the computation of two-phase length of the capillary tube and Mikol (1963) friction factor correlation was used for the prediction of friction factor inside the capillary tube. Jung *et al.* (1999) formulated a selection procedure for the flow of refrigerants R-22 and the alternatives, viz. R-134a, R-407C and R-410A through an adiabatic capillary tube. Stoeker's model (1982) with modifications was employed in the development of the mathematical model. It was concluded that McAdams *et al.* (1942) two-phase viscosity correlation gave a better prediction than the Dukler *et al.* (1964) two-phase viscosity correlation model. Jung *et al.* (1999) generated data from their model and subsequently developed a semi-empirical correlation to predict the refrigerant mass flow rate of R-22, R-134a, R-407C and R-410A. Sami and Maltais (2000) developed a mathematical model by using fluid flow conservation equations written for homogenous refrigerant fluid flow under saturated, subcooled and two phase flow conditions. The model was validated with their own experimental data of R-22, R-410A, R-410B and R-407C. The results from the model indicated that a system using R-407C would experience smaller pressure drop compared to R-410A and R-410B. Wongwises *et al.* (2000b) developed a mathematical model for computation of the capillary length for a given mass flow rate in an adiabatic capillary tube. The fourth order Runge-Kutta method was used to solve a system of partial differential equations

obtained by the application of the laws of conservation of momentum, mass and energy. The characteristic curves under same operating conditions for traditional refrigerants and their alternatives were drawn and compared. It was concluded that for all pairs of refrigerants, the traditional refrigerants consistently gave lower pressure drops for both single phase and two phase flow than the eco-friendly alternative refrigerants Wongwises *et al.* (2002) developed another mathematical model for determine the flow characteristics of refrigerants through capillary tube. Trisaksri and Wongwises (2003) develop two phase model in which Churchill (1977) correlation is used for finding friction factors and McAdams (1942), Dukler (1964) correlation was used for viscosity measurement.

Bansal and Wang (2004) presents a homogeneous simulation model for choked flow conditions for pure refrigerants (R134a, R600a) in adiabatic capillary tubes. Chingulpitak and Wongwises (2011) develop another two phase flow model for a comparison of flow characteristics of refrigerants flowing through adiabatic straight and helical capillary tubes. In it Churchill (1977) correlation was used for computation of friction factor & McAdams viscosity model was used for computation of two phase flow viscosity. The viscosity models were used depending on each refrigerant following recommendations of past research. The Dukler (1964) model was used for simulations with R12 and R22, and the Cicchitti (1960) model for R134a, while the McAdams (1942) model, as the best all-around predictor, was used for the remaining refrigerants.

Chapter - III

MATHEMATICAL MODELLING

In this chapter, a mathematical model has been developed to predict the flow characteristics of a refrigerant through geometries of straight capillary tube. A computer program coded in MATLAB has been developed to compute the length of capillary tube and the refrigerant mass flow rate. The developed model for straight capillary tube geometries have been validated with the experimental data of previous studies. Finally the effect of various geometric parameters like diameter, degree of subcooling, condenser temperature, relative roughness on length of capillary tube for given set of input operating conditions has been carried out.

3.1 DEVELOPMENT OF MATHEMATICAL MODEL

The mathematical modelling of the straight capillary tube has been carried out by applying mass, momentum and energy conservation equations on required geometry of capillary tube.

For the purpose of analysis, the physical domain has been converted to computational domain, as shown in Fig.3.1. The refrigerant from condenser enters the capillary tube at section 1 in a subcooled liquid state. Due to sudden contraction at the capillary tube inlet, the refrigerant pressure is dropped and state point 2 is reached. Subsequently, a single phase liquid flow in the capillary tube is established. Since the flow of refrigerant through the capillary tube is adiabatic, the temperature of the flowing liquid refrigerant remains constant. The pressure inside the capillary tube drops linearly as long as the flow is in liquid state. The point of inception of vaporization is termed as flashing point, labeled as point 3. This point marks the onset of two-phase flow of refrigerant. In the two-phase region of the capillary tube, the temperature and pressure of refrigerant starts falling rapidly till the evaporator pressure or the choking point is attained.

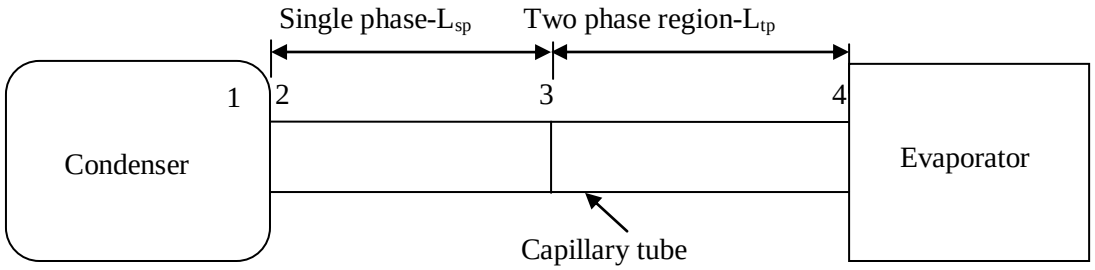

Fig. 3.1: Computational domain of straight adiabatic capillary tube

Thus, the flow of refrigerant through an adiabatic capillary tube has been divided into following three distinct regions:

1 – 2 represents pressure drop due to sudden contraction at capillary inlet.

2 – 3 represents single-phase subcooled flow region.

3 – 4 represents liquid-vapor two-phase flow region.

Following assumptions have been made during the analyses of straight adiabatic capillary tubes:

- the capillary tube is of uniform cross-section and roughness.
- the capillary tube is perfectly insulated.
- pure refrigerant is flowing through the capillary tube.
- one dimensional and steady state flow.
- the flow is homogenous in the two-phase region.

Consider an infinitesimal fluid element of length 'dL' within the capillary tube, shown in Fig.3.2 and applying the equations of conservation of mass, momentum and energy.

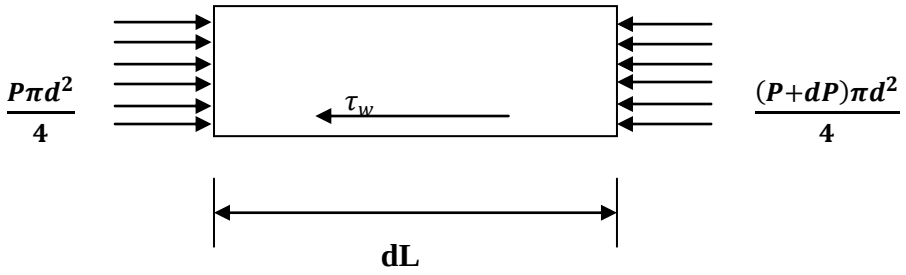

Fig. 3.2: Free body diagram of fluid element of straight tube

Mass Balance

Application of continuity equation results into the following

$$m = \rho VA \text{ or } \quad G = \frac{m}{A} = \rho V \tag{3.1}$$

Momentum Balance

On applying the principle of momentum conservations, the following equation will result

$$P.A - (P + dP).A - \tau_w(\pi d)dL = mdV \tag{3.2}$$

on simplification, the Equation (3.2) reduces to the following Equation (3.3)

$$dL = -\frac{2d}{f}\left(\frac{\rho\, dP}{G^2} + \frac{dV}{V}\right) \tag{3.3}$$

Taking log both sides of Equation (3.1) and then differentiating and simplifying

$$-\frac{dV}{V} = \frac{d\rho}{\rho} \tag{3.4}$$

Equation (3.3) reduces to

$$dL = \frac{2d}{f}\left(\frac{\rho dP}{G^2} - \frac{d\rho}{\rho}\right) \tag{3.5}$$

Energy Balance

On applying the steady flow energy equation for adiabatic flow with no external work and neglecting the elevation difference, the following Equation (3.6) is obtained

$$h + \frac{V^2}{2} = \text{constant} \tag{3.6}$$

3.1.1 Straight Capillary Tube

The mathematical analysis and the development of model for a straight tube are discussed below:

3.1.1.1 Single-phase region

In the single phase liquid region, the refrigerant density is almost constant as the liquids are practically incompressible (ρ = constant) and with tube cross sectional area being constant, from mass balance represented by Equation (3.1), the velocity is constant.

Integrating Equation (3.5), the length of single-phase liquid region

$$L_{sp} = \frac{d}{f_{sp}}\left[\frac{2}{\rho V^2}(P_2 - P_3)\right] = \frac{2d\rho(P_2 - P_3)}{f_{sp}G^2} \tag{3.7}$$

Pressure loss due to entrance effects

$$P_1 - P_2 = k\frac{\rho V^2}{2} \tag{3.8}$$

where '*k'* is the entrance loss coefficient, value of '*k*' is taken as 1.5 from Zhou and Zhang (2006).

From Equations (3.7) and (3.8)

$$L_{sp} = \frac{d}{f_{sp}}\left[\frac{2\rho}{G^2}(P_1 - P_3) - k\right] \tag{3.9}$$

where f_{sp} is the single phase friction factor

A number of friction factor correlations are available in literature and some of the correlations have been mentioned in Table 3.1. Out of these three correlations, Churchill correlation (1977) has been widely accepted and has been used by a number of researchers in the development of their model. In the proposed model for straight capillary tube, Churchill's correlation (1977) has been used.

Table 3.1 Friction factor correlation models

Researchers	***friction factor correlations***
Moody (1944)	$f = \dfrac{1.325}{\left[ln\left(\dfrac{e/d}{3.7} + \dfrac{5.74}{Re^{0..9}}\right)\right]^2}$
Colebrook (1939)	$\dfrac{1}{\sqrt{f}} = 1.14 - 2log\left(\dfrac{e}{d} + \dfrac{9.3}{Re\sqrt{f}}\right)$
Churchill(1977)	$f = 8\left[\left(\dfrac{8}{\mathrm{Re}}\right)^{12} + \left(\dfrac{1}{(A+B)^{1.5}}\right)\right]^{\frac{1}{12}}$ where $A = 2.457\ln\left(\dfrac{1}{(7/\mathrm{Re})^{0.9} + 0.27(e/d)}\right)^{16}$ and $B = \left(\dfrac{37530}{\mathrm{Re}}\right)^{16}$

3.1.1.2 Two-phase region

a

Applying continuity equation between sections 3 and 4

$$\dot{m} = \frac{V_3 A}{v_3} = \frac{V_4 A}{v_4} \tag{3.10}$$

Applying steady flow energy equation, with no external work, heat transfer and potential energy, between sections 3 and 4

$$h_3 + \frac{V_3^2}{2} = h_f + xh_{fg} + \frac{G^2}{2}(v_f + xv_{fg})^2 \tag{3.11}$$

Equation (3.11) is quadratic in x and the quality x can be expressed as

$$x = \frac{-h_{fg} - G^2 v_f v_{fg} + \sqrt{\left(G^2 v_f v_{fg} + h_{fg}\right)^2 - 2G^2 v_{fg}^2 \left(\frac{G^2 v_f^2}{2} - h_3 - \frac{V_3^2}{2} + h_f\right)}}{G^2 v_{fg}^2} \tag{3.12}$$

The two-phase friction factor f_{tp} can be calculated using Churchill's correlation (1977). The Reynolds number in two-phase region has to be determined by

$$\mathrm{Re}_{tp} = \frac{Vd}{\mu_{tp} v_{tp}} \tag{3.13}$$

where, μ_{tp} is the two-phase dynamic viscosity correlations are available in literature and some of them are listed below in Table 3.2.

Table 3.2 Two-phase viscosity correlation models

Researchers	***viscosity models***
McAdams (1942)	$\frac{1}{\mu_{tp}} = \frac{x}{\mu_g} + \frac{1-x}{\mu_f}$
Cicchitti (1960)	$\mu_{tp} = x\mu_g + (1-x)\mu_f$
Dukler *et al.* (1964)	$\mu_{tp} = \frac{x v_g \mu_g + (1-x) v_f \mu_f}{x v_g + (1-x) v_f}$

A number of researchers have suggested the use of different viscosity correlation for the prediction of two-phase length of capillary tube. For example, Bittle *et al.* (1994) have suggested the use of Dukler's model (1964) for simulations with R-12 and R-22 and Cicchitti's model for R-134a.Wongwises *et al.* (2001) have found that McAdams correlation (1942) gives a better

prediction than the Dukler's correlation (1964).So to judge which one is giving more accurate results these all viscosity correlations are compared with given experimental data. The one, which will be accurate will be used for simulation of different refrigerants.

The two-phase region of the tube, i.e., section 3-4, is divided into small elements with uniform pressure drop, *ΔP*, across each element. The computational domain for two phase region is shown in Fig. 3.3.

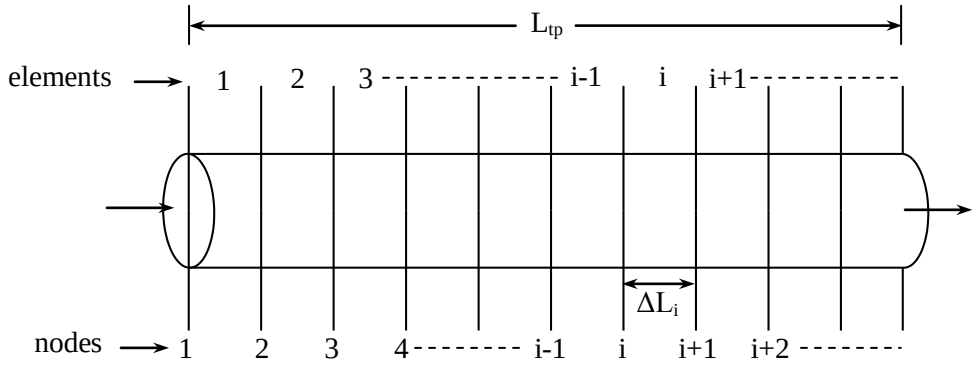

Fig. 3.3: Computational domain for two phase region

Applying conservation of energy equation, as given by Equation (3.6), between inlet (i^{th} node) and outlet ($i+1^{th}$ node) of an i^{th} element lying in the two phase region:

$$h_i + \frac{V_i^2}{2} = h_{f,i+1} + x_{i+1}h_{fg,i+1} + \frac{G^2}{2}\left(v_{f,i+1} + x_{i+1}v_{fg,i+1}\right)^2 \qquad (3.14)$$

The thermodynamic and transport properties of the refrigerant at the outlet of the i^{th} element can then be determined from the known value of quality, x_{i+1}, and pressure, P_{i+1}.

The pressure at the outlet of 'i^{th}' element is given by

$$P_{i+1} = P_3 - i\Delta P \qquad (3.15)$$

where, P_3 is the refrigerant pressure at the end of single phase liquid flow region, i.e., $P_3 = P_v$. With the pressure P_i corresponding quality, x_i, can be calculated from Equation (3.15), the entropy at the 'i^{th}'*element* can be determined from

$$s_i = s_f + x_i s_{fg} \qquad (3.16)$$

The incremental length, dL, is calculated from section after section. For each element pressure, temperature, vapour quality, friction factor and entropy are calculated. It has been found that the

entropy kept on increasing and after attaining certain value it decreases. The calculations have been made up to the point of maximum entropy. The pressure of the elemental section where entropy is maximum ($P_{i,smax}$), is then compared to the evaporator pressure (P_e)

if $P_{i,smax} = P_e$ then $P_4 = P_e$

if $P_{i,smax} \neq P_e$ then $P_4 = P_{i,smax}$

Integrating Eq. (2) for the section 3 - 4

$$L_{tp} = 2d\left(\frac{-1}{G^2}\int_{P_3}^{P_{s\,max}} \frac{\rho}{f_{tp}}dP + \int_{P_3}^{P_{s\,max}} \frac{d\rho}{\rho f_{tp}}\right) \tag{3.17}$$

The elemental length for two phase flow is calculated using discretized form of equation 3.5

$$\Delta L_i = \frac{2d}{f_{tpm,i}}\left(\frac{-\rho_{m,i}\Delta P}{G^2} + \frac{\Delta\rho_i}{\rho_{m,i}}\right) \tag{3.18}$$

Where, $\rho_{m,i}$ *and* $f_{tpm,i}$ are mean density and mean friction factor respectively over the 'ith' element in two phase region.

Finally, element lengths are added to calculate two-phase length. Thus the total length of capillary tube is the sum of single and two-phase lengths, i.e.,

$$L = L_{sp} + L_{tp} \tag{3.19}$$

Chapter - IV

RESULTS AND DISCUSSION

4.1 Validation of Mathematical Model

In order to validate the proposed model for straight capillary tube, the mass flow rates of refrigerants measured by Melo *et al.* (2002), Fiorelli *et al.* (1999) and Jabaraj *et al.* (2006) are compared with those predicted by the model. The details of the database used for the validation of model are listed in Table 4.1.

Table 4.1: Database used for validation of mathematical model for straight capillary tube

Parameters	**Melo *et al.* (1999)**	**Fiorelli *et al.* (2002)**	**Jabaraj *et al.* (1991)**
Refrigerant	R-12, R-134a, R-600a	R-407C,R-410A	R-22, M-20
Capillary tube length (L), m	2.926	1.5	0.75, 1.5, 1.25
Capillary tube diameter (d), mm	0.77	1.101,1.394,1.641	1.1176,1.27,1.397
Relative roughness of capillary tube (e/d)	9.74×10^{-4}	$(0.219\text{-}0.360)\times10^{-3}$	0
Condenser temperature (T_{cd}), °C	37.5-70.5	34-47	37-47
Degree of subcooling (ΔT_{sub}), °C	2-16	1.5-6.0	5-14

4.1.1 Validation of mathematical model with Melo *et al.* (1999) experimental data for R-12.

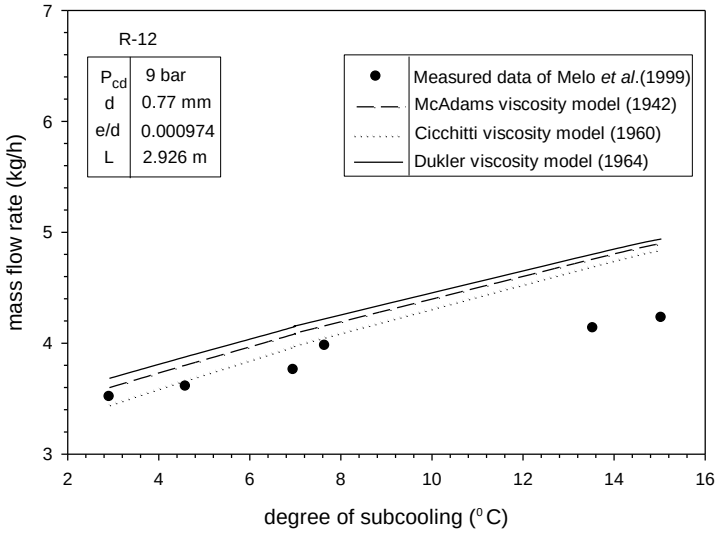

Fig.4.1 (a): Comparison of Melo *et al.* (1999) experimental data with present numerical results at condenser pressure of 9 bar for the flow of R-12.

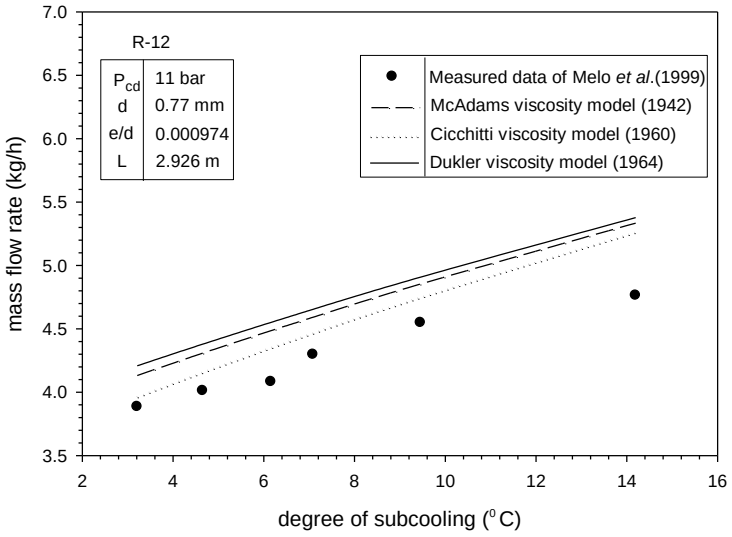

Fig.4.1 (b): Comparison of Melo *et al.* (1999) experimental data with present numerical results at condenser pressure of 11 bar for the flow of R-12.

Fig.4.1 (a) and (b) shows comparison of Melo *et al*.(1999) experimental data with present models for condenser pressure of 9 bar and 11 bar respectively for R-12. Tube length, diameter and relative roughness are 2.926 m, 0.77 mm and 0.000974 respectively. It has been found that mass flow rate increases with increase in degree of subcooling. This is due to the fact that, at higher inlet subcooling a larger liquid length is required to drop refrigerant pressure to the saturation pressure corresponding to refrigeration temperature. The closest estimate here is given by the Cicchitti viscosity model (1960) which gives an average error of -5.19 % for condenser pressure of 9 bar and of -4.83 % for 11 bar pressure.

4.1.2 Validation of mathematical model with Melo *et al.* (1999) experimental data for R-134a.

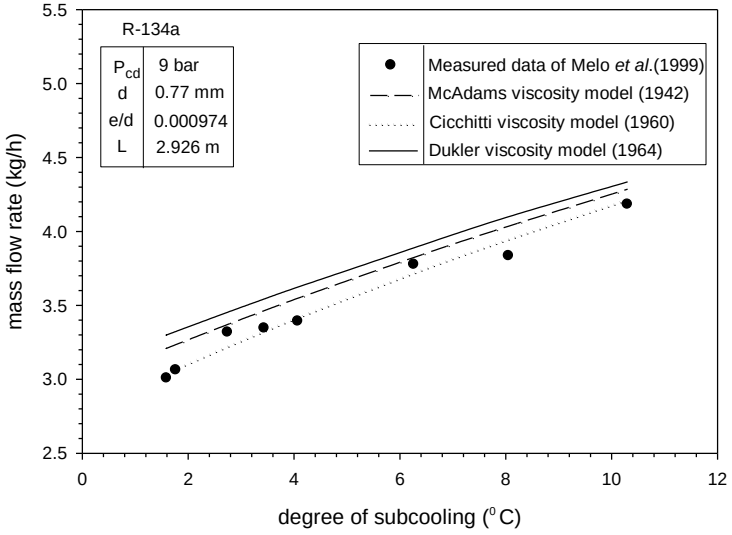

Fig.4.2 (a): Comparison of Melo *et al.* (1999) experimental data with present numerical results at condenser pressure of 9 bar for the flow of R-134a.

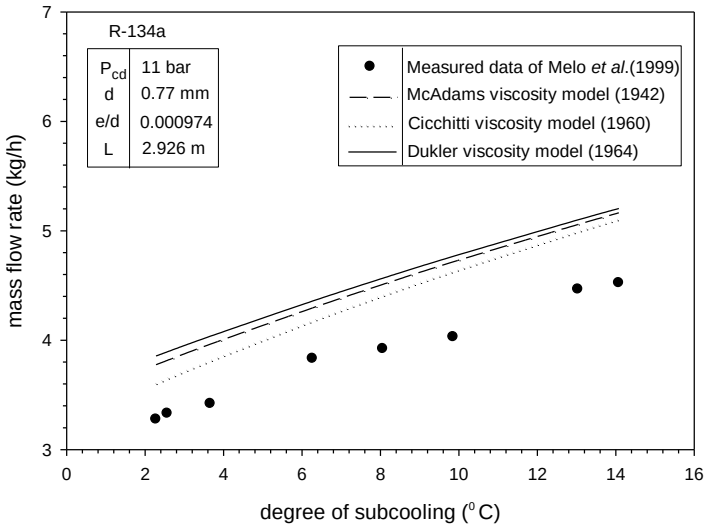

Fig.4.2 (b): Comparison of Melo *et al.* (1999) experimental data with present numerical results at condenser pressure of 11 bar for the flow of R-134a.

Fig.4.2 (a) and (b) shows comparison of modelling results of R-134a from present numerical models with Melo *et al.* (1999) experimental data for mass flow rate versus degree of subcooling at condenser pressure of 9 bar and 11 bar respectively. The tube diameter is 0.77 mm and length of tube is 2.926 m. It has been found that mass flow rate increases with increase in degree of subcooling. This is due to the fact that higher the degree of subcooling at capillary inlet higher will be the liquid length of the capillary tube. It is a known fact that the resistance of the fluid flow is low in the liquid region of capillary as compared to that in the two-phase liquid-vapour flow region. Therefore, increase in refrigerant mass flow rate can be associated with increase in liquid length of the capillary tube The Cicchitti viscosity model (1960) results are in good agreement with experimental data which gives an average error of -0.077 % for condenser pressure of 9 bar and -10.81 % for condenser pressure of 11 bar.

4.1.3 Validation of mathematical model with Melo *et al.* (1999) experimental data for R-600a.

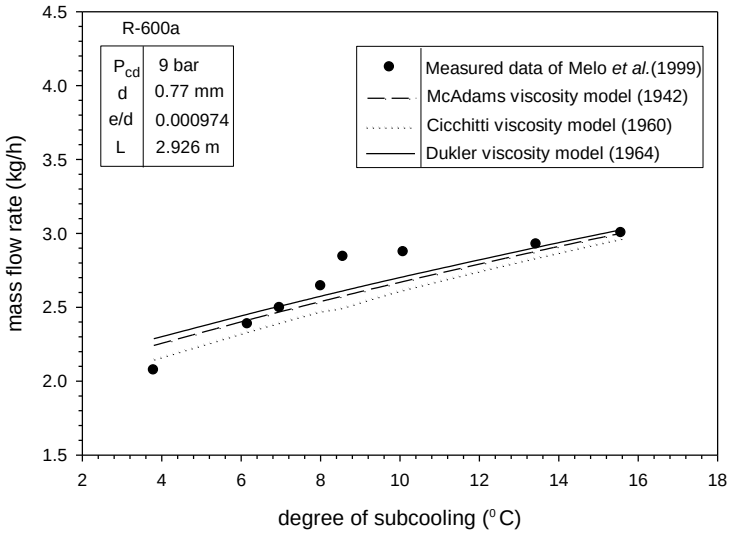

Fig.4.3 (a): Comparison of Melo *et al.* (1999) experimental data with present numerical results at condenser pressure of 9 bar for the flow of R-600a.

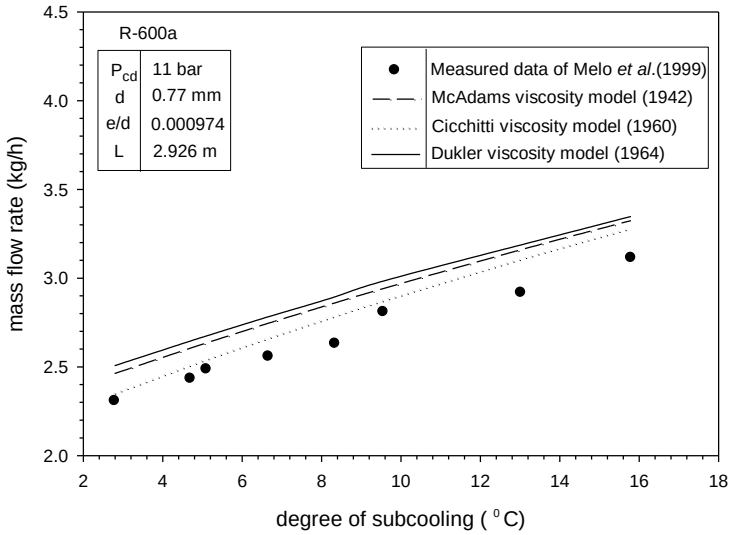

Fig.4.3 (b): Comparison of Melo *et al.* (1999) experimental data with present numerical results at condenser pressure of 11 bar for the flow of R-600a.

Fig.4.3 (a) and (b) has been drawn with mass flow rate as ordinate and capillary inlet subcooling of refrigerant as abscissa. The tube diameter is 0.77 mm and length is 2.926 m. The closest estimate is given by the Dukler viscosity model (1964) which gives an average error of 0.64 % for condenser pressure of 9 bar. For 11 bar pressure Cicchitti viscosity model (1960) is closest with average error of -3.70 %.

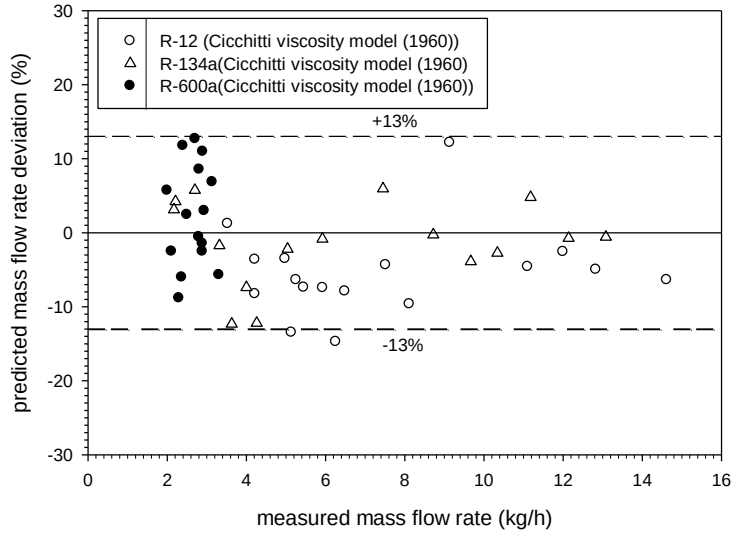

Fig.4.4 (a): Comparison between measured mass flow rate and predicted mass flow rate in percentage for R-12, R-134a and R-600a using Cicchitti viscosity model (1960).

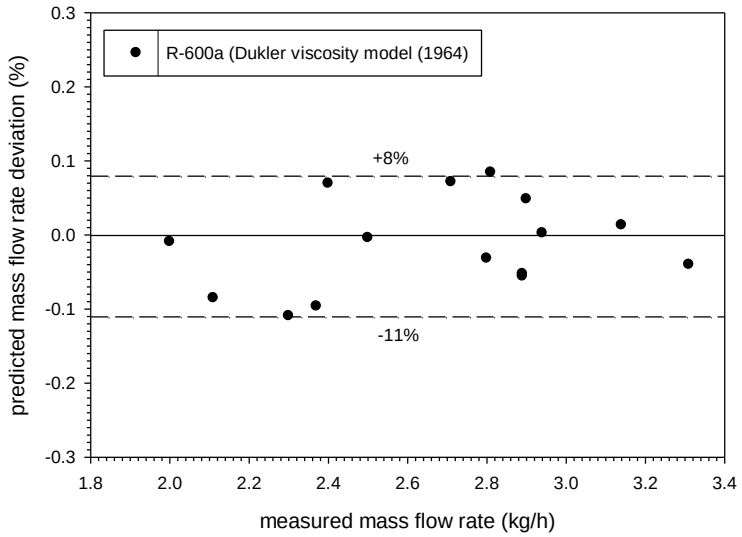

Fig.4.4 (b): Comparison between measured mass flow rate and predicted mass flow rate deviation for R-600a using Dukler viscosity model (1964).

Fig.4.4 (a) shows comparison of Melo *et al.*(1999) measured mass flow rate with predicted mass flow rate deviation (%) using Cicchitti viscosity model (1960) which is the more accurate model in validation for R-12, R-134a and R-600a. But in some results of R-600a, Dukler viscosity model (1964) gives accurate results in validation as shown in Fig.4.4 (b). During their result with Cicchitti viscosity model it has been found that for all three refrigerants approximately all data lies in between error band of $\pm$13%.With Dukler viscosity model (1964) for R-600a all data lies in between error band of +8% to -11%.

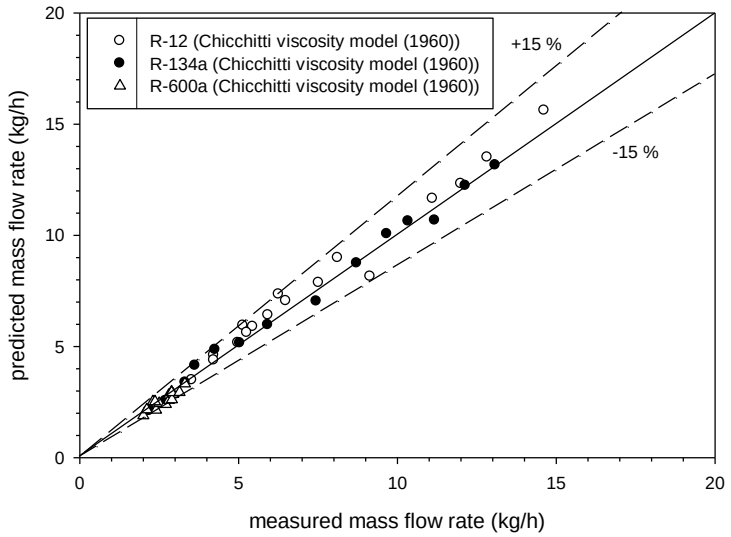

Fig.4.5: Comparison of measured mass flow rate with those predicted by model for refrigerants R-12,R-134a and R-600a.

Fig.4.5 shows the comparison of experimental mass flow rates of Melo *et al.* (1999) with the numerical mass flow rates predicted by the proposed model. It is observed that 96 percent experimental data of refrigerants R-12, R-134a and R-600a acquired from the present study are predicted by the model in the deviation range of -15 % to +15 % with mean deviation of -1.21 %.

4.1.4 Validation of mathematical model with Fiorelli *et al.* (2002) experimental data for R-407C.

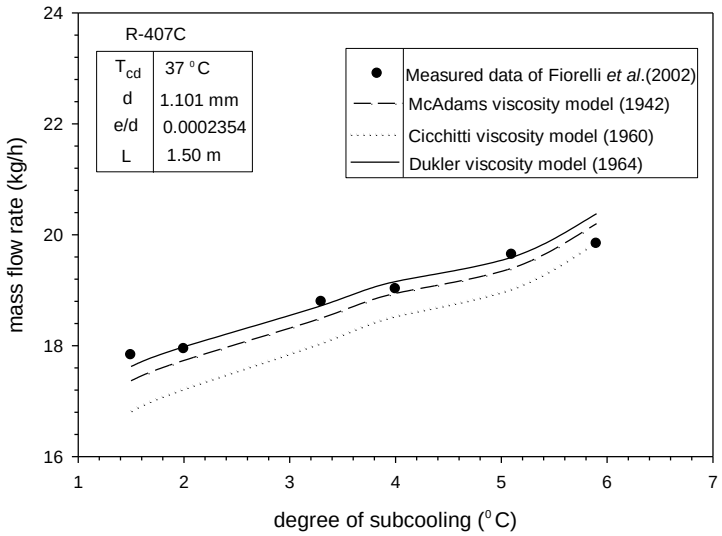

Fig.4.6: Comparison of Fiorelli *et al.* (2002) experimental data with present numerical results at condenser temperature of 37 °C and diameter of 1.101 mm for the flow of R-407C.

Fig.4.6 shows comparison of Fiorelli *et al.* (2002) results with present model results for R-407C.The tube diameter is 1.101 mm, condenser temperature is 37 °C and relative roughness is 0.0002354. It is observed that with the rise in refrigerant's inlet subcooling there is a linear increase in the mass flow rate of refrigerant. As the inlet subcooling is increased from 1.5 °C to 6 °C, the refrigerant mass flow rate is increased nearly by 12 %.The present numerical results from the Dukler viscosity model (1964) are in good agreement with measured data which gives an average error of 15.63% respectively.

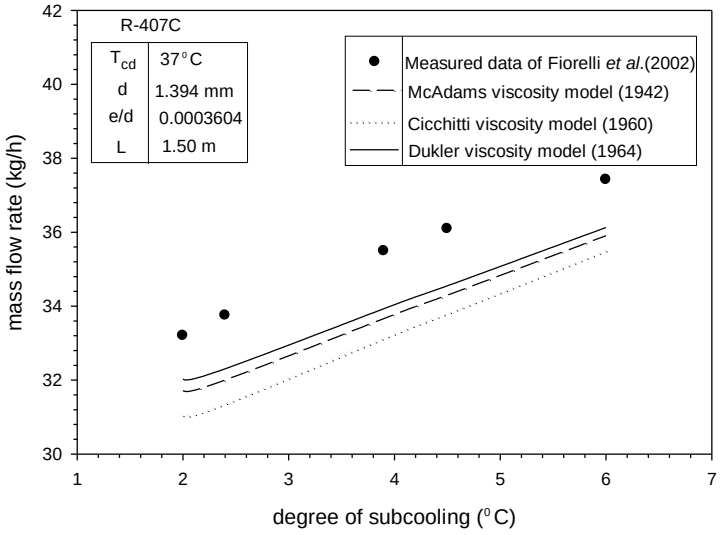

Fig.4.7: Comparison of Fiorelli *et al.* (2002) experimental data with present numerical results at condenser temperature of 37 °C and diameter of 1.394 mm for the flow of R-407C.

Fig.4.7 shows modelling results of R-407C for diameter 1.394 mm, condenser temperature of 37 °C and relative roughness of 0.0003604. The Dukler viscosity model (1964) underpredicts the Fiorelli *et al.* (2002**)** results with an average error of 12.71% respectively.

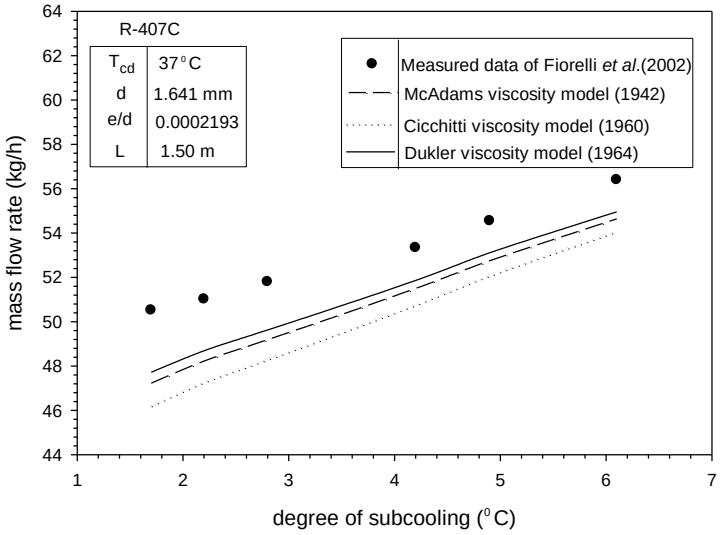

Fig.4.8: Comparison of Fiorelli *et al.* (2002) experimental data with present numerical results at condenser temperature of 37 °C and diameter of 1.641 mm for the flow of R-407C.

Fig.4.8 shows comparison of experimental data with present models for diameter of 1.641 mm, condenser temperature of 37 °C and relative roughness of 0.0002193. It has been found that Dukler viscosity model (1964) gives a good agreement with measured data and gives an average error of 15.16 % respectively.

4.1.5 Validation of mathematical model with Fiorelli *et al.*(2002) experimental data for R-410A.

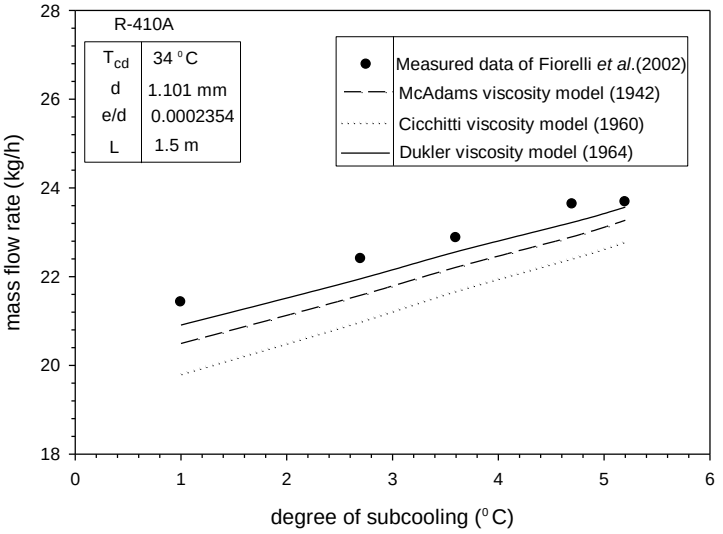

Fig.4.9: Comparison of Fiorelli *et al.* (2002) experimental data with present numerical results at condenser temperature of 34 °C for the flow of R-410A.

The variation of R-410A mass flow rate with degree of subcooling for tube of diameter 1.101 m has been shown in Fig.4.9. The condensing temperature is 34 °C and relative roughness is 0.0002354 .The closest estimate is given by the Dukler viscosity model (1964) which underpredicts the Fiorelli *et al.* (2002) results with an average error of 12.71 % respectively.

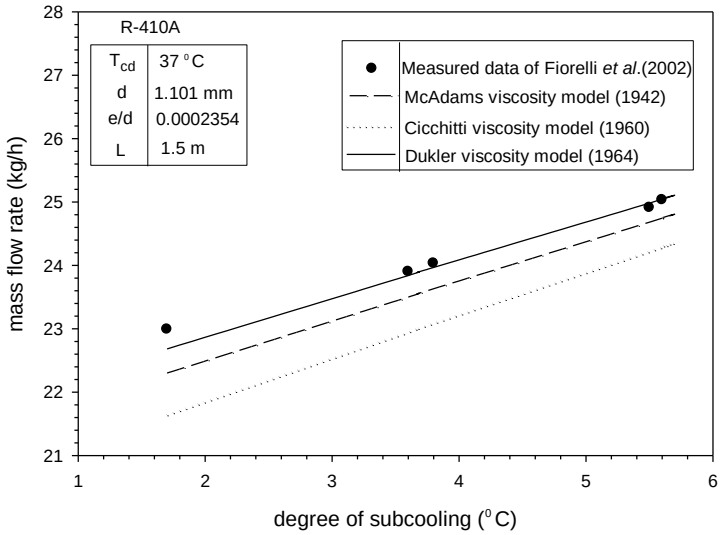

Fig.4.10: Comparison of Fiorelli *et al.* (2002) experimental data with present numerical results at condenser temperature of 37 °C for the flow of R-410A.

Fig 4.10 shows comparison of experimental data with present models for diameter of 1.101 mm, condensing temperature of 37 °C and relative roughness of 0.0002354. Further, it is noted that the Dukler viscosity model (1964) model gives good agreement with experimental data results. Model underpredicts the refrigerant mass flow rate up to 10.47 % for Fiorelli *et al.*(2002) experimental data.

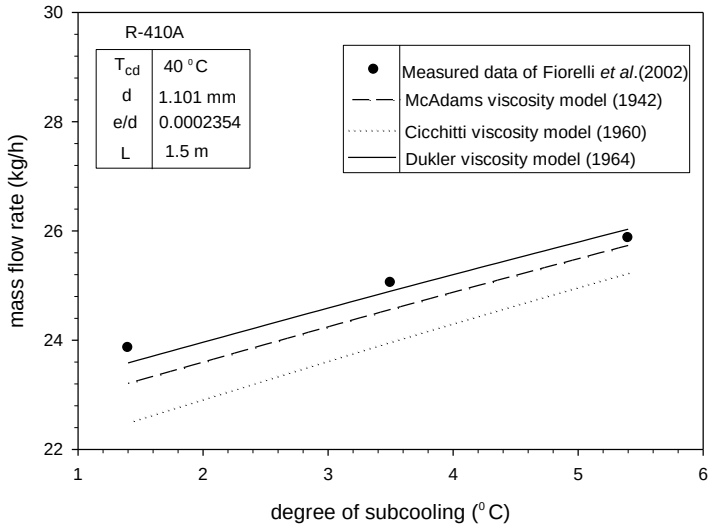

Fig.4.11: Comparison of Fiorelli *et al.* (2002) experimental data with present numerical results at condenser temperature of 40 °C for the flow of R-410A.

Fig.4.11 has been drawn with capillary inlet subcooling of refrigerant as abscissa and refrigerant mass flow as ordinate. As the inlet subcooling is increased from 1.5 °C to 6 °C the refrigerant mass flow rate is increased nearly by 7.8 %.The Dukler viscosity model (1964) underpredicts the experimental data with an average error of 3.94 % .

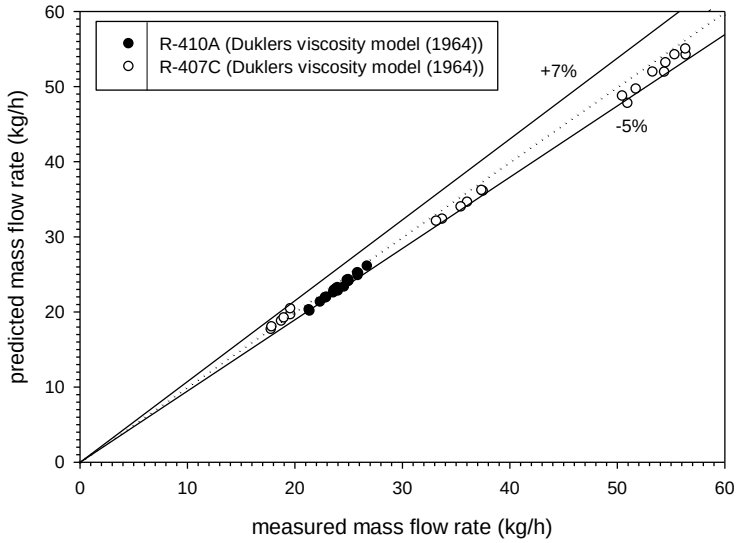

Fig.4.12: Comparison of measured mass flow rate with those predicted by model for refrigerants R-407C and R-410A.

Fig.4.12 shows the comparison of experimental mass flow rates of Fiorelli *et al.* (2002) with the numerical mass flow rates predicted by the proposed model. It is observed that 97 percent experimental data of refrigerants R-407C and R-410A fall within -5 % to +7 % deviation with mean deviation of 3.55 %.

4.1.6 Validation of mathematical model with Jabaraj *et al.* (2006) experimental data for R-22.

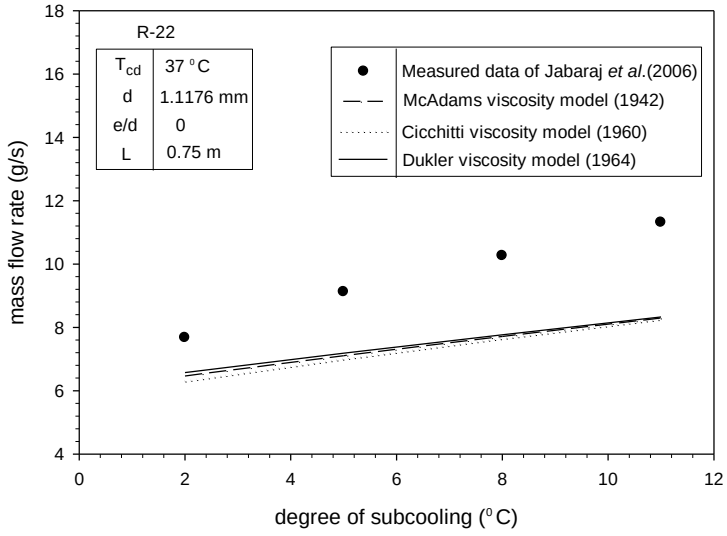

Fig.4.13 (a): Comparison of Jabaraj *et al.* (2006) experimental data with present numerical results at condenser temperature of 37 °C and length of 0.75 m for the flow of R-22.

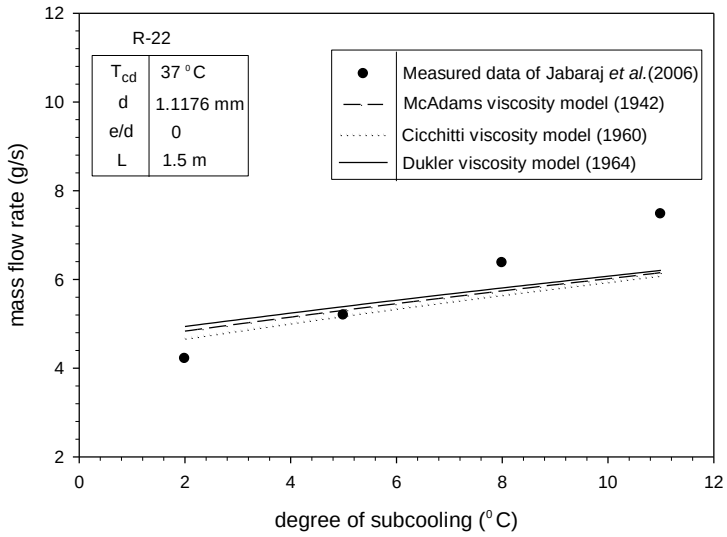

Fig.4.13 (b): Comparison of Jabaraj *et al.* (2006) experimental data with present numerical results at condenser temperature of 37 °C and length of 1.5 m for the flow of R-22.

Fig.4.13 (a) and (b) have been drawn to validate the proposed model with present Jabaraj *et al.* (2006) experimental data for capillary tube diameter of 1.1176 mm , condensing temperature of 37 at different lengths. It has been found that mass flow rate varies inversely with length of capillary tube. With increase in length of tube the resistance to refrigerant flow will increase which result in lesser mass flow rate as compared to capillary tube of shorter length. The closest estimate is given by the Dukler viscosity model (1964) which gives an average error of 27.8 % for length of 0.75 m and -2.91 % for length equal to 1.5 m.

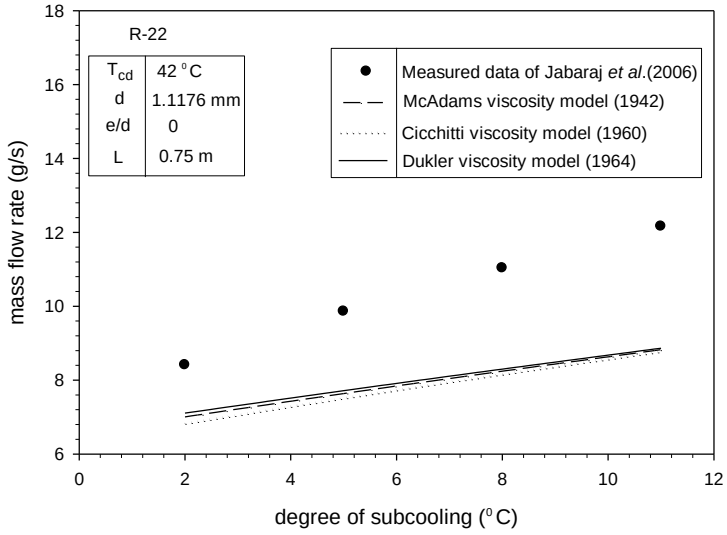

Fig.4.14 (a): Comparison of Jabaraj *et al.* (2006) experimental data with present numerical results at condenser temperature of 42 °C and length of 0.75 m for the flow of R-22.

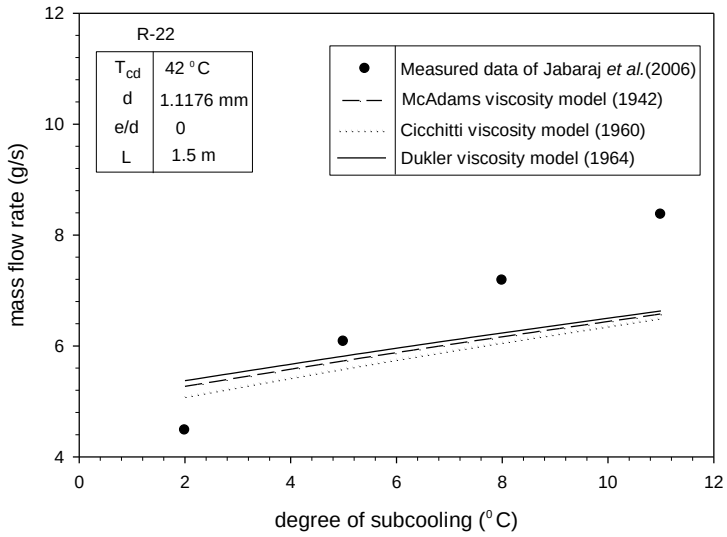

Fig.4.14 (b): Comparison of Jabaraj *et al.* (2006) experimental data with present numerical results at condenser temperature of 42 °C and length of 1.5 m for the flow of R-22.

Mass flow rate variation with degree of subcooling for different lengths have been drawn in Fig.4.14 (a) and (b) in order to validate experimental data with present models for tube diameter of 1.1176 mm and condensing temperature of 42 °C. Due to increase in condensing temperature the mass flow rate increases. The Dukler viscosity model (1964) results are in good agreement with experimental data, which gives an average error of 29.02 % for length equal to 0.75 m and 7.31 % for length equal to 1.5 m.

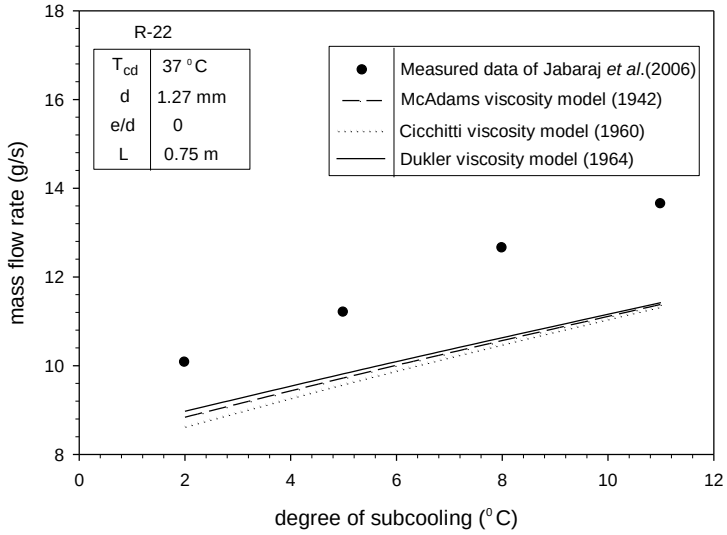

Fig.4.15 (a): Comparison of Jabaraj *et al.* (2006) experimental data with present numerical results at condenser temperature of 37 °C and length of 0.75 m for the flow of R-22.

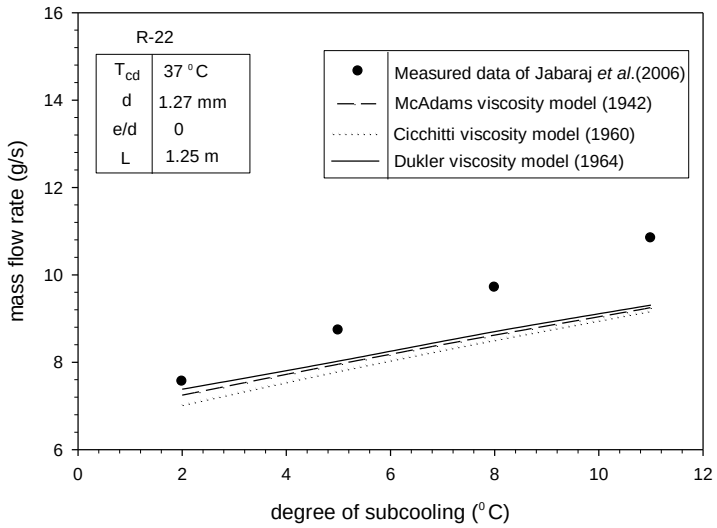

Fig.4.15 (b): Comparison of Jabaraj *et al.* (2006) experimental data with present numerical results at condenser temperature of 37 °C and length 1.25 m for the flow of R- 22.

Fig.4.15 (a) and (b) shows comparison of experimental data with present models for mass flow rate versus degree of subcooling with diameter equal to 1.27 mm, condenser temperature of 37 °C for different lengths. It is observed that with increase in diameter the mass flow rate increases due to reduced pressure drop for refrigerant flowing through capillary tube. The modelling results of Dukler viscosity model (1964) are in good agreement with experimental data which gives an average error of 16.17 % for length of 0.75 m and 9.67 % for tube length of 1.25 m.

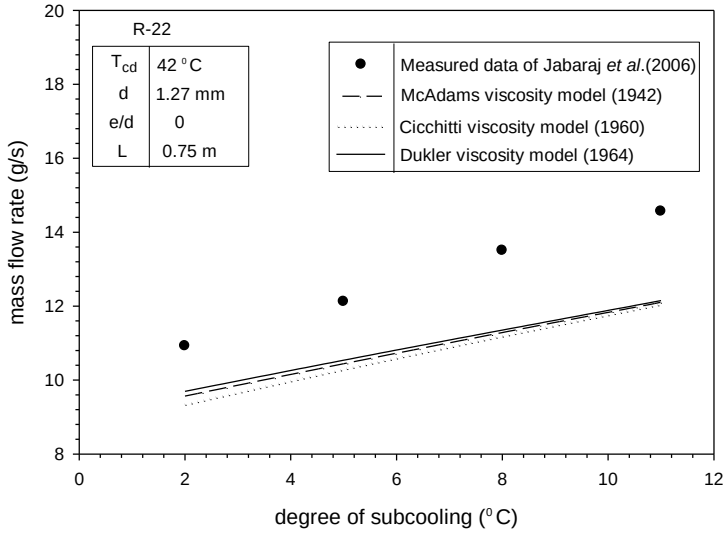

Fig.4.16 (a): Comparison of Jabaraj *et al.* (2006) experimental data with present numerical results at condenser temperature of 42 °C and length of 0.75 m for the flow of R-22.

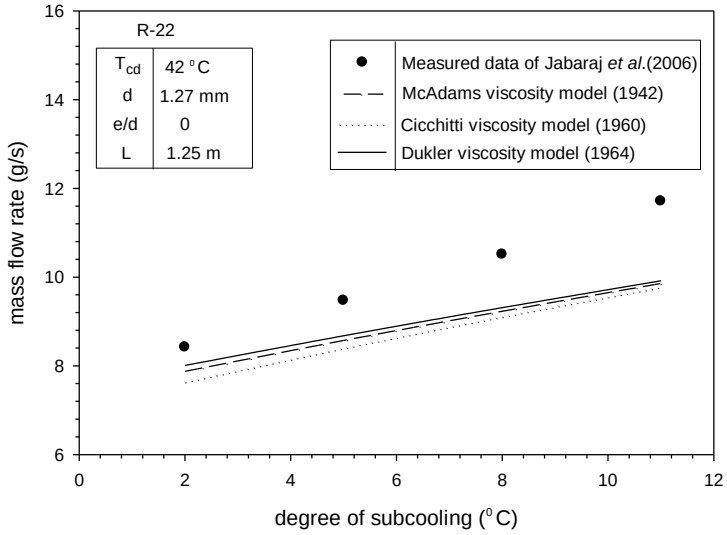

Fig.4.16 (b): Comparison of Jabaraj *et al.* (2006) experimental data with present numerical results at condenser temperature of 42 °C and length of 1.25 m for the flow of R-22.

Fig.4.16 (a) and (b) shows comparison of modelling results from present models for R-22 with Jabaraj *et al.* (2006) experimental data at different lengths. The tube diameter and condenser temperature are 1.27 mm, 42 °C respectively. The closest estimate is given by the Dukler viscosity model (1964) which gives an average error of 16.6 % for length of tube equal to 0.75 m and 11.29 % for length equal to 1.25 m.

4.1.7 Validation of mathematical model with Jabaraj *et al.*(2002) experimental data for M-20.

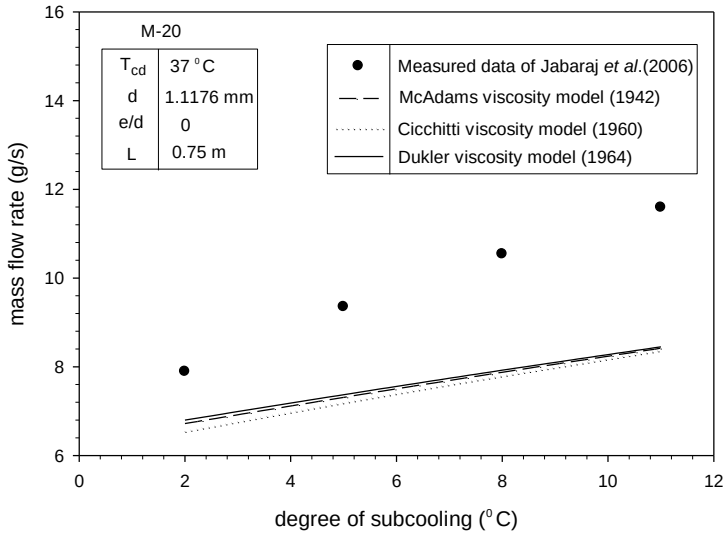

Fig.4.17 (a): Comparison of Jabaraj *et al.* (2006) experimental data with present numerical results at condenser temperature of 37 °C and length of 0.75 m for the flow of M-20.

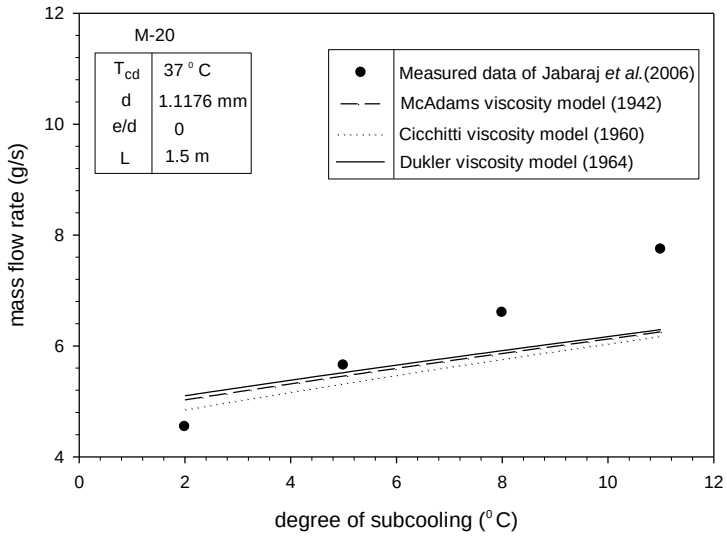

Fig.4.17 (b): Comparison of Jabaraj *et al.* (2006) experimental data with present numerical results at condenser temperature of 37 °C and length of 1.5 m for the flow of M-20.

Fig.4.17 (a) and (b) shows comparison of experimental data with present models for M-20 through capillary tube of diameter 1.1176 mm and condenser temperature of 37 °C at different lengths. Similar to R-22 the mass flow rate of M-20 increases for shorter capillary tube as compared to longer capillary length. The proportion of mass flow rate for M-20 has been found to be more than that of R-22 in same operating conditions. This is due to lower viscosity of M-20 as compared to R-22. The closest estimate is given by the Dukler viscosity model (1964) which gives an average error of 28.26 % for length of tube equal to 0.75 m and 6.45 % for length equal to 1.5 m.

.

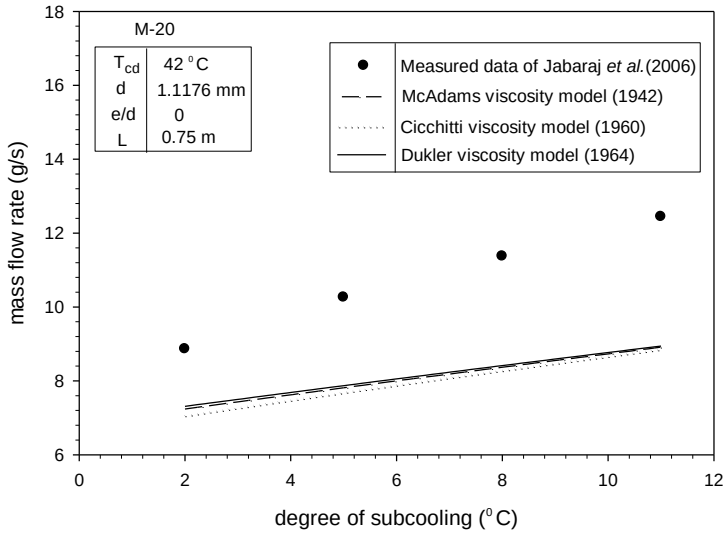

Fig.4.18 (a): Comparison of Jabaraj *et al.* (2006) experimental data with present numerical results at condenser temperature of 42 °C and length of 0.75 m for the flow of M-20.

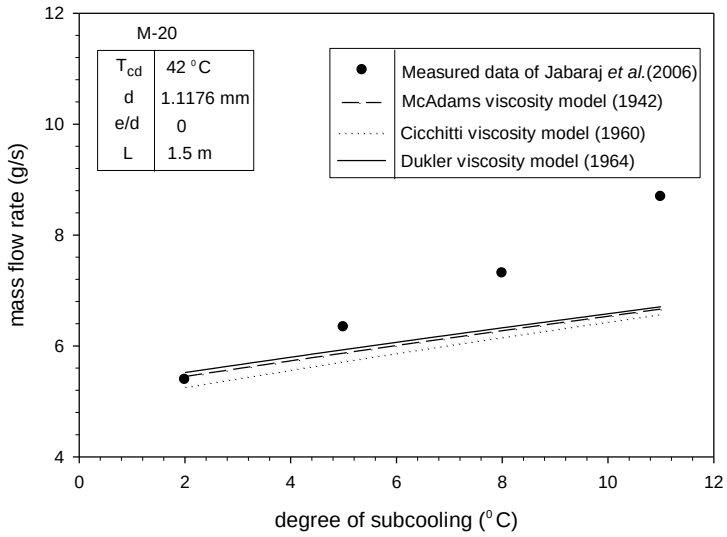

Fig.4.18 (b): Comparison of Jabaraj *et al.* (2006) experimental data with present numerical results at condenser temperature of 42 °C and length of 1.5 m for the flow of M-20.

To validate the proposed model with present experimental data, Fig.4.18 (a) and (b) has been drawn taking degree of subcooling as abscissa and refrigerant mass flow rate as ordinate. The tube diameter is 1.1176 mm and condenser temperature is 42 °C. With increase in diameter the mass flow rate of M-20 increases. The Dukler viscosity model (1964) underpredicts mass flow rate by 31.14% for length of tube 0.75 m and 12.39 % for tube length of 1.5 m from Jabaraj *et al.* (2006) experimental data generated for M-20.

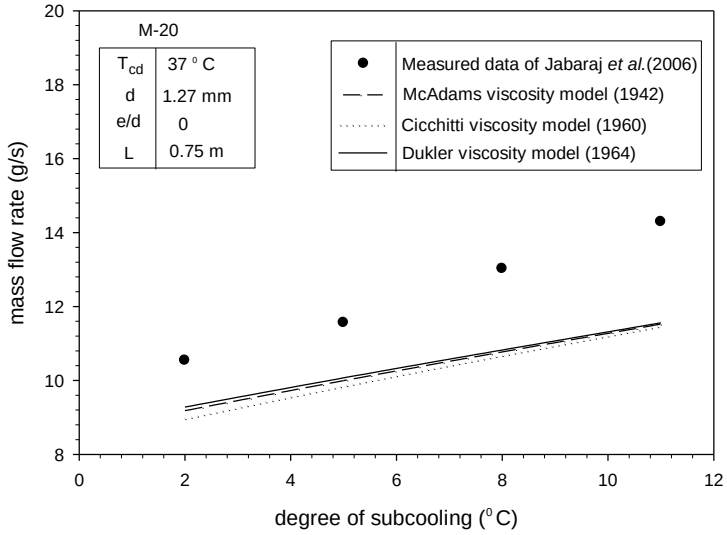

Fig.4.19 (a): Comparison of Jabaraj *et al.* (2006) experimental data with present numerical results at condenser temperature of 37 °C and length of 0.75 m for the flow of M-20.

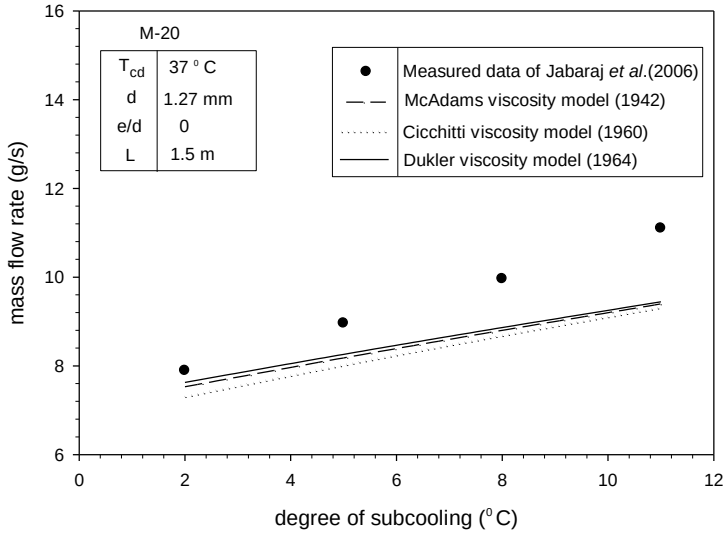

Fig.4.19 (b): Comparison of Jabaraj *et al.* (2006) experimental data with present numerical results at condenser temperature of 37 °C and length of 1.5 m for the flow of M-20.

Fig.4.19 (a) and (b) shows comparison of experimental data with present models for diameter equal to1.27 mm. It has been found that mass flow rate increases with increase in diameter of tube. This is due to the fact that pressure drop decreases with increase in diameter. The closest estimate is given by the Dukler viscosity model (1964) which gives an average error of 18.05% for length of tube equal to 0.75 m and 10.44 % for length equal to 1.5 m.

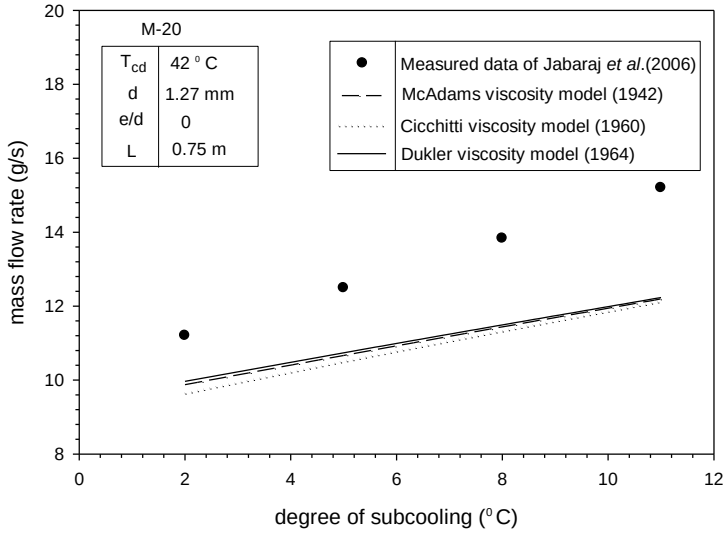

Fig.4.20 (a): Comparison of Jabaraj *et al.* (2006) experimental data with present numerical results at condenser temperature of 42 °C and length of 0.75 m for the flow of M-20.

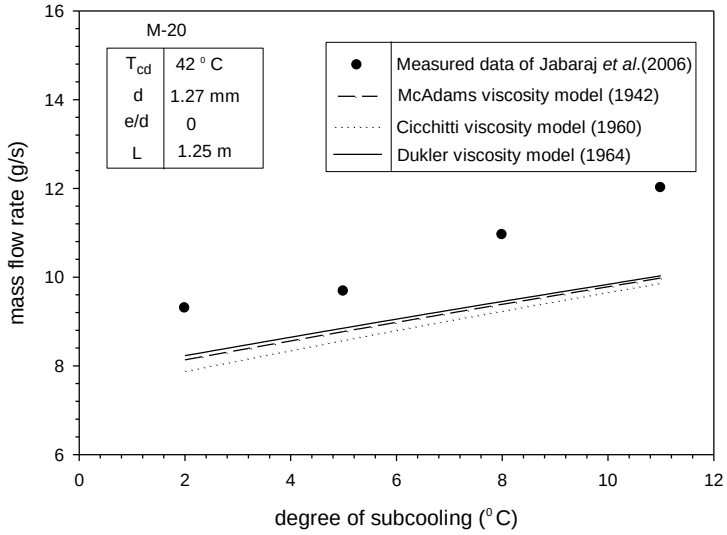

Fig.4.20 (b): Comparison of Jabaraj *et al.* (2006) experimental data with present numerical results at condenser temperature of 42 °C and length of 1.25 m for the flow of M-20.

Fig.4.20 (a) and (b) shows comparison of experimental data with present models for diameter equal to 1.27 mm and condenser temperature of 42 °C. As the condenser temperature increases the mass flow rate increases. As seen from this figure predicted results of Dukler viscosity model (1964) are in good agreement with experimental data, and give an average error of 18.31% for length of tube equal to 0.75 m and 14.49 % for length equal to 1.25 m.

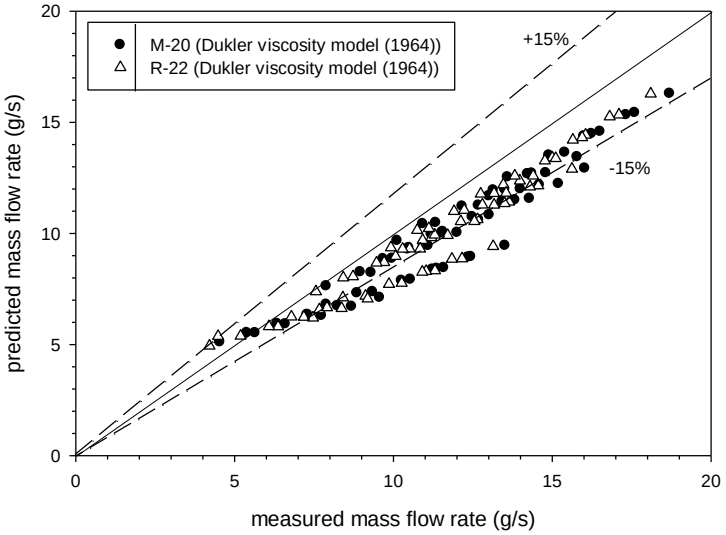

Fig.4.21: Comparison of measured mass flow rate with those predicted by model for refrigerants M-20 and R-22.

Fig.4.21 shows the comparison of experimental mass flow rates of Jabaraj *et al.* (2006) with the numerical mass flow rates predicted by the proposed model. It is observed that 80 percent

experimental data of refrigerants M-20 and R-22 acquired from the present study are predicted by the model in the deviation range of -15 % to +15 % with mean deviation of 15.95 %.

After validation simulation is done between different refrigerants with different operating conditions of pressure, temperature, subcooling, diameter. R-12, R-134a, R-600a, R-407C, R-410A, R-22, M-20 are the various refrigerants used for simulation to analyse their characteristics at various operating conditions.

4.1.8 Simulation of refrigerants M-20 and R-22 using Dukler viscosity model (1964).

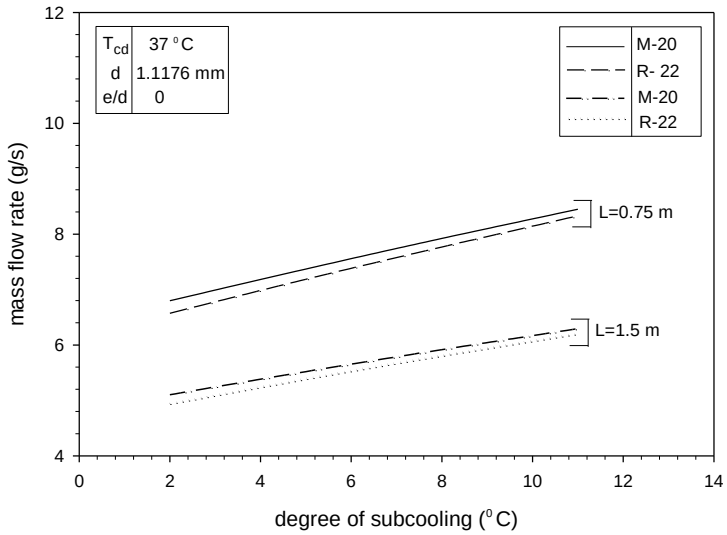

Fig.4.22 (a): Mass flow rate variation with degree of subcooling for different capillary length at 1.1176 mm diameter with condenser temperature of 37 °C.

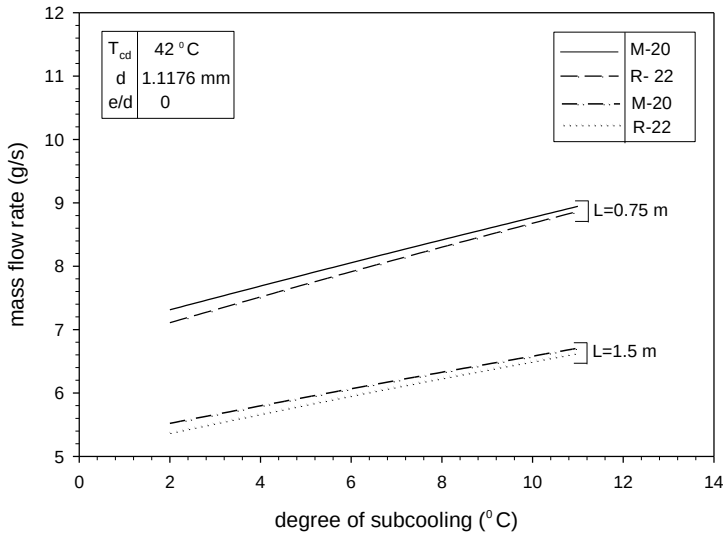

Fig.4.22 (b): Mass flow rate variation with degree of subcooling for different capillary length at 1.1176 mm diameter with condenser temperature of 42 °C.

Fig.4.22 (a) and (b) represents mass flow rate variation with respect to degree of subcooling for M-20 and R-22 at condensing temperature of 37 °C and 42 °C respectively, through capillary tube of diameter 1.1176 mm for different capillary length. M-20 shows a higher mass flow rate for given degrees of subcooling, which is 1.43-3.43% higher than that of R-22 at different degree of subcooling and lengths for condensing temperature of 37 °C. With condensing temperature of 42 °C M-20 mass flow rate is greater than R-22 by 0.89-2.86%.It is observed that mass flow rate of R-22 seems to be closer to M-20 at higher degree of subcooling and deviates at lower degree of subcooling.

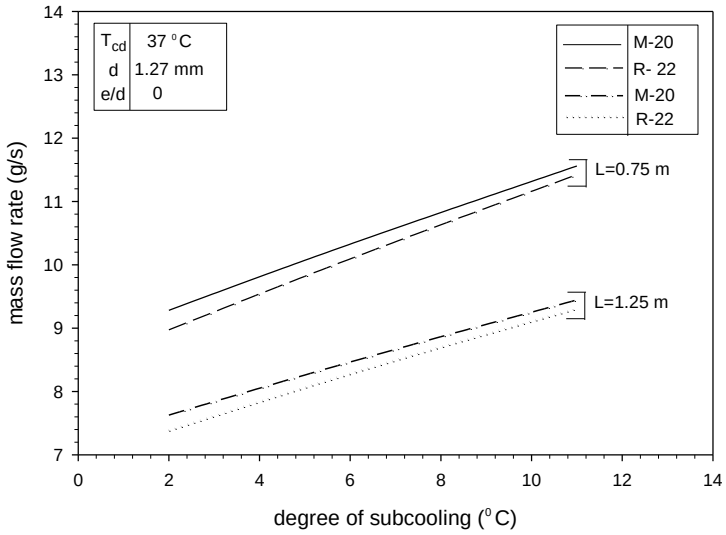

Fig.4.23 (a): Mass flow rate variation with degree of subcooling for different capillary length at 1.27 mm diameter with condenser temperature of 37 °C.

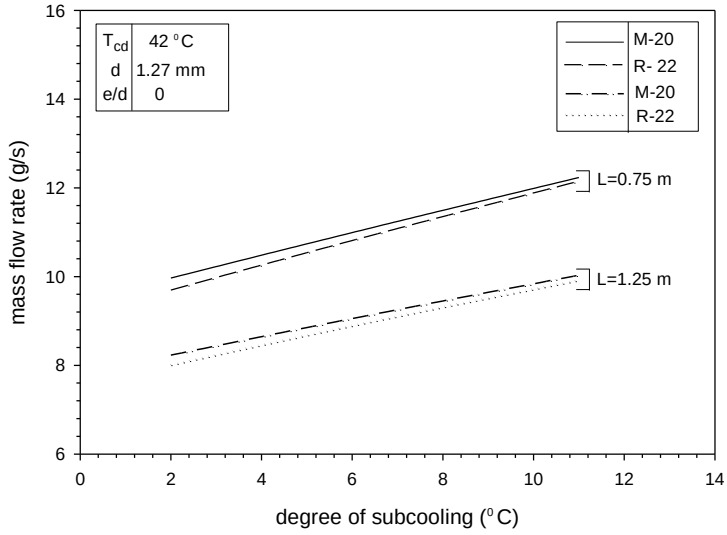

Fig.4.23 (b): Mass flow rate variation with degree of subcooling for different capillary length at 1.27 mm diameter with condenser temperature of 42 °C.

In simulation of M-20 and R-22 effect of degree of subcooling has been shown in Fig.4.23 (a) and (b). Mass flow rate is plotted against degree of subcooling at condensing temperature of 37 °C and 42 °C respectively. The tube diameter is 1.27 mm, with lengths of capillary tube as 0.75 m and 1.5 m. It is observed that with increase in diameter the mass flow rate also increases. At condensing temperature of 37 °C, M-20 shows a higher mass flow rate for given degrees of subcooling and length, which is 1.20-3.43 % higher than that of R-22. Mass flow rate for M-20 increases as condensing temperature increases to 42 °C, it is 0.68-2.79 % greater for M-20 mass flow rate is than R-22.

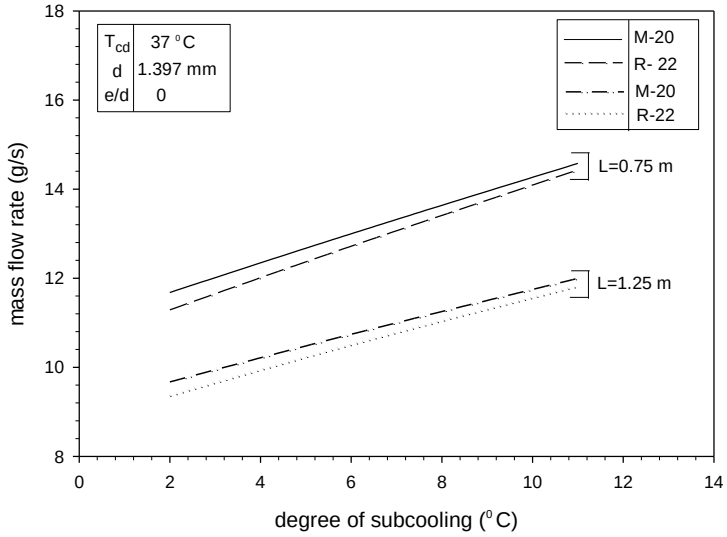

Fig.4.24 (a): Mass flow rate variation with degree of subcooling for M-20 and R-22 with different capillary length at 1.397 mm diameter with condenser temperature of 37 °C.

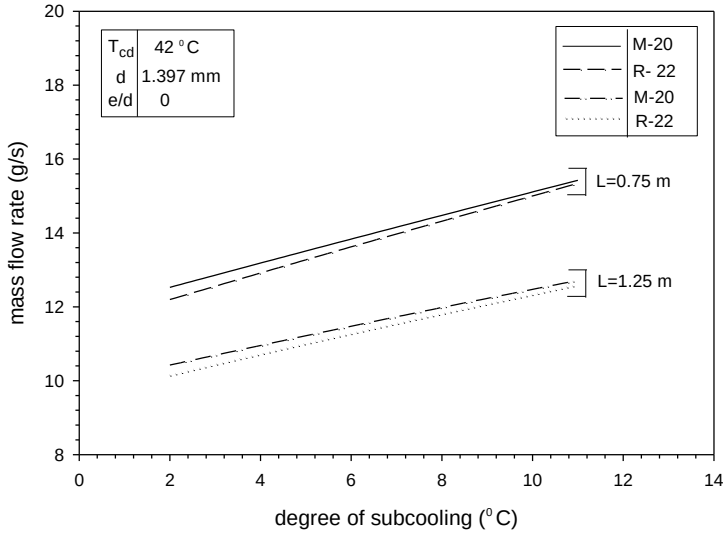

Fig.4.24 (b): Mass flow rate variation with degree of subcooling for different capillary length at 1.397 mm diameter with condenser temperature of 42 °C.

Fig.4.24 (a) and (b) plots the mass flow rate against degree of subcooling at condensing temperature of 37 °C and 42 °C respectively. With tube diameter of 1.397 mm, M-20 mass flow rate is 1.01-3.45 % higher than that of R-22 at condensing temperature of 37 °C. As above case, proportion of M-20 mass flow rate which increases with increase in condensing temperature to 42 °C is 0.54-2.72% from R-22.

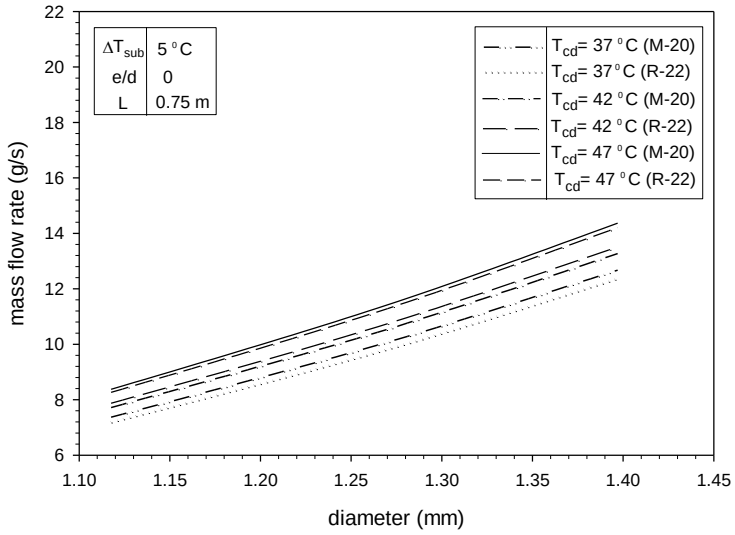

Fig.4.25: Mass flow rate variation with diameter for refrigerants M-20 and R-22 at same degree of subcooling.

Fig.4.25 represents effect of capillary tube diameter on mass flow rate for a length of 0.75 m at subcooling of 5 °C. It is found that as capillary tube diameter increases, the mass flow rate increases significantly due to reduced pressure drop. M-20 has greater mass flow rate as compared to R-22 at particular subcooling. This is due to the fact that viscosity of M-20 is less than R-22 which cause an increase in its mass flow rate. When diameter is increased from 1.1176 to 1.397 mm for condensing temperature of 37 °C mass flow rate increases by 71.94 % for M-20. Similarly for condensing temperature of 42 °C and 47 °C it increases by 71.63% and 71.55% respectively. It is predicted that M-20 mixture shows 1.19-4.31 % higher mass flow rate than that of R-22 at various diameters and condensing temperatures.

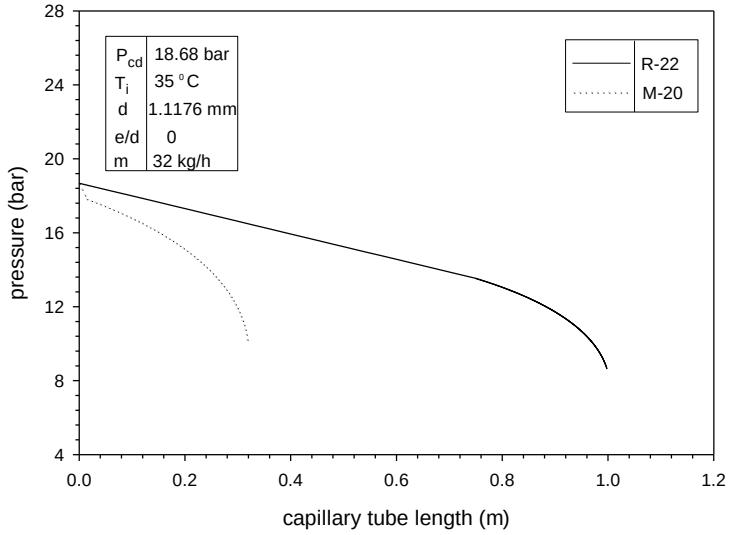

(a)

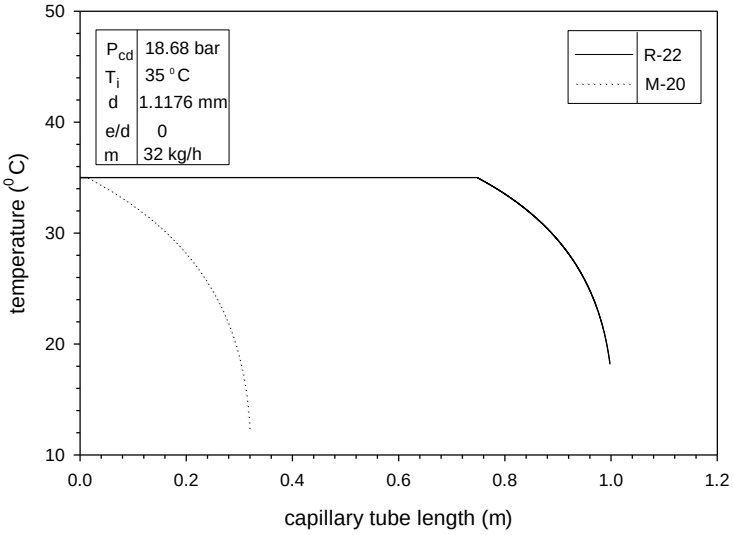

(b)

Fig.4.26: Pressure and temperature variation with capillary tube length for refrigerants M-20 and R-22, at same condenser pressure and inlet temperature to capillary tube.

Fig.4.26 represents the pressure and temperature distribution along capillary tube for refrigerants R-22 and M-20 at 18.68 bar condenser pressure and 35 °C inlet temperature to capillary tube. At these conditions R-22 has greater subcooled single phase length than M-20, as a result total capillary tube length is more than M-20.

4.1.9 Simulation of refrigerants R-410A, R-407C, M-20, R-22, R-12 and R-134a using Dukler viscosity model (1964) for R-410A, R-407C, M-20, R-22 and Cicchitti model (1960) for R-12 and R-134a.

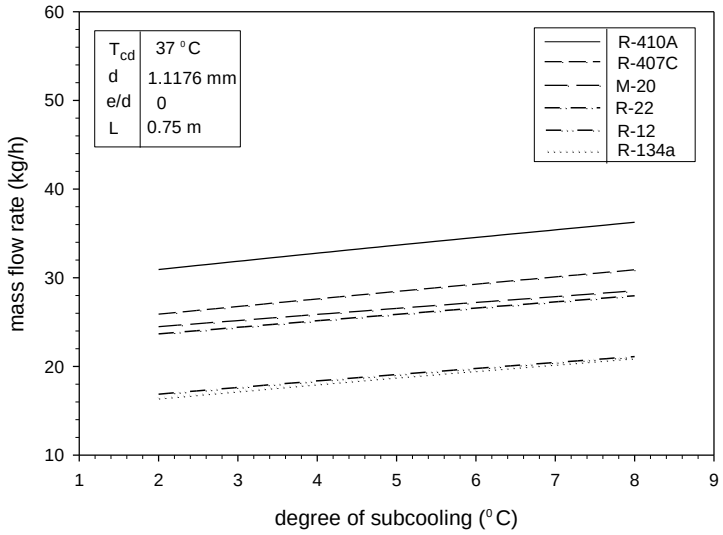

Fig.4.27: Mass flow rate variation with degree of subcooling for R410A, R-407C, M-20, R-22, R-12 and R-134a at condenser temperature of 37 °C.

Fig.4.27 shows effect of degree of subcooling. The mass flow rate is plotted against degree of subcooling for refrigerants at condensing temperature of 37 °C, diameter equal to 1.1176 mm and length of 0.75 m.

In simulation following observations are made from Fig.4.27.

- Mass flow rate on an average is maximum for R-410A as compared to other refrigerants for given level of subcooling. This is due to the fact that saturation temperature of R-410A is greater than other refrigerants.
- R-410A has 73.1-88.5% greater mass flow rate from R-134a and from R-12 its value is greater by 71.7-83.3%.
- While comparing with R-407C its value is 17.3-19.4% greater.
- R-22 lags behind by 29.6-30.6% of mass flow rate and from M-20 mass flow rate of R-410A is higher by 26.3-27%.

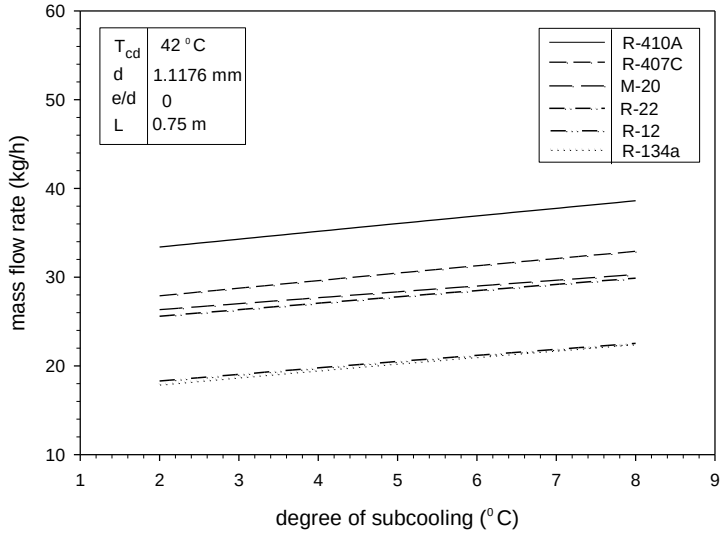

Fig.4.28: Mass flow rate variation with degree of subcooling for R410A, R-407C, M-20, R-22, R-12 and R-134a at condenser temperature of 42 °C.

Fig.4.28 describe the mass flow rate variation with respect to degree of subcooling for refrigerants at condensing temperature of 42 °C, diameter of 1.1176 mm and length equal to 0.75 m. It is observed that with increase in condenser temperature mass flow rate increases for each refrigerant.This is due to the fact with increase in condensing temperature the length of subcooled single phase region increases which result an increase mass flow rate. From figure it is cleared that mass flow rate is maximum for R-410A as compared to other refrigerants for given level of subcooling.With increase in condenser temperature mass flow rate for all refrigerants will also increase. R-410A, R407C, M-20, R-22, R-12 and R-134a mass flow rate values get increase by 6.93 %, 7.11 %, 6.88 %, 7.49 % 7.58 %, 8.26 % respectively.

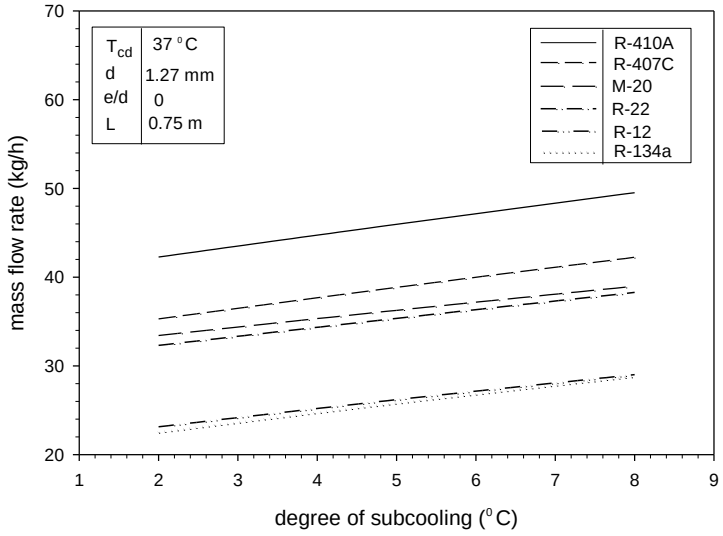

Fig.4.29: Mass flow rate variation with degree of subcooling for R410A, R-407C, M-20, R-22, R-12 and R-134a with condenser temperature of 37 °C and diameter of 1.27 mm.

Fig.4.29 shows effect of mass flow rate with degree of subcooling for refrigerants at condensing temperature of 37 °C, diameter of 1.27 mm and length of 0.75 m. With increase in capillary tube diameter the mass flow rate increases due to decrease in pressure drop. It can be seen that the average value of mass flow rate is maximum for R-410A as compared to other refrigerants for given level of subcooling. R-410A has greater average value of mass flow rate from R-134a, R-12, R-407C, R-22 and M-20 by 79.85 %, 76.70 %, 18.45 %, 30.05 % and 26.7 % respectively.

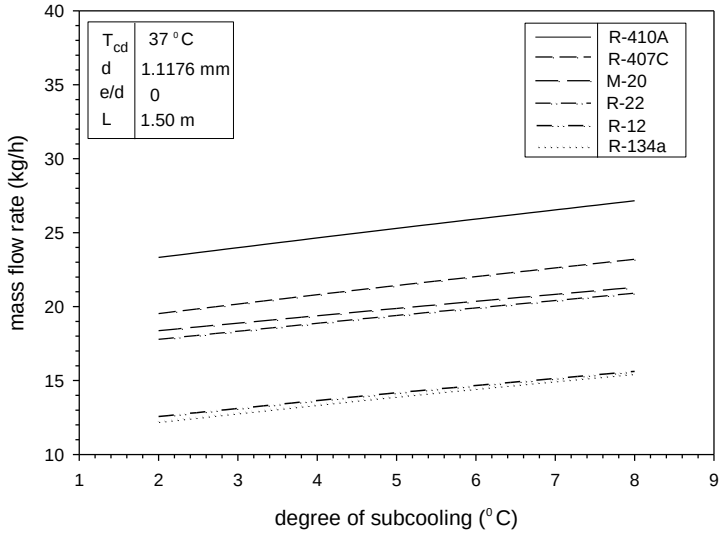

Fig.4.30: Mass flow rate variation with degree of subcooling for R410A, R-407C, M-20, R-22, R-12 and R-134a with condenser temperature of 37 °C and diameter of 1.1176 mm.

Fig.4.30 shows mass flow rate variation with respect to degree of subcooling for refrigerants at condensing temperature of 37 °C, diameter of 1.1176 mm and length of 1.50 m. From graph it can be seen that with increase in length of capillary tube the amount of refrigerant flowing through the tube will decrease at same operating conditions. According to flow characteristics of R-410A, the average value of mass flow rate is maximum for R-410A as compared to other refrigerants for given level of subcooling.

R-12 and R-134a have almost same increase in mass flow rate with increase in degree of subcooling. They slightly diverge at lower subcooling and coincide at higher subcooling. Mass flow rate for R-410A on average is greater from R-134a by 83.2 %. From R-12 flow rate for R-410A is greater by 79.7 %. Similarly from R-407C, R-22 and M-20 its value is 18.45 %, 30.45 % and 27.15 % higher respectively.

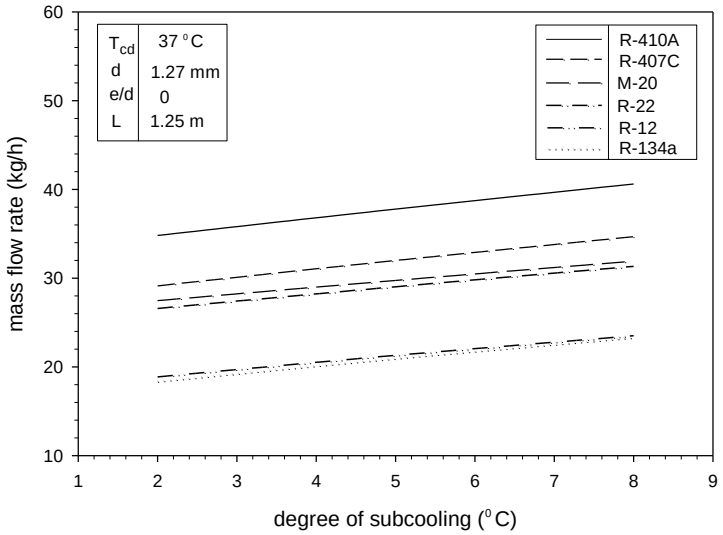

Fig.4.31: Mass flow rate variation with degree of subcooling for R410A, R-407C, M-20, R-22, R-12 and R-134a with condenser temperature of 37 °C and diameter of 1.27 mm.

Fig.4.31 shows effect of degree of subcooling on mass flow rate for refrigerants at condensing temperature of 37 °C, diameter of 1.27 mm and length of 1.25 m. At same operating conditions, with increase in length the increment in mass flow rate proportion gets reduced due to increase in pressure drop in capillary tube.

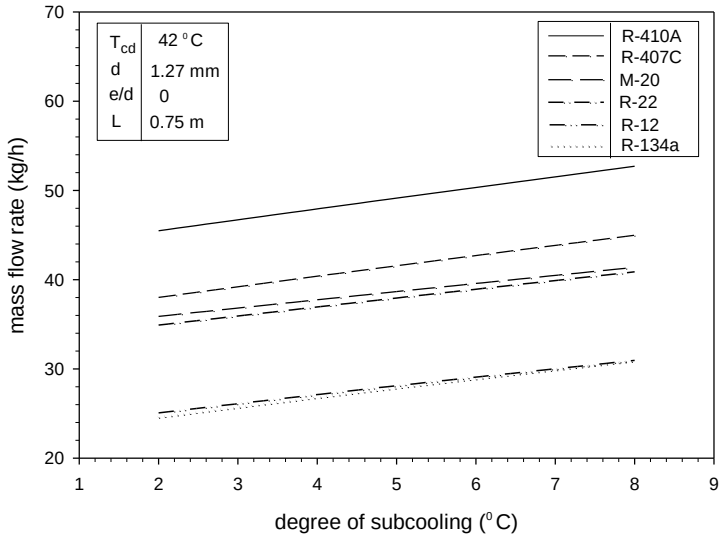

Fig.4.32: Mass flow rate variation with degree of subcooling for R410A, R-407C, M-20, R-22, R-12 and R-134a with condenser temperature of 42 °C and diameter of 1.27 mm.

In simulation of refrigerants R410A, R-407C, M-20, R-22, R-12 and R-134a as shown in Fig.4.32 mass flow rate is taken as ordinate and degree of subcooling as abscissa at condensing temperature of 42 °C, diameter of 1.27 mm and length of 0.75 m. With increase in condenser temperature the subcooled liquid length increases and two-phase region length decreases. But the increase in

subcooled liquid region is more which result in total length.

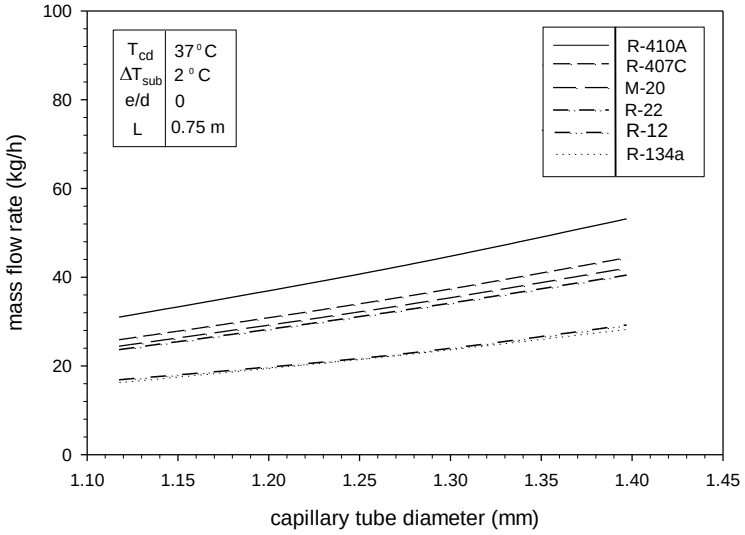

Fig.4.33: Mass flow rate variation with capillary tube diameter for R410A, R-407C, M-20, R-22, R-12 and R-134a at condenser temperature of 37 °C with subcooling of 2 °C.

Fig.4.33 shows mass flow rate variation with respect to diameter of capillary tube at fixed length of 0.75 m, condenser temperature of 37 °C and subcooling of 2 °C. It has been found that at particular condenser temperature mass flow rate start increases with increase in diameter. This is due to the fact that resistance offer to refrigerant flow decreases which result in increase mass flow rate through capillary tube. From results, it is cleared that R-12 and R-134a have almost same increase in mass flow rate. R-22, M-20 and R-407C are seems to be close to each other at smaller diameter but they start diverging from each other at higher diameter.

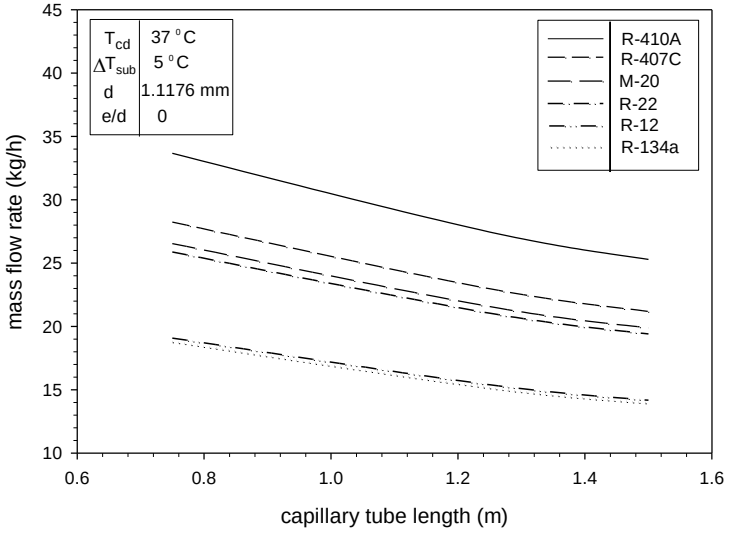

Fig.4.34: Mass flow rate variation with capillary tube length for R410A, R-407C, M-20, R-22, R-12 and R-134a at 1.1176 mm diameter with same condenser temperature and subcooling.

Fig.4.34 shows effect of capillary tube length. Mass flow rate is plotted against length of capillary tube at condensing temperature of 37 °C, subcooling of 5 °C and diameter of 1.1176 mm. It is cleared from figure that capillary tube length start decreasing with increase in mass flow rate. This is because with increase in length pressure drop also increases, so to maintain constant pressure drop mass flow rate must decrease.

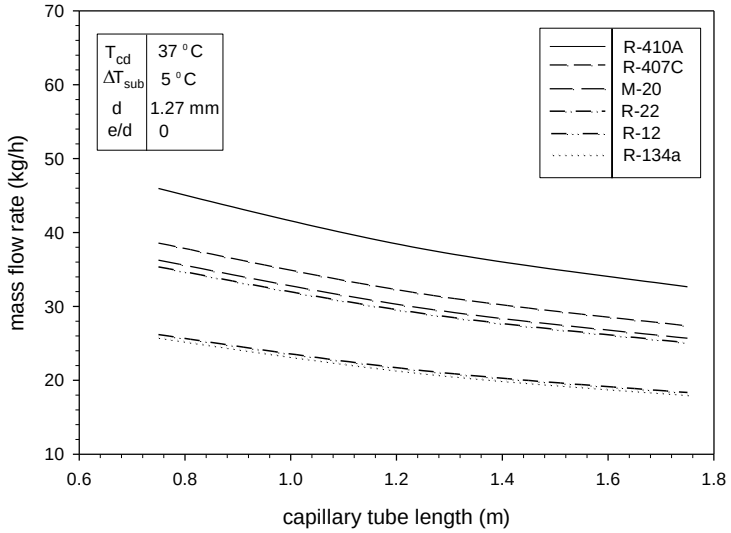

Fig.4.35: Mass flow rate variation with capillary tube length for R410A, R-407C, M-20, R-22, R-12 and R-134a at 1.27 mm diameter with same condenser temperature and subcooling.

Fig.4.35 shows mass flow rate variation with respect to length of capillary tube. From Fig.4.34 and 4.35 it is observed that with increase in diameter from 1.1176 to 1.27 mm at same conditions of condenser temperature and subcooling mass flow rate increases. This is due to the fact that the pressure drop of refrigerant flowing through adiabatic capillary tube decreases due to less restriction to the flow of refrigerant through large diameter capillary tube. But at same time mass flow rate will decrease with increase in length of capillary tube as depicted in Fig.4.34 and 4.35.The mass flow rate for R-410A, R-407C, M-20, R-22, R-12 and R-134a increases by 34.68 %, 34.87 %, 34.87 %, 34.89 %,35.34 % and 35.36 % respectively when diameter increases from 1.1176 to 1.27 mm.

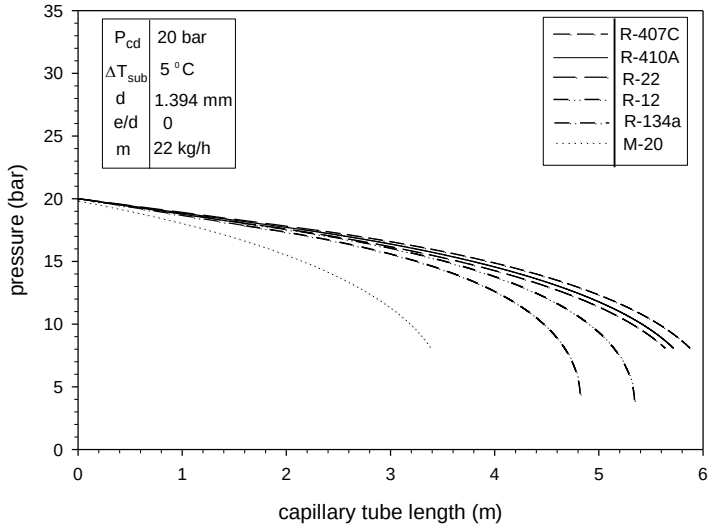

Fig.4.36: Pressure variation along capillary tube length for refrigerants R410A, R-407C, M-20, R-22, R-12, R-134a at same condenser pressure and subcooling to capillary tube.

Fig.4.36 represents pressure distribution along the capillary tube for refrigerants R-410A, R-407C, R-134a, R-12, R-22 and M-20 at subcooling of 5 °C and 20 bar condenser pressure. The total pressure drop across the capillary tube for refrigerants R-410A, R-407C, R-22, M-20 are almost same but there is difference in capillary tube lengths. Similarly for R-12 and R-134a have almost same total pressure drop, but different capillary tube lengths. Since for R-407C the linear pressure drop due to frictional effects is more as compared to other refrigerants, which result in increase in single phase length and hence the total capillary tube length is longest for R-407C.

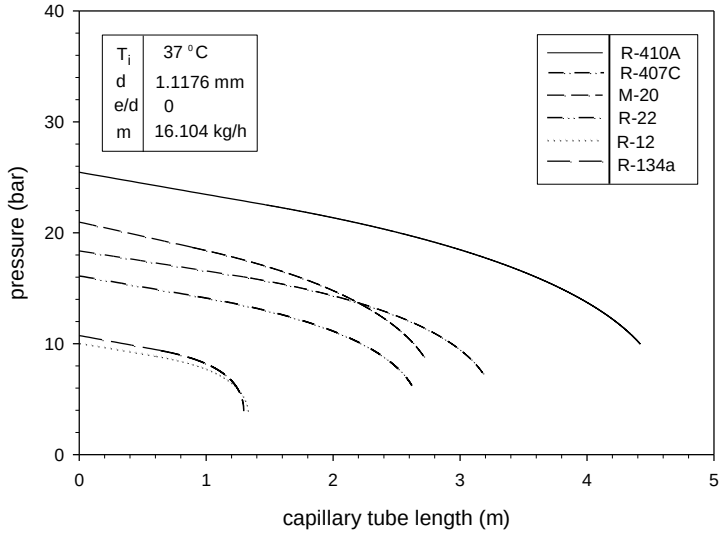

(a)

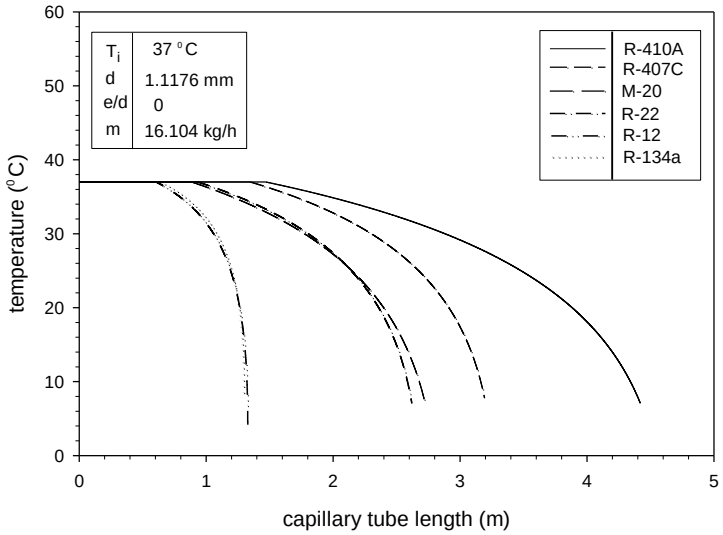

(b)

Fig.4.37: Pressure and temperature variation along capillary tube length for refrigerants R410A, R-407C, M-20, R-22, R-12, R-134a at same inlet temperature to capillary tube.

Fig.4.37 represents the pressure and temperature distribution along capillary tube for refrigerants R-410A, R-407C, R-134a, R-12, R-22 and M-20 at 37 ℃ inlet temperature. For R-410A the saturation pressure is greater than other refrigerants, as a result the single phase length and total capillary tube length is more than other refrigerants. The pressure drop for R-410A is 2.937 bar, for R-407C is 2.441 bar, for M-20 is 2.269 bar, for R-22 is 1.854 bar, for R-134a is 1.349 bar and for R-12 is 1.167 bar. Greater the pressure drop more will be the capillary tube length for particular refrigerant. The total length for R-410A is greater from R-407C, M-20, R-22, R-12, R-134a by 28.15%, 38.28 %, 40.91%, 69.48% and 70.19% respectively.

4.1.9 Simulation of refrigerants R-12, R-134a, R-407C, M-20 and R-22 using Dukler viscosity model (1964) for R-407C, M-20 and R-22 and Cicchitti model (1960) for R-12 and R-134a.

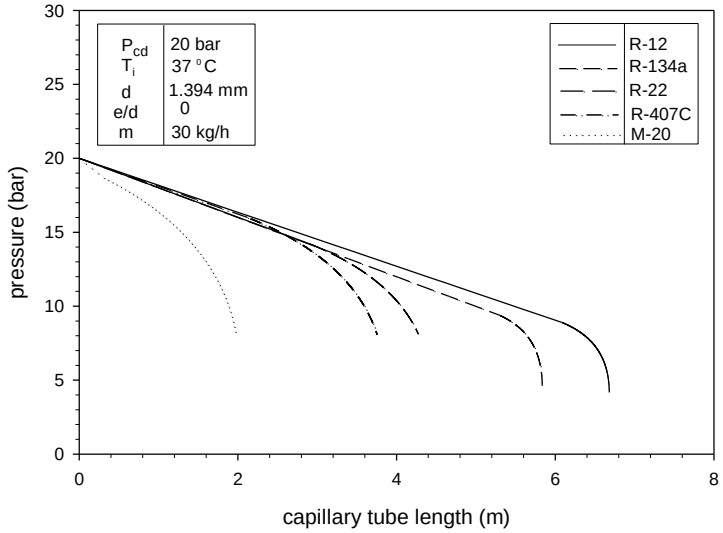

(a)

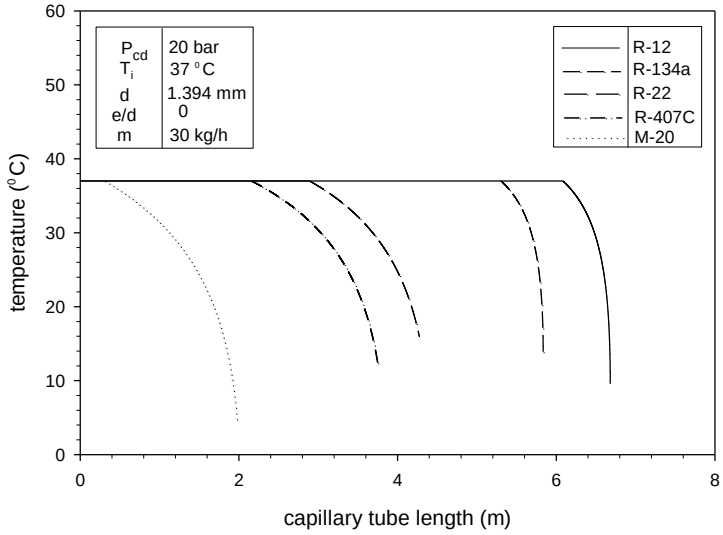

(b)

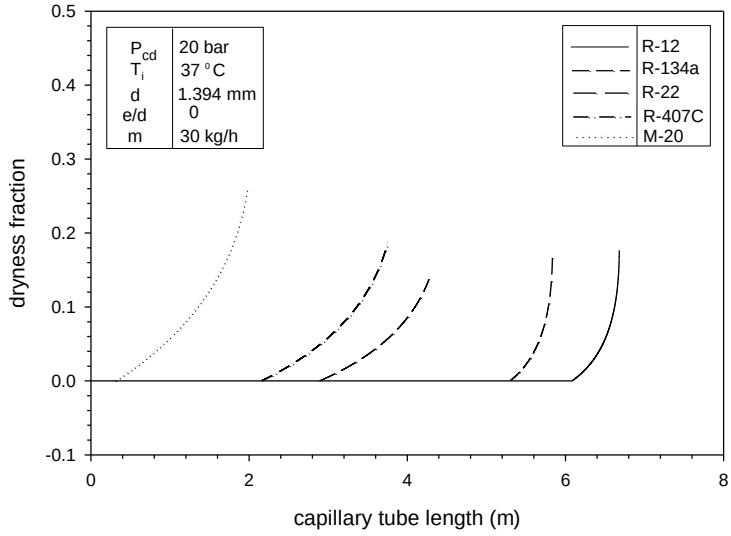

(c)

Fig.4.38: Pressure, temperature and dryness fraction variation along capillary tube length for refrigerants R-407C, M-20, R-22, R-12, R-134a at same condenser pressure and inlet temperature to capillary tube.

Fig.4.38 represents the pressure, temperature and dryness fraction distribution along capillary tube length for refrigerants at 37 °C inlet temperature to capillary tube. It is observed that at same condenser pressure and inlet temperature R-12 has more length as compare to other refrigerants. This is due to the fact that at this condenser pressure and inlet temperature R-12 has high subcooled liquid region length and high pressure drop which cause its total capillary tube length to be greater as compared to other refrigerants. R-12 has greater length from R-134a, R-22, R-407C and M-20 by 12.71 %, 36.15 %, 43.88 % and 70.57 % respectively.The dryness fraction is greater

for M-20 as compared to other refrigerants.

4.1.10 Simulation of refrigerants R-12, R-134a and R-600a using Cicchitti viscosity model (1960).

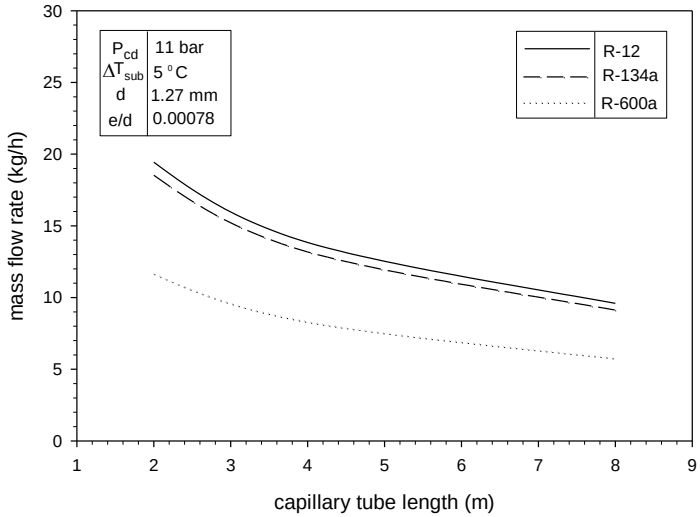

Fig.4.39: Mass flow rate variation with capillary tube length for R-12, R-123a and R-600a at 11 bar condenser pressure with 5 °C of subcooling at inlet to capillary tube.

Mass flow rate variation against capillary tube length has been shown in Fig.4.39 for 11 bar condenser pressure, subcooling of 5 °C and diameter of 1.27 mm for R-12, R-134a and R-600a. It shows that refrigerant R-12 has greater mass flow rate for given capillary tube lengths as compared to R-134a and R-600a.

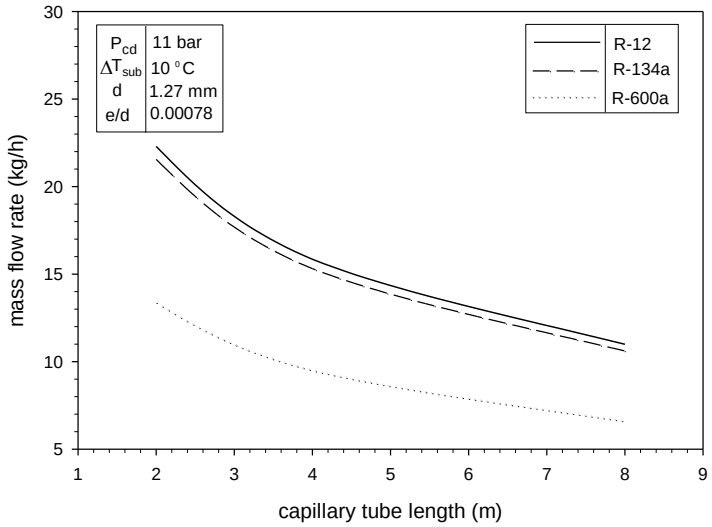

Fig.4.40: Mass flow rate variation with capillary tube length for R-12, R-134a and R-600a at 11 bar condenser pressure with 10 °C of subcooling at inlet to capillary tube.

Fig.4.40 shows mass flow rate variation against capillary tube length for 11 bar pressure, and subcooling of 10 °C. It is observed that at same pressure for R-12 the mass flow rate for subcooling of 10 °C is greater by 14.60 % on average as compared to ΔT_{sub}=5 °C. For R-134a mass flow rate on average is greater by 14.56 % from R-12 and by 16.27 % from R-600a.

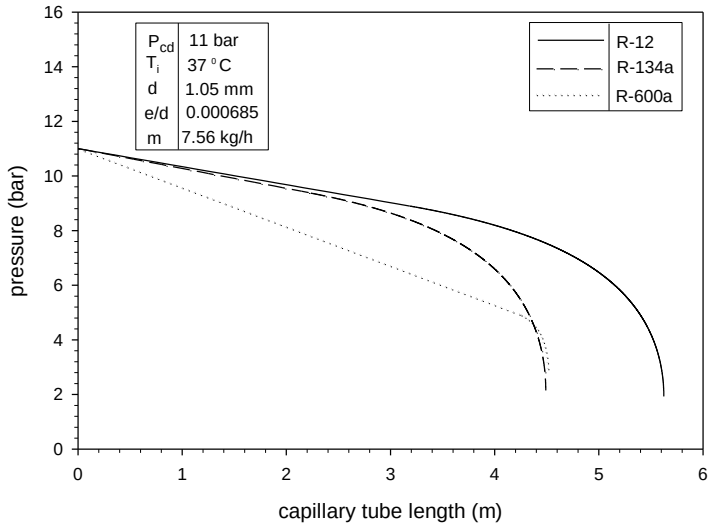

(a)

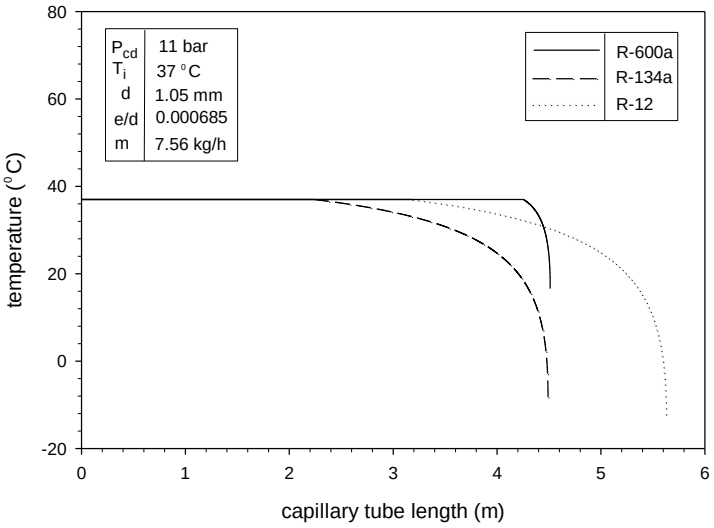

(b)

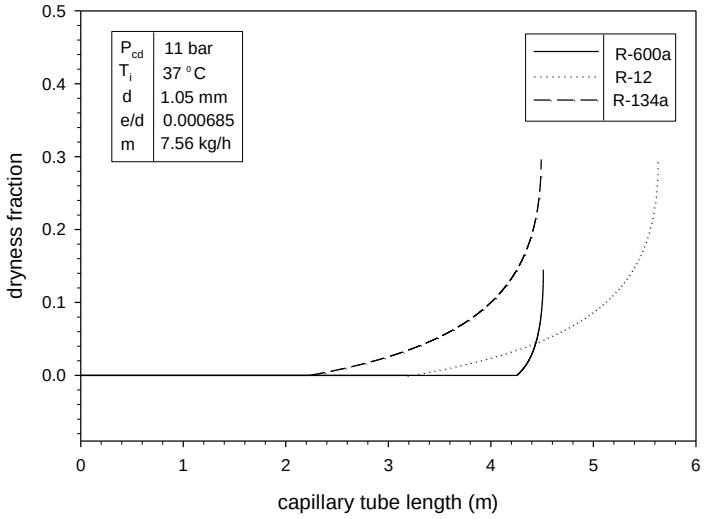

(c)

Fig.4.41: Pressure, temperature and dryness fraction variation along capillary tube length for R-12, R-134a and R-600a at same condenser pressure and inlet temperature to capillary tube.

Fig.4.41 has been drawn to depict pressure, temperature and dryness fraction distribution along capillary tube length for condenser pressure of 11 bar and inlet temperature of 37 °C to capillary tube. The tube diameter is equal to 1.05 mm. In study it is observed that R-12 and R-134a has same pressure drop but different tube lengths.R-12 has high capillary tube length as compared to R-600a and R-134a.This is because R-12 has high subcooled liquid region length.

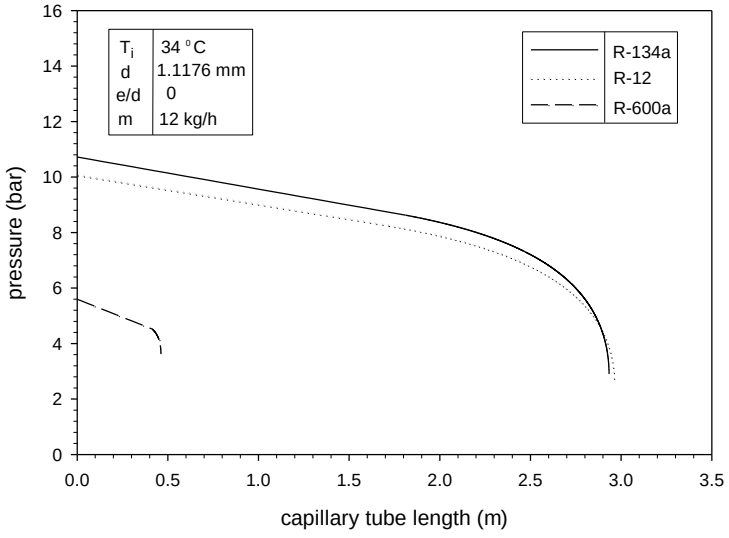

Fig.4.42: Pressure variation along capillary length for R-134a, R-12 and R-600a at same inlet temperature to capillary tube.

Fig.4.42 shows pressure distribution along capillary tube length for inlet temperature of 37 °C and diameter of 1.1176mm for refrigerants R-12, R-134a and R-600a. In study it is observed that the

condenser pressure is more for R-134a but length is more for R-12.This is because pressure drop for R-12 is more, which result in high capillary tube length as compare to R-134a and R-600a.

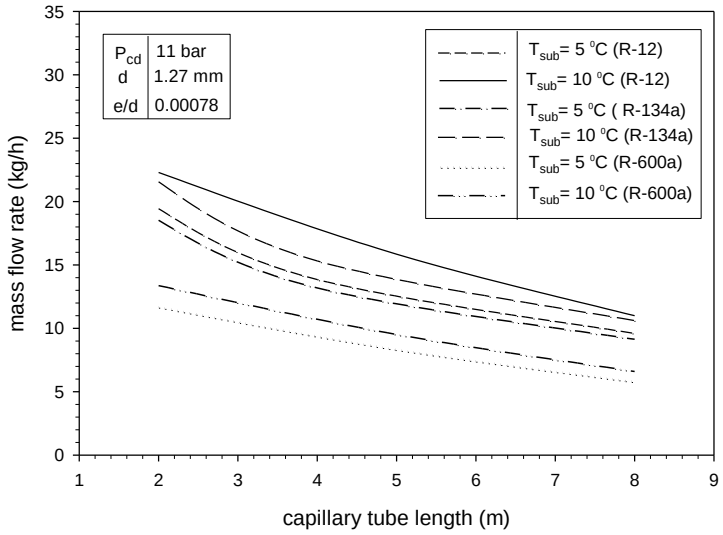

Fig.4.43: Mass flow rate variation along capillary tube length for R-12, R-134a and R-600a at same condenser pressure.

Fig.4.43 shows mass flow rate variation with capillary tube length for condenser pressure of 11 bar and diameter of 1.27 mm. In simulation of R-12, R-134a and R-600a it is observed that R-12 has high mass flow rate as compared to R-134a and R-600a for both ΔT_{sub}=5 °C and ΔT_{sub}=10 °C. The mass flow rate for R-12 is greater by average value of 12.74 % for ΔT_{sub}=10 °C as compared to ΔT_{sub}=5 °C. For R-134a its value leads by 16.27 %, whereas for R-600a it is greater by average value of 14.48 %.

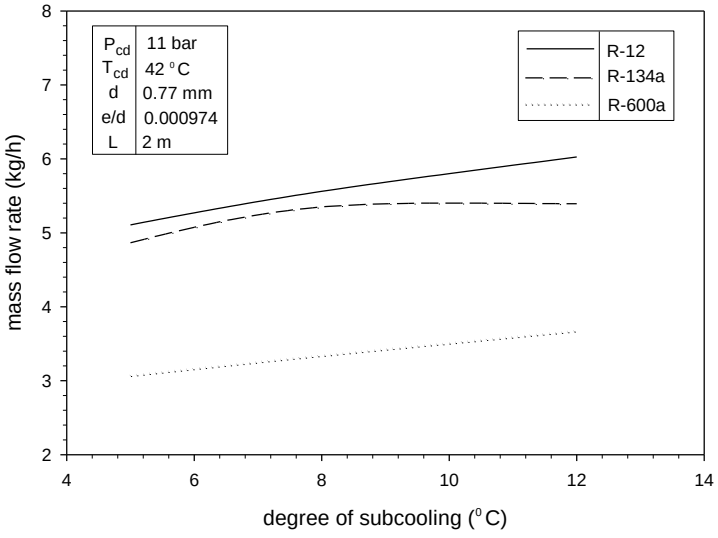

Fig.4.44: Mass flow rate variation with respect to degree of subcooling for R-12, R-134a and R-600a at same condenser pressure and temperature.

Mass flow rate is taken as ordinate and degree of subcooling is taken as abscissa as shown in Fig.4.44 at condensing pressure and temperature of 11 bar and 42 °C respectively. Results revealed that R-12 has high mass flow rate for given degree of subcooling as compared to R-134a and R-600a. R-12 has greater mass flow rate by average value of 7.01 % from R-134a and by average value of 6.57% from R-600a

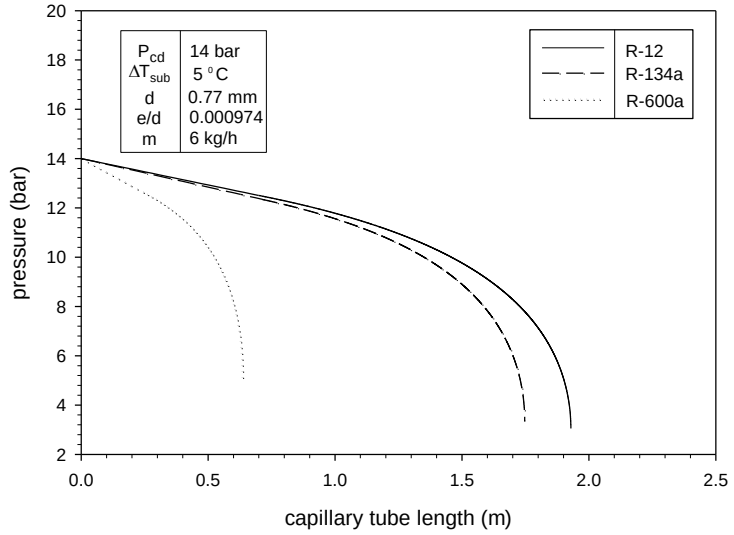

(a)

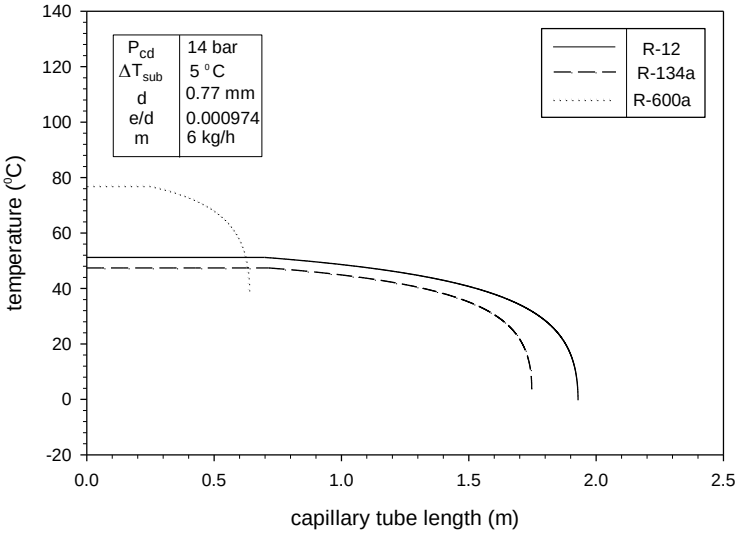

(b)

Fig.4.45: Pressure and temperature variation along capillary tube length for R-12, R-134a and R-600a at same condenser pressure and same degree of subcooling.

Fig.4.45 describe the pressure and temperature distribution along capillary tube length at same condenser pressure of 14 bar and subcooling of 5 °C. For same condenser pressure and subcooling the pressure drop for R-12 is high from R-134a and R-600a which results in large total capillary tube length as compared to R-134a and R-600a. Here Fig. 4.45 (b) shows that exit temperature for refrigerant R-12 and R-134a is almost same, however the exit temperature of R-600a is much higher. So it can be said that flow characteristics of R-12 and R-134a are almost same at same condenser pressure and degree of subcooling at inlet of capillary tube.

4.1.11 Simulation of refrigerants R-22, R-407C and R-410A using Dukler viscosity model (1964).

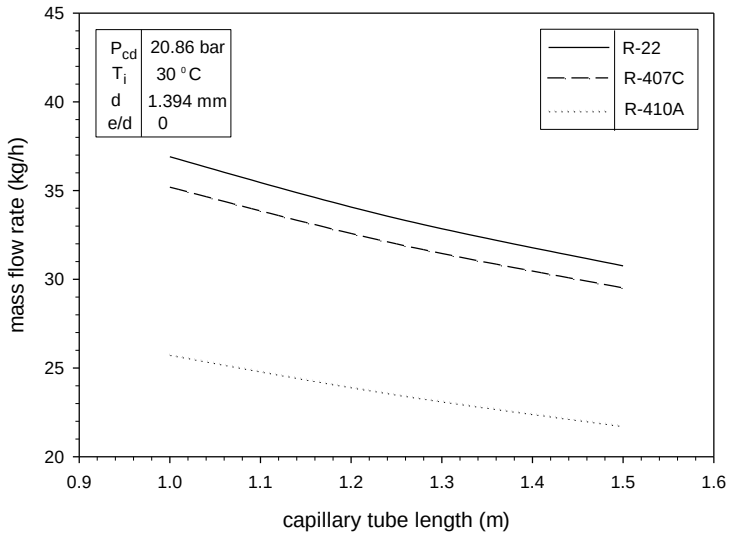

Fig.4.46: Mass flow rate variation along capillary tube length for R-22, R-407C and and R-410A at same condenser pressure and inlet temperature to capillary tube.

Fig.4.46 shows mass flow rate variation with respect to capillary tube length for three refrigerants R-22, R-407C and R-410A at inlet temperature of 30 °C and condenser pressure of 20.86 bar for diameter 1.394 mm. From graph it is cleared that as the length increases mass flow rate decreases because with increase in length pressure drop also increases, so to maintain constant pressure drop mass flow rate must also decrease. R-22 has greater mass flow rate for give lengths of capillary tube.This is due to the fact that R-22 has greater pressure drop as compared to R-407C and R-410A.Mass flow rate for R-22 on an average increases by 4.34%, 29.78 % from R-407C and R-410A respectively.

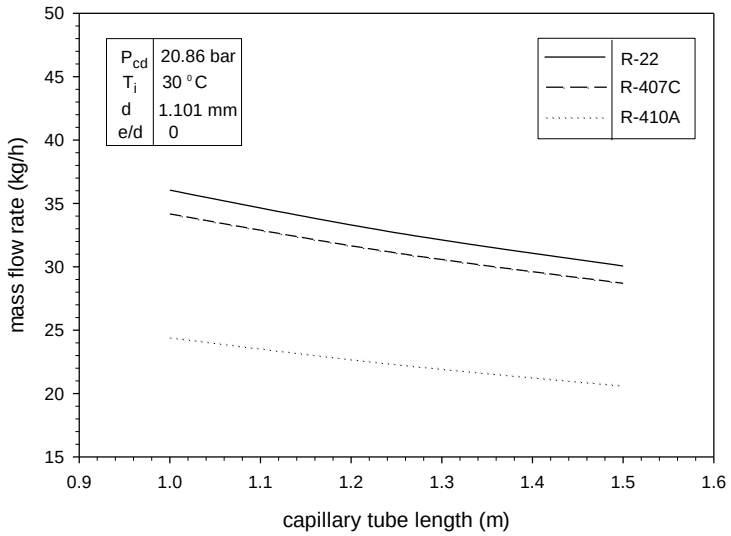

Fig.4.47: Mass flow rate variation with capillary tube length for R-22, R-407C and R-410A at same condenser pressure and inlet temperature to capillary tube.

Fig.4.47 shows mass flow rate variation with respect to capillary tube length for three refrigerants R-22, R-407C and R-410A for same pressure and inlet temperature of 20.86 bar and 30 °C respectively, with diameter of 1.101 mm. Averagely, mass flow rate for R-22 increases by 4.34 % from R-407C and by 29.78 % from R-410A.With decrease in diameter the mass flow rate decreases for each refrigerant. For R-22 it decreases by 2.85 %, for R-407C it decreases by 2.34 % and for R-410A it decreases by 5.34%.

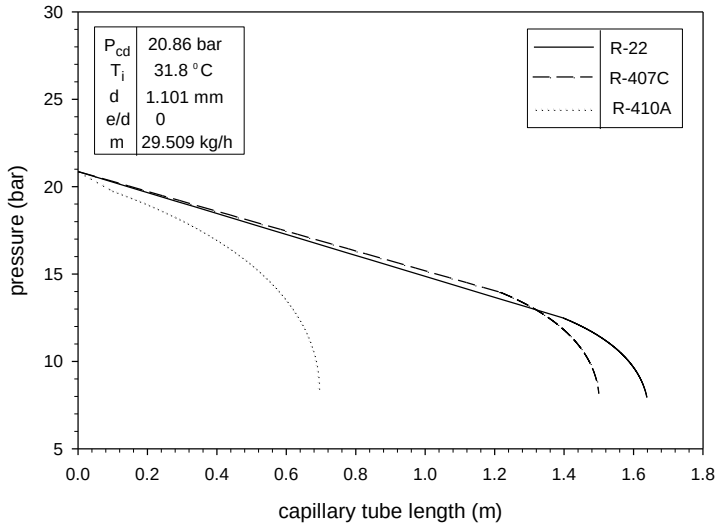

(a)

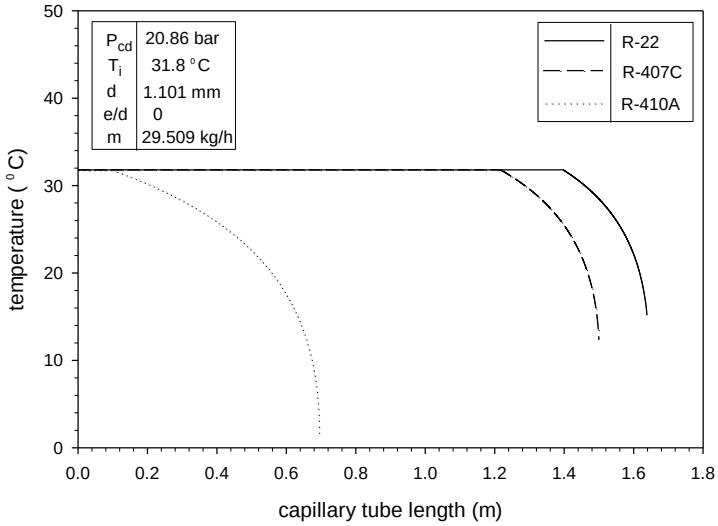

(b)

Fig.4.48: Pressure and temperature variation with capillary tube length for R-22, R-407C and R-410A at same condenser pressure and inlet temperature to capillary tube.

Fig.4.48 describe the pressure and temperature distribution along the Capillary tube for refrigerants R-22, R-407C and R-410A at same condenser pressure and temperature at the inlet of capillary tube. The total pressure drop across the capillary tube is almost same for all these refrigerants, but there is difference in capillary tube length. At a condenser pressure of 20.86 bar and inlet temperature of 31.8 °C, the degree of subcooling for R-22, R-407C and R-410A are 21.33, 15.58, 2.09 °C respectively. Since the degree of subcooling for refrigerants R-22 is highest, therefore single phase length and hence the total capillary tube length is longest for refrigerant R-22.

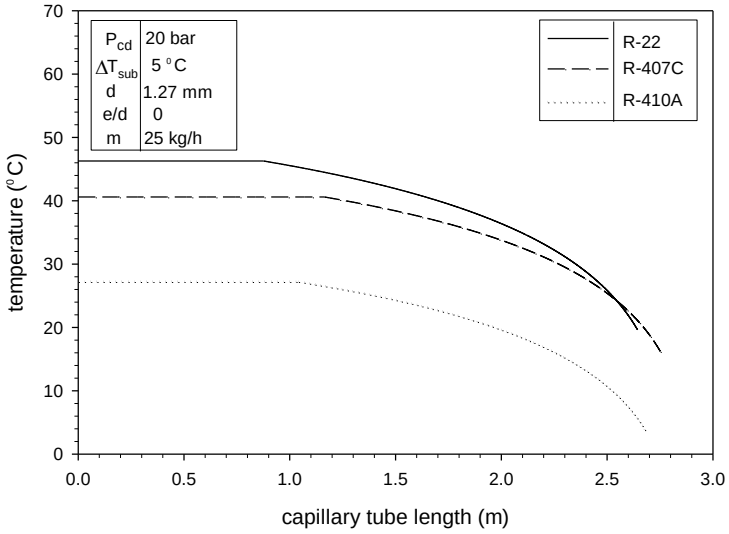

Fig.4.49: Temperature variation with capillary tube length for R-22, R-407C and R-410A at same condenser pressure and subcooling.

Fig.4.49 shows temperature distribution along capillary tube length at same condenser pressure of 20 bar and same degree of subcooling i.e ΔT_{sub}=5 °C. Here graph shows that exit temperature of R-22 is higher compared to R-407C and R-410A.Capillary tube length is more for R-407C due to large subcooled liquid region length. R-22 and R-410A has large difference in their inlet temperature to capillary tube but lengths are very near to each other. R-410A capillary tube length is more from R-22 but by little amount.

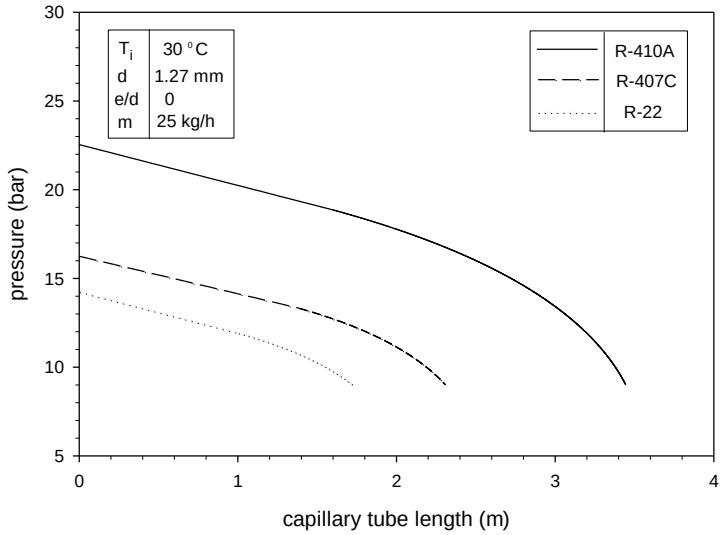

(a)

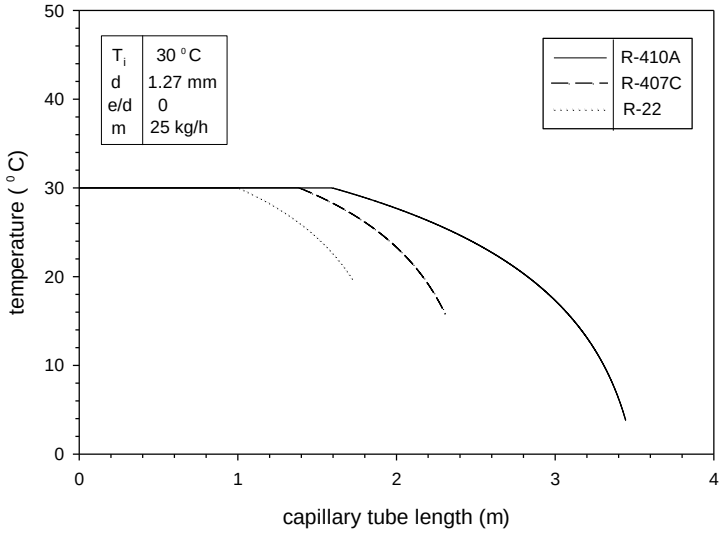

(b)

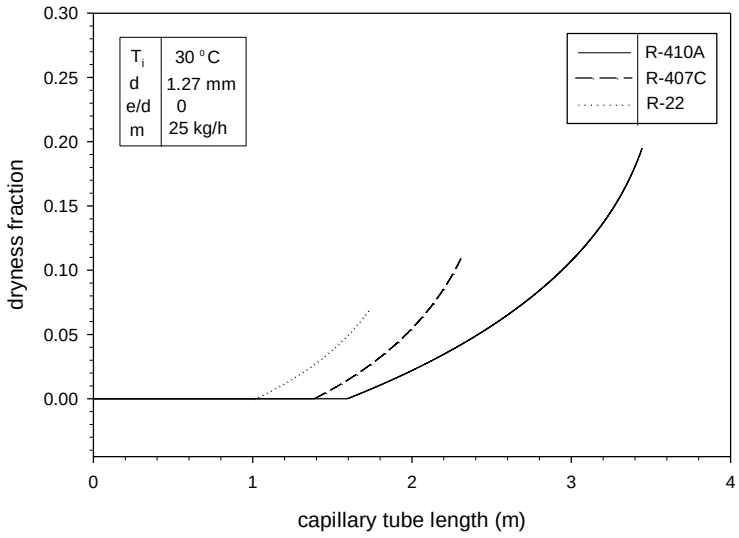

(c)

Fig.4.50: Pressure, temperature and dryness fraction variation along capillary tube length for R-22, R-407C and R-410A at same inlet temperature to capillary tube.

Fig.4.50 describe the pressure, temperature and dryness fraction distribution along the capillary tube for refrigerant R-22, R-407C and R-410A at same inlet temperature of 30 °C. At the same inlet temperature, the saturation pressure of R-410A and R-407C is higher than that of R-22. Higher pressure at capillary tube inlet results in higher pressure drop, which result an increase in capillary tube length for same mass flow rate. So, due to this capillary tube length is higher for Refrigerant R-410A and R-407C than that of R-22 at same inlet temperature and mass flow rate.

4.1.12 Simulation of refrigerants R-22, R-407C and M-20 using Dukler viscosity model (1964).

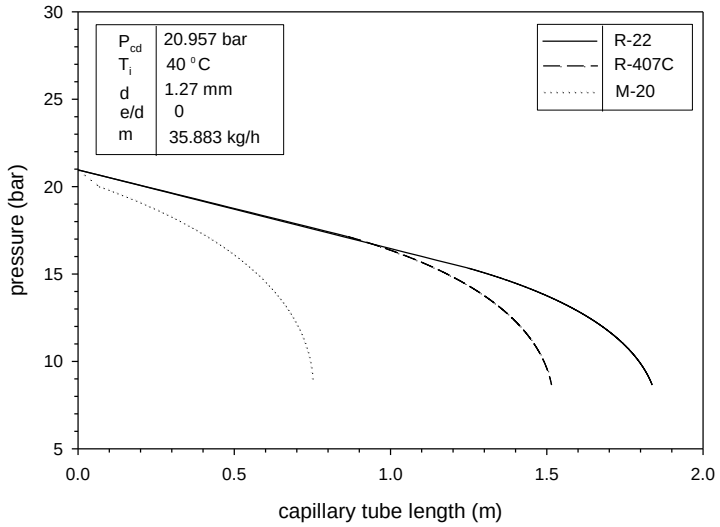

Fig.4.51: Pressure variation with capillary tube length for R-22, R-407C and M-20 with capillary tube diameter of 1.27 mm.

Fig.4.51 presents the pressure distribution along the capillary tube for refrigerants R-22, R-407C and M-20 at same condenser pressure and temperature at the inlet of capillary tube with diameter 1.27 mm. The degree of subcooling for R-22, R-407C and M-20 are 13.339, 7.585, 7.43 °C respectively. Since the degree of subcooling for refrigerants R-22 is highest, therefore single phase length and hence the total capillary tube length is longest for refrigerant R-22.

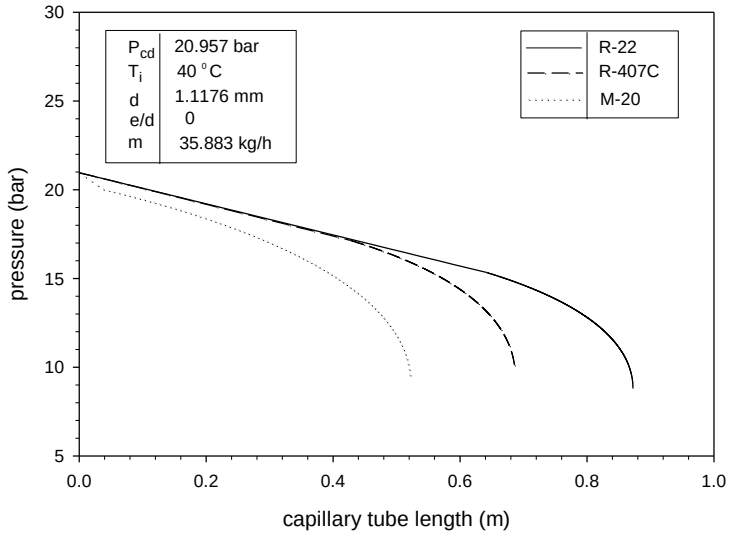

Fig.4.52: Pressure variation with capillary tube length for R-22, R-407C and M-20 with capillary tube diameter of 1.1176 mm.

Fig.4.52 presents the pressure distribution along capillary tube length for refrigerants R-22, R-407C and M-20 for diameters 1.1176 mm at same condenser pressure and inlet temperature to capillary tube. In study it is analysed that the pressure drop for all three refrigerants remain same, but there is difference in capillary tube lengths. As shown in Fig.4.51 and 4.52, for 1.27 mm diameter, value of lengths are more as compared to diameter 1.1176 mm for refrigerants R-22, R-407C and M-20 as shown in. R-22 length increases by 52.38 %, R-407C mass flow rate increases by 54.72 %, M-20 length increases by 30.52 %.All this is due to minor frictional effects take place for large diameter capillary tube.

4.1.13 Simulation of refrigerants R-12, R-134a, R-407C and R-410A using Cicchitti viscosity model (1960) for R-12 and R-134a and Dukler viscosity model (1964) for R-407C and R-410A.

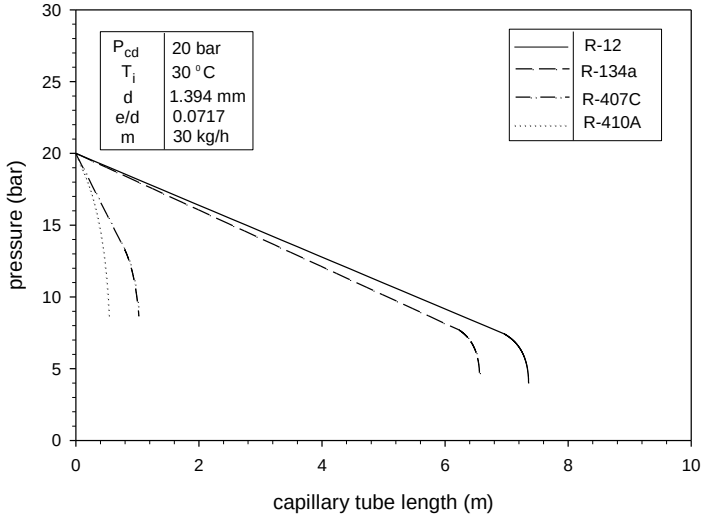

(a)

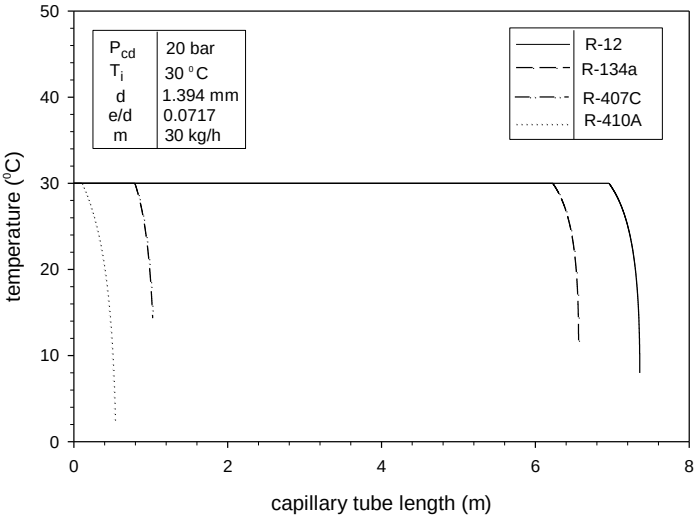

(b)

Fig.4.53: Pressure and temperature variation with capillary tube length for R-12, R-134a, R-407C and R-410A at same condenser pressure and inlet temperature to capillary tube.

Fig.4.53 represents the pressure and temperature distribution along the capillary tube for refrigerant R-22, R-134a, R-407C and R-410A at same pressure of 20 bar and, inlet temperature of 30 °C. It has been found that the degree of subcooling for R-22, R-134a, R-407C and R-410A are 43.02, 37.48, 15.59, 2.22 °C respectively. Since the degree of subcooling for refrigerants R-12 is highest, therefore single phase length and hence the total capillary tube length is longest for refrigerant R-12.

4.1.14 Simulation of refrigerants R-407C, M-20, R-12 and R-134a using Dukler viscosity model (1964) for R-407C and M-20 whereas Cicchitti model for R-12 and R-134a (1960).

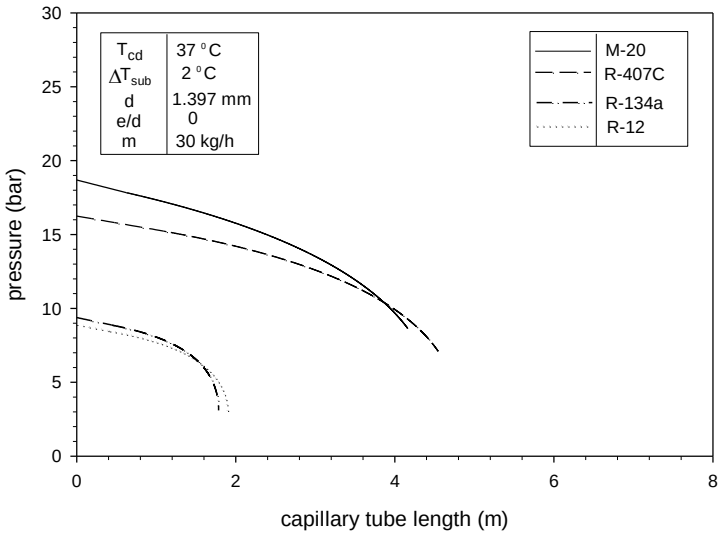

Fig.4.54: Pressure variation with capillary tube length for M-20, R-407C, R-134a and R-12 at same condenser temperature and subcooling at inlet to capillary tube.

Fig.4.54 has been drawn taking capillary tube length as abscissa and pressure as ordinate. M-20, R-407C and R-134a and R-12 at 37 °C condenser temperature with subcooling of 2 °C. At the same condenser temperature, pressure drop for these refrigerants M-20, R-407C, R-12, R-134a are as 1.104, 0.855, 0.502 and 0.438 bar respectively. M-20 has high pressure drop which results in largest total capillary tube length.

4.1.15 Simulation of refrigerants R-22, R-134a, R-407C and M-20 using Cicchitti viscosity model (1960) for R-134a whereas R-22 , R-407C and M-20 using Dukler viscosity model (1964).

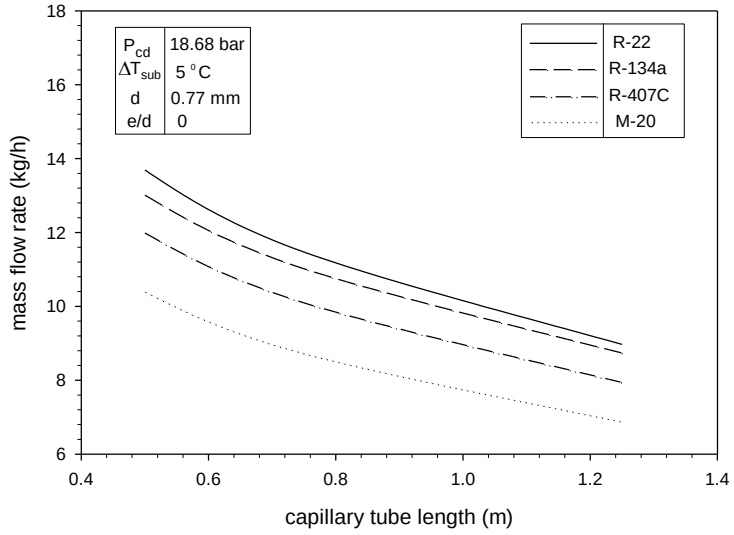

(a)

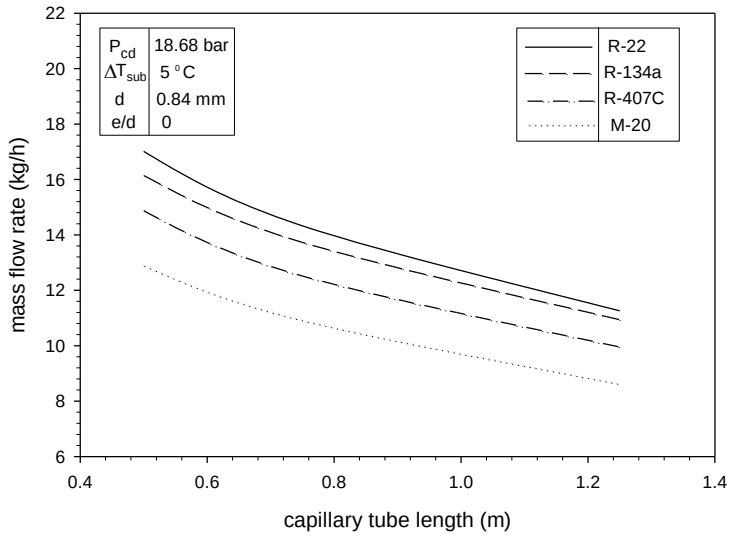

(b)

Fig.4.55: Mass flow rate variation along capillary tube length for R-22, R-134a, R-407C and M-20 at same condenser pressure and subcooling with different diameters.

Simulation of R-22, R-134a, R-407C and M-20 for diameter 0.77 and 0.84 mm has been shown in Fig.4.55. Mass flow rate is varied along capillary tube length at condenser pressure of 18.68 bar and subcooling of 5 °C. It is predicted that R-12 has greater mass flow rate as compared to other refrigerants at diameter of 0.77 mm as shown in Fig.4.55a. This is due to the fact that R-12 has higher pressure drop and subcooled liquid region length. From R-134 its mass flow rate is greater by 2.71-5.24 %, from R-407C its value is greater by 13.02-14.24% and from M-20 it is greater by 30.40-31.71%.As the diameter changes to 0.84 mm the value of mass flow rate for R-12 increases by 2.95-5.40 % from R-134a, from R-407C it increases by 13.14-14.43 % and from M-20 by 30.58-31.96 %.

Chapter - V

CONCLUSIONS AND SCOPE OF FUTURE WORK

5.1 Conclusions

The present work leads to the following conclusions:

- The mathematical model for adiabatic straight capillary tube has been developed. The proposed model can predict the capillary tube length for a given refrigerant mass flow rate. The proposed model for each capillary tube is validated with the data of previous researchers.
- The proposed model for straight capillary tube predicts the experimental data of Melo *et al.* (1999), Fiorelli *et al.* (2002), and Jabaraj *et al.* (2006) .Model predicts with experimental data of Melo *et al.* (1999) in the error band of ±15 % with mean deviation of -1.21 %, with Fiorelli *et al.* (2002) it predicts in the error band of -5 % to 7 % with mean deviation of 3.55 % and for Jabaraj *et al.*(2006) the model predicts in error band of ±15 % with mean deviation of 15.95 %. The proposed model for straight capillary tube has predicted our own experimental data very closely.
- The flow characteristics of R-12 and R-134a are close to each other at same condenser pressure and same degree of subcooling
- The flow characteristics of R-22 and R-407C are close to each other at same condenser pressure and same degree of subcooling.
- The pressure drop for refrigerants R-410A, R-407C, M-20 and R-22 are close to each other at same condenser pressure and same degree of subcooling.
- By varying the model input parameters it has been found that for all refrigerants, the mass flow rate increases with increase in degree of subcooling, increases as diameter increases, increases as condenser temperature increases, decreases as roughness increases and decreases as length increases.

5.2 Scope of future work

Over the past 10 years or so, the refrigeration industry has been going through challenging time because of continuing debate on environmental issues such as depletion of ozone, global warming and energy efficiency. In order to find suitable substitutes for conventional refrigerants various alternative refrigerant mixtures should be included in future work based on

homogenous flow mathematical model to analyse their flow characteristics through adiabatic capillary tube. This will help to find suitable refrigerants to be used in refrigeration industry. Such mixtures should also include sizing of adiabatic capillary tubes in order to evaluate how they affect performance of refrigeration cycles as well as design of cycle components.

REFERENCES

1. Bansal PK, Rupasinghe AS. 1996. An empirical model for sizing capillary tubes. *International Journal of Refrigeration* Vol. 19: 497-505.

2. Bansal PK, Rupasinghe AS. 1998. A homogenous model for adiabatic capillary tubes. *Applied Thermal Engineering* Vol. 18: 207-219.

3. Beattie, whalley. 1981. A simple two-phase frictional pressure drop calculation method *Int.J.Multiphase* flow: 83-87.

4. Bittle RR, Pate MB. 1994. A theoretical model for predicting adiabatic capillary tube performance with alternative refrigerants. *ASHRAE Transaction* Vol. 100: 52-64.

5. Bolstad MM, Jordan RC. 1948. Theory and use of the capillary tube expansion device. *Refrigerating Engineering* Vol. 56: 577-583.

6. Bolstad MM, Jordan RC. 1949. Theory and use of the capillary tube expansion device. Part II, Non–adiabatic flows. *Refrigerating Engineering* June: 577-583.

7. Cicchitti A, Lombardi C, Silvestri M. Soldaini G, Zavattarelli R. 1960. Two-phase cooling experiments-pressure drop, heat transfer and burnout measurements. *Energia Nucleare* Vol. 7: 407-425.

8. Chang SD, Ro ST. 1996. Experimental and numerical studies on adiabatic flow of HFC mixtures in capillary tubes. *International Conference, Purdue, J.E.. Braun, E.A. Groll,* 1996: 83-88.

9. Chinglupitak, Wongwises. 2011. A comparison of flow characteristics of refrigerants through adiabatic straight and helical capillary tubes. *Applied Thermal Engineering* Vol. 30: 1927-1936.

10. Choi J, Kim Y, Kim HY. 2003. Generalized correlation for refrigerant mass flow rate through adiabatic capillary tubes. *International Journal of Refrigeration* Vol. 26: 881-888.

11. Choi J, Kim Y, Chung JT. 2004. An empirical correlation and rating charts for the performance of adiabatic capillary tubes with alternative refrigerants. *Applied Thermal Engineering* Vol. 24: 29-41.

12. Churchill SW. 1977. Frictional equation apans all fluid flow regimes. *Chemical engineering* Vol. 84: 91-92.

13. Coolebrook CF. 1939. Turbulent flow in pipes with particular reference to the transition region between the smooth and rough pipes laws J. *Inst. Civ. Eng.* Vol. 11:133-156.

14. Cooper L. 1957. Simple selection method for capillaries derived from physical flow conditions. *Refrigerating Engineering* July: 37-41.

15. Dudley JC. 1962. A photographic study of the two phase flow of Freon in small bore tubes. *MSc Thesis,University of Wisconsin.*

16. Dukler AE, Wicks M, Cleveland RG. 1964. Frictional pressure drop in two-phase flow part A and B. *AIChE Journal* Vol. 10: 38-51.

17. Fiorelli FAS, Huerta AAS, Silvares OM. 2002. Experimental analysis of refrigerant mixtures flow through adiabatic capillary tubes. *Experimental Thermal and Fluid science* Vol. 26: 499-512.

18. Hopkins NE. 1950. Rating the Restrictor Tube. *Refrigerating Engineering*: 1087-1095.

19. Jabaraj DB, Kathirvel AV, Lal DM. 2006. Low characteristics of FFC407C/HFC600a/HC290 refrigerant mixture in adiabatic capillary tubes. *Applied thermal Engineering* Vol. 26: 1621-1628.

20. Jung D, Park C, Park B. 1999. Capillary tube selection for HCFC22 alternatives. *International Journal of Refrigeration.* Vol. 22: 604-614.

21. Kim Y, O'Neal DL. 1994. The effect of oil on the two phase critical flow of refrigerant R-134a through short tube orifices. *International Journal of Heat and Mass transfer* Vol. 37: 1377-1385.

22. Koizumi H, Yokoyama K. 1980. Characteristics of refrigerant flow in capillary tube. *ASHRAE Transactions Vol*. 86: 19-27.

23. Lathrop HF.1948. Application and characteristics of capillary tubes. *Refrig. Engg* August.

24. Li RY, Lin S, Chen ZH. 1990. Numerical modelling of thermodynamic non-equilibrium flow of refrigerant through capillary tubes. *ASHRAE Transaction* Vol. 96: 542-549.

25. Lin S, Kwok CCK, Li RY, Chen, Z.H. and Z.Y. Chen. 1991. Local frictional pressure drop during vaporization of R12 through capillary tubes. *Int. J. Multiphase Flow* Vol.17: 83-87.

26. Marcy GP. 1949. Pressure drop with change of phase in a capillary tube. *Refrigerating engineering*: 53-57.

27. McAdams WH, Wood WK, Bryan RL. 1942. Vaporization inside horizontal tubes, II. Benzene–oil mixture. *Transaction ASME* 64:193.

28. McLinden MO, Klein SA, Lemmon EW. 1998. REFPROP-thermodynamic and transport properties of refrigerants and refrigerant mixtures, NIST Standard Reference Database-version 6.01.

29. Melo C, Ferreira RTS, Boabaid NC, Goncalves JM, Mezavi MM. 1999. An experimental analysis of adiabatic capillary tubes. *Applied Thermal Engineering* Vol. 19: 669-684.

30. Mikol EP. 1963. Adiabatic single-and two-phase flow in small bore tubes. *ASHRAE Journal* Vol. 5: 75-86.

31. Moddy F, Princeton NJ. 1944. Friction factors for pipe flow. *Transactions of the ASME* November Vol. 66:671-684.

32. Motta SFY, Parise JAR, Braga SL. 2002. A visual study of R-404A/oil flow through adiabatic capillary tubes. *Int. J. Refrigeration* Vol. 25: 586-596.

33. Sami SM, Tribes C. 1998. Numerical prediction of capillary tube behavior with pure and binary alternative refrigerants. *Applied Thermal Engineering* Vol. 18: 491-502.

34. Sami SM, Maltais H. 2000. Experimental analysis of capillary tubes behavior with some HCFC-22 alternative refrigerants. *International Journal of Energy Research* Vol. 25: 1233-1247.

35. Stoecker WF, Jones JW. 1982. Refrigeration and Air Conditioning. *McGraw-Hill* New York.

36. Trisaksri, Wongwises. 2003. Correlations for sizing adiabatic capillary tubes. *Int. J.Energy Res*. Vol. 27:1145-1164.

37. Vins V. 2009. Two phase flow analyses during throttling process. *Int. J. Thermophys* Vol. 30: 1179-1196.

38. Whitesel HA. 1957. Capillary two phase flow. *Refrigerating engg*. Vol. 98: 42-43.

39. Wong TN, Ooi KT. 1996. Evaluation of capillary tube performance for CFC12 and HFC134a. *International Communications in Heat and Mass Transfer* Vol. 23: 993-1001.

40. Wongwises S, Chan P, Luesuwannatat N, Purattanark T. 2000. Two-Phase separated flow model of refrigerant flowing through capillary tubes. *International Communications in Heat and Mass Transfer* Vol. 27: 343-356.

41. Wongwises S, Pirompak W. 2001. Flow characteristics of pure refrigerants and refrigerant mixtures in adiabatic capillary tubes. *Applied Thermal Engineering* Vol. 21: 845-861.

42. Yang L, Wang W.2008. A generalized correlation for the characteristics of adiabatic capillary tubes. *Int J. Refrigeration* Vol. 31, 197-203.

43. Zhang CL.2004. Intensive parameter analysis of adiabatic capillary tube using approximate analytic solution. *International Journal of Refrigeration* Vol. 27: 456-463.